

Modelling and characterization of an
airlift-loop bioreactor



CENTRALE LANDBOUWCATALOGUS

0000 0248 1147

Promotoren: dr. ir. K. van 't Riet,
hoogleraar in de levensmiddelenproceskunde

ir. K. Ch. A. M. Luyben,
hoogleraar in de bioprocestechnologie
aan de Technische Universiteit Delft

P. Verlaan

Modelling and characterization of an airlift-loop bioreactor

Proefschrift

ter verkrijging van de graad van
doctor in de landbouwwetenschappen,
op gezag van de rector magnificus,
dr. C. C. Oosterlee,
in het openbaar te verdedigen
op vrijdag 20 november 1987
des namiddags te vier uur in de aula
van de Landbouwuniversiteit te Wageningen.

STELLINGEN

1. In de historische beeldvorming is de door Nederland in 1901 ingezette "Ethische politiek" nagenoeg uitsluitend met Oost-Indië in verband gebracht, in West-Indië is echter een zelfde beleid gevoerd, maar door het nadelige effect ervan is dat niet als zodanig onderkend.

E.B. Pultrum, doctoraalverslag, Rijksuniversiteit Leiden, 1986.

2. Het karakteriseren van axiale dispersie in een bellenkolom door middel van het dimensieloze Bodenstein kental dient vermeden te worden.
3. De veronderstelling dat het uitwisselingsoppervlak tussen de gas- en de vloeistoffase in een airlift-loop reactor door expansie en coalescentie van de gasbellen constant is over de hoogte, lijkt in tegenspraak met de resultaten uit dit proefschrift.

C.S. Ho et al., Biotechnol. and Bioeng., 19 (1977) 1503-1522.

4. Naarmate de schaal van een airlift-loop reactor toeneemt, neemt het belang van een juist ontwerp van de gasverdeler met betrekking tot de zuurstofoverdracht, af.
5. In de exacte wetenschappen wordt bij de opzet van mathematische modelvergelijkingen ten onrechte veelvuldig gebruik gemaakt van het germanisme "aanname", daar waar men veronderstelling bedoelt.
6. De definitie: "Een model is een vereenvoudigde voorstelling van de werkelijkheid" doet aan de voorstelling van de werkelijkheid van sommige onderzoekers ernstige twijfel ontstaan.
7. Het is te hopen dat de taakuitbreiding van de brandweer met de rampenbestrijding hier te lande, door deze organisatie zodanig zal worden opgevat dat die bestrijding tot een sanering van de diverse opleidingen tot brandweerfunctionaris zal kunnen leiden.
8. Het verdient aanbeveling om voor het besturen van motorrijwielen met een zuigerverplaatsing van meer dan 500 cm³ behalve een rijbewijs ook een psychologische test verplicht te stellen.

Stellingen behorende bij het proefschrift: "Modelling and characterization of an airlift-loop bioreactor" van P. Verlaan. Wageningen, 20 november 1987.

Ter nagedachtenis aan mijn vader.

VOORWOORD

Dit werk had niet tot stand kunnen komen zonder de medewerking van een groot aantal personen. In het bijzonder geldt dit voor de studenten die, als onderdeel van hun doctoraalwerk, onder mijn leiding aan het airlift-project hebben bijgedragen. Aan al deze mensen ben ik veel dank verschuldigd.

Toch wil ik er enkelen bij name noemen en persoonlijk bedanken:

Prof. dr. ir. J. Tramper, voor de inzet waarmee je de taak als "dagelijks begeleider", uitvoerde en voor de boeiende discussies over syntaxis en semantiek tijdens het schrijven van de artikelen.

De beide promotoren, prof. dr. ir. K. van 't Riet en prof. ir. K.Ch.A.M. Luyben, voor jullie inzet en vooral ook voor de enthousiaste wijze waarop jullie ideeën naar voren brachten tijdens onze werkbesprekingen.

CONTENTS

	page
CHAPTER 1: General introduction.	1
CHAPTER 2: A hydrodynamic model for an airlift-loop bioreactor with external loop.	11
CHAPTER 3: Estimation of axial dispersion in individual sections of an airlift-loop reactor.	31
CHAPTER 4: Isobaric and non-isobaric modelling of dynamic gas-liquid oxygen transfer in an airlift-loop bioreactor.	53
CHAPTER 5: From bubble column to airlift-loop reactor: Hydrodynamics of the transition flow regime.	75
CHAPTER 6: From bubble column to airlift-loop reactor: Axial dispersion and oxygen transfer.	93
CHAPTER 7: Hydrodynamics, axial dispersion and gas-liquid oxygen transfer in an airlift-loop bioreactor with three-phase flow.	107
CHAPTER 8: Summary/Samenvatting.	121

CHAPTER ONE

GENERAL INTRODUCTION

Biotechnology is currently a rapidly expanding field of interdisciplinary research. This appears amongst others from the development of a number of new types of bioreactors. The traditional stirred-tank reactor is no longer a priori the standard bioreactor, mainly because of economic considerations and the intrinsic properties of the bio-phase used [1,2]. Especially the airlift-loop reactor (ALR), as a result of several features which will be explained below, is a good example of the coming bioreactor. The ALR concept has been evolved from that of the bubble column (BC) and was first described by Lefrançois et al. [3]. The special feature of the ALR is the recirculation of the liquid through a downcomer connecting the top and the bottom

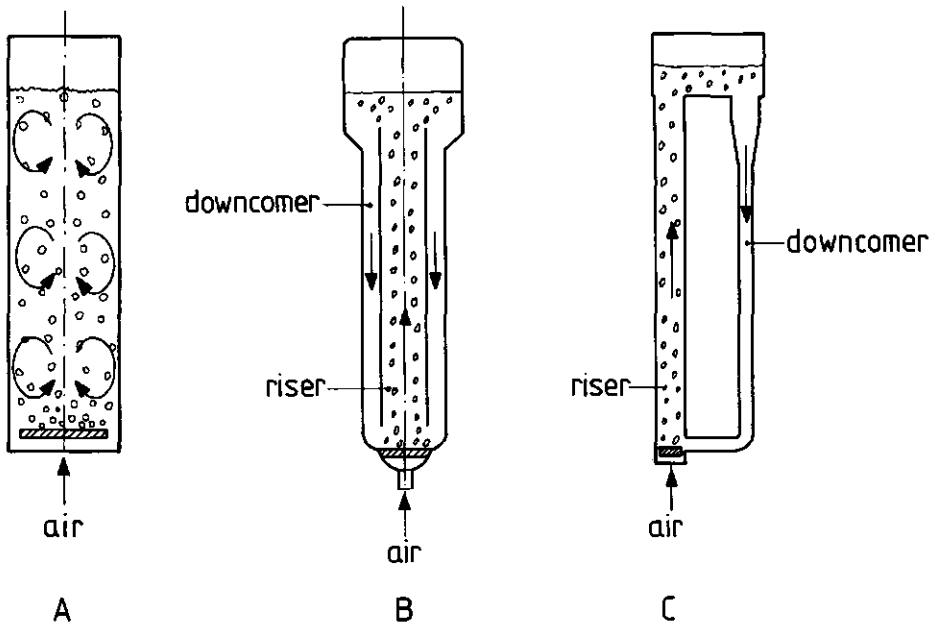


Fig. 1 Schematic representations of a bubble column (A), an internal-loop airlift reactor (B) and an external-loop airlift reactor (C).

of the main bubbling section (the riser, see figure 1). Due to the high

circulation-flow rate, efficient mixing is combined with a controlled liquid flow in the absence of mechanical agitators and thus absence of large shear forces. Moreover, an ALR can satisfy a high oxygen demand particularly in larger ALR configurations (50-150 m) [4,5]. These properties make the ALR a suitable reactor for shear sensitive organisms requiring a controlled dissolved oxygen concentration (DOC). An example of such an application is the production of secondary metabolites by plant cells [6].

Design and construction of the ALR

An ALR is a reactor which essentially consists of a riser and a downcomer which have an open connection at the bottom and the top. There exist two different types of ALRs: the ALR with an internal loop (AILR) and the ALR with an external loop (AELR) as shown in figure 1. Continuous injection of air at the bottom of the riser creates a density difference with the downcomer as the air escapes at the top of the reactor. Due to this density difference, a liquid flow from the bottom to the top exist in the riser and from the top to the bottom in the downcomer, thus resulting in the circulation of the continuous liquid phase.

Advantages of the ALR in comparison to more conventional bioreactors like the standard fermenter, are the absence of mechanically moved parts in the ALR and a low rate of shear, the relative simple construction and with that a low fault sensitivity, an adequate gas-phase disengagement at the top, a large specific interfacial contact area at a low energy input, a unique combination of controlled flow and good mixing properties and due to the controlled flow, a well defined residence time for all phases including the solid (bio-)phase. Furthermore, it should be noted that the ALR can be easily operated under sterile conditions as result of its simple construction. The main additional advantage of the AILR is the very simple geometry: a bubble column with a shaft in it. The AELR has several additional advantages in comparison to the AILR:

- * a well defined residence time in the individual sections of the AELR
- * an adjustable gas-phase disengagement at the top
- *accessability for measurement and control in both the riser and the downcomer

- * A simple valve between the riser and the downcomer enables control of the liquid velocity independent of the gas-input rate
- * An excellent heat exchange and temperature control
- * A simple geometry of the individual parts (tubes) justifies the use of a simple model
- * An optimal hydraulic diameter for both the riser and downcomer and therefore a low friction rate
- * Visual admittance to the process if the AELR is constructed of transparent elements

For the present study the above-mentioned features tipped the balance in the advantage of the AELR to use this type of ALR for our experiments. An extended overview of the characteristics for the ALR and other type of loop reactors is given by Blenke [7].

Aim

The aim of the present research is the modelling and characterization of the physical behaviour of a multi-phase flow in an ALR in order to give unambiguous information for the design and scale-up of an ALR for a given biotechnological production process using immobilized biocatalysts.

Scope and objectives

The study of this type of reactor was at the time initiated in view of its application as bioreactor for conversion with immobilized biocatalysts [8] and plant cells [6,9,10]. From the viewpoint of this, efficient oxygen transfer and a controlled DOC in the ALR has to be realized, which requires knowledge of hydrodynamic, mixing and oxygen transfer characteristics. In the present study these are the basic elements of investigation.

Hydrodynamics

The behaviour of an ALR (and of a bioreactor in general) is determined not only by its geometry but also by its hydrodynamic properties. Therefore knowledge of liquid velocity and (local) gas hold-up is a requisite for reliable predictions of mixing and mass transfer characteristics. In contrast to bubble columns, in an ALR the above-mentioned hydrodynamic parameters predetermine each other, thereby impeding a fundamental prediction of gas hold-up and liquid velocity. Several investigators have reported work on characterising an ALR by liquid velocities, gas hold-ups and reactor geometries for air-water systems [11-19]. From this literature can be concluded that correlations and a few empirical hydrodynamical models concerning air-water systems are available. Several of these models have been proposed in order to describe flow behaviour in an ALR but in most cases these models have been based on empirical correlations specific to the particular ALR used [17,18,20]. A more general description of the hydrodynamics does not exist, while some authors present contradictory findings [13,14]. Chapter 2 deals with the hydrodynamic properties of an ALR for an air water system aiming at a more general description and understanding for reactor design and scale-up.

Mixing

Mixing in an ALR is a result of two different phenomena: axial dispersion and liquid circulation. Axial dispersion is mass transport by diffusion-like disturbances on a plug flow occurring in the reactor tubes of an ALR. The liquid circulation cumulates the individual axial dispersion contributions during one liquid circulation, to a final mixing result generally expressed by a single parameter: the mixing time. In an ALR, axial dispersion has an influence on oxygen and other substrate profiles, thus effecting the kinetics of (immobilized) biocatalysts and with that the design of the ALR. Fields and Slater [21] for instance, investigated the influence of liquid mixing in an ALR on the respiration of micro-organisms and found that respiratory quotients are affected by the local mixing behaviour. In view of biological processes in which small characteristic times (time constants) are of importance, it is essential to investigate not only axial dispersion

for the reactor as a whole, but also for the different sections of the ALR: riser, topsection (gasdisengagement section) and downcomer.

In contrast to bubble columns, where numerous investigators reported results on the characterization of axial dispersion [22-24], there is a lack of knowledge on the mixing behaviour in ALRs, especially in the individual sections of the ALR. Several investigators reported results on axial dispersion in the ALR as a whole and in the individual sections [10,17,18,25,26], but the mathematical methods they applied to assess these values entailed serious problems due to the liquid circulation in the ALR [18,21].

In chapter three a parameter estimation method is presented yielding the axial dispersion parameter which is not affected by the nature of the tracer nor by the circulation flow of the loop reactor. It will also be shown that axial dispersion in the reactor as a whole can be calculated from the contributions of the individual sections.

Oxygen transfer

As the ALR is especially a reactor for aerobic biotechnological processes, the aeration capacity and performance is of main interest for its application as a bioreactor. Moreover, because of the controlled liquid flow, the geometry of the reactor and the hydrostatic pressure differences, intolerable variations in the local DOC may occur during a fermentation. As a result, the characterisation of the aeration in an ALR does not only require a thorough knowledge of the overall aeration characteristics but also of local gas-liquid oxygen transfer, including oxygen transfer in the gas-sparger region.

Several investigations have been carried out on the mass transfer capacity of airlift contactors [15,17,25,27], however these results are based on empirical correlations which in most cases are specific to the situation and often do not contribute to a more perspicacious view on this matter. A few workers introduced mathematical models describing oxygen transfer in an ALR [18,28,29]. Unfortunately, the assumptions proposed, restricts a more general approach. In one case for instance, only the steady-state situation was considered [28], while in other cases fundamental parameters were obtained from empirical correlations making large scale predictions doubtful [28,29]. Other examples are: 1. the assumption on the mixing behaviour was

not based on a thorough knowledge of mixing in an ALR [29] leading to false interpretations, 2. not the entire reactor was incorporated in the model [18], 3. gas phase dynamics were neglected [18] and 4. the theoretical work was not verified experimentally [29].

Clearly, a real theoretical base for the description of oxygen transfer and the estimation of oxygen-transfer coefficients in an ALR is lacking in the literature. On the basis of the research reported in the chapters two and three, a dynamic, non-isobaric gas-liquid transfer model was developed which was used to estimate the aeration coefficient and to investigate the influence of the air-sparger region on the overall oxygen transfer. This model is presented in chapter four. Carbondioxide and nitrogen transports are included in the model as mass transfer of these components between the gas and the liquid phase is able to severely influence the DOC or the mole fraction of oxygen in the gas phase. Moreover, large carbondioxide concentrations in the liquid phase can influence the metabolism of biomass [30].

Transition phenomena

An ALR has a plug flow for both the liquid and the gas-phase with the liquid phase circulating through the reactor. In some cases, depending on the dimensions of the ALR, the difference between an ALR and a bubble column can become very small as a result of a hampered liquid flow. Such a situation occurs in an ALR when for instance gas redispersion plates are mounted, when the downcomer diameter is designed very small in order to obtain a small residence time in this part, or when voluminous monitoring devices are fitted in the reactor tubes. If the liquid flow is hampered, the upflow region can loose its typical plug-flow characteristics and gradually can transfer into a BC-type of flow. The intermediate region between an unhampered ALR flow and a BC flow is what we call the transition flow regime and depends on the process conditions of the ALR.

A major problem in designing and modelling the physical behaviour of an ALR, in particular with respect to the aspects mentioned in the previous three paragraphs, is the exact definition of the flow regimes in the column; in other words, whether to deal with a BC or an ALR. Each flow pattern has its own responsive chord on reactor performance. This problem has been

recognized earlier in the literature but until now, little results have been reported on this topic. Merchuk and Stein [12] investigated the hydrodynamics in the transition flow regime and summarized their results in an empirical correlation from which no general prediction for the onset of change in flow pattern can be obtained.

A few workers investigated axial dispersion [15,25] and oxygen transfer [15] in an ALR and compared the results between bubble column and airlift operation in the same unit, but no information of axial dispersion and oxygen transfer in the transition flow regime between an ALR and a BC is existing. Chapter five is dedicated to the hydrodynamics of the transition flow regime. A criterium is presented by which transition from bubble column to ALR hydrodynamics can be predicted. This criterium also indicates whether the general hydrodynamic model for an ALR, presented in chapter two, is valid or not.

Chapter six is dedicated to axial dispersion and oxygen transfer in the transition flow regime. The results presented in that chapter can be an important tool in scaling-up and designing ALRs.

Three-phase flow

The research mentioned in the previous sections concerned the physical behaviour of gas-liquid flow in an ALR. In many cases immobilized biocatalysts or micro-organisms growing in aggregates are used in biotechnological production processes. This means that the biophase in the reactor is concentrated in or on beads with diameters up to several millimeters. Also in this case an ALR seems a suitable reactor having excellent suspension characteristics due to the high liquid velocity.

Little research has been reported until now on the influence on bioreactor performance of relatively large (2-3 mm) particles with a neutral buoyancy e.g. gel-entrapped biocatalysts. Recently, results were published on the influence of neutral buoyant calcium alginate beads with a diameter of 2,2 mm on oxygen transfer in a stirred-tank reactor [31]. For ALRs no such data is available. Therefore the aim of chapter 7 is to give a concise overview of the physical ALR properties and the interaction with relatively large solid particles in order to provide essential information for three-phase-ALR design. In chapter 7, results are reported on the physical

influence on ALR performance of neutral buoyant polystyrene or calcium-alginate beads with diameters ranging from 2.4 to 2.7 mm.

Notes on thesis lay out

The chapters in this thesis all are similarly presented as independent contributions, each of which forms a part that can be read apart from the others. Each chapter has been closed with literature references and a list of symbols used.

REFERENCES

- [1] P. Verlaan. Airlift-loop bioreactor. PT-procestechniek. 40 nr.10 (1985) 60-63 (in Dutch).
- [2] P. Verlaan. Karakterisering van een airlift-loop bioreactor. Voedingsmiddelentechnologie (VMT). 12 (1987) 31-34 (in Dutch).
- [3] M.L. Lefrançois, C.G. Mariller and J.V. Mejane. Effectionnements aux procedes de cultures forigiques et de fermentations industrielles. Brevet d'Invention, France, no. 1 102 200 (1955).
- [4] M.L. Hemming. General biological aspects of waste-water treatment including the deep-shaft process. Wat. Pollut. Control. 78 (1979) 312-325.
- [5] S. Shioya, N.D.P. Dang and I.J. Dunn. Bubble column fermenter modeling: a comparison for pressure effects. Chem. Eng. Sci. 33 (1978) 1025-1030.
- [6] A.C. Hulst, P. Verlaan, H. Breteler and D.H. Ketel. Thiophene production by *Tagetes patula* in a pilot plant airlift-loop reactor. Proc. 4th Europ. Congress on Biotechnology. 2 (1987) 401-404. (O.M. Neijssel, R.R. van der Meer, K.Ch.A.M. Luyben eds.) Elsevier Science Publishers B.V., Amsterdam.
- [7] H. Blenke. Biochemical loop reactors, VCH, Weinheim, 1985.
- [8] J. Tramper and J. Vlak. Some engineering and economic aspects of continuous cultivation of insect cells for the production of Baculoviruses. Ann. N.Y. Acad. Sci. 469 (1986) 279-286.
- [9] D.H. Ketel. Callus and cell culture of *Tagetes* species in relation to production of thiophenes. Thesis, Agricultural University, Wageningen, 1987.
- [10] P. Verlaan, A.C. Hulst, J. Tramper, K. van 't Riet and K.Ch.A.M. Luyben. Immobilization of plant cells and some aspects of the application in an airlift fermentor. Proc. 3rd Europ. Congress on Biotechnol., vol. 1, München, GDR, 10-14 sept. (1984) 151-157.
- [11] U. Onken and P. Weiland. Hydrodynamics and mass transfer in an airlift loop fermentor. Eur. J. Appl. Microbiol. Biotechnol. 10 (1980) 31.
- [12] J.C. Merchuk and Y. Stein. Local hold up and liquid velocity in airlift reactors. AIChE J. 27 (1981) 377-388.
- [13] D.G. Mercer. Flow characteristics of a pilot-scale airlift fermentor. Biotechnol. & Bioeng., 23 (1981) 2421-2431.
- [14] W.J. McManamey, D.A.J. Wase, S. Raymahasay and K. Thayamithy. The influence of gas inlet design on gas hold-up values for water and various solutions in a loop-type air-lift fermenter. J. Chem. Technol. Biotechnol., 34B (1984) 151-164.
- [15] R.A. Bello, C.W. Robinson and M. Moo-Young. Gas hold-up and overall volumetric oxygen transfer coefficient in airlift contactors. Biotechnol. & Bioeng. 27 (1985) 369-381.
- [16] N.N. Clark and R.L. Flemmer. Predicting the hold up in two-phase bubble upflow and downflow using the Zuber and Findlay drift-flux model. AIChE J., 31 (1985) 500-503.
- [17] R.T. Hatch. Experimental and theoretical studies of oxygen transfer

- in the airlift fermentor. Thesis, M.I.T., Cambridge, 1973.
- [18] R.G.J.M. van der Lans. Hydrodynamics of a bubble column loop reactor, Thesis, Delft University of Technology, Delft, 1985.
- [19] A.G. Jones. Liquid circulation in a draft-tube bubble column. *Chem. Eng. Sci.* 40 (1985) 449-462.
- [20] H. Kubota, Y. Hosono and K. Fujie. Characteristic evaluations of ICI air-lift type deep shaft aerator. *J. Chem. Eng. Jap.*, 11 (1978) 319-325.
- [21] P.R. Fields and N.K.H. Slater. The influence of fluid mixing upon respiratory patterns for extended growth of a methylotroph in an air-lift fermentor. *Biotechnol. & Bioeng.* 26 (1984) 719-726.
- [22] R.W. Field and J.F. Davidson. Axial dispersion in bubble columns. *Trans. I. Chem. Eng.* 58 (1980) 228-235.
- [23] K.H. Mangartz and Th. Pilhofer. Interpretation of mass transfer measurements in bubble columns considering dispersion of both phases. *Chem. Engng. Sci.* 36 (1981) 1069-1077.
- [24] J.B. Joshi and Y.T. Shah. Hydrodynamic and mixing models for bubble column reactors. *Chem. Eng. Commun.* 11 (1981) 165-199.
- [25] P. Weiland. Untersuchung eines Airliftreaktors mit Äußerem Umlauf im Hinblick auf seine Anwendung als Bioreaktor. Thesis, University of Dortmund, Dortmund, 1978.
- [26] P.R. Fields and N.K.H. Slater. Tracer dispersion in a laboratory air-lift reactor. *Chem. Engng. Sci.* 38 (1983) 647-653.
- [27] C.H. Lin, B.S. Fang, C.S. Wu, H.Y. Fang, T.F. Kuo and C.Y. Hu. Oxygen transfer and mixing in a tower cycling fermentor. *Biotechnol. & Bioeng.* 18 (1976) 1557-1572.
- [28] J.C. Merchuk and Y. Stein. A distributed parameter model for an airlift fermentor. *Biotechnol. & Bioeng.* 22 (1980) 1189-1211.
- [29] C.S. Ho, L.E. Erickson and L.T. Fan. Modeling and simulation of oxygen transfer in airlift fermentors. *Biotechnol. and Bioeng.* 19 (1977) 1503-1522.
- [30] A.V. Quirk and R.W.H. Plank. The effect of carbon dioxide on the production of an extracellular nuclease of staphylococcus aureus. *Biotechnol. & Bioeng.* 25 (1983) 1083-1093.
- [31] J.J. Frijlink. Physical aspects of gassed suspension reactors. Thesis, University of Technology, Delft, 1987.

CHAPTER TWO**A HYDRODYNAMIC MODEL FOR AN AIRLIFT-LOOP BIOREACTOR
WITH EXTERNAL LOOP**

P. Verlaan, J. Tramper and K. van 't Riet,
Department of Food Science, Food and Bioengineering Group,
Agricultural University,
De Dreyen 12, 6703 BC Wageningen, The Netherlands.

K.Ch.A.M. Luyben, Department of Biochemical Engineering,
Delft University of Technology,
Julianalaan 67, 2628 BC Delft.

ABSTRACT

A simple model is introduced for the hydrodynamic description of an airlift-loop bioreactor with external loop. The model is based on the drift flux model of Zuber and Findlay (1965) for a two-phase flow and predicts the liquid velocity and the local gas hold-up in both the upflow and downflow region in relation to the gas input rate and the reactor dimensions. The model is non-isobaric and takes into account non-uniform flow profiles. Liquid velocity and local gas hold up in airlift-loop reactors from laboratory to pilot plant scales are predicted to within 5-10% accuracy.

INTRODUCTION

At present, various types of bioreactors are used in biotechnological processes, e.g. the conventional stirred tank reactor and the more modern airlift-loop reactor. An airlift-loop reactor (ALR) combines efficient oxygen transfer and mixing with controlled liquid flow and low shear forces. The behaviour of a bioreactor is determined not only by the reactor geometry but also by its hydrodynamic properties. Therefore knowledge of liquid velocity and (local) gas hold-up is essential for reliable predictions of mixing and mass transfer characteristics. In contrast to bubble columns, in an ALR the above-mentioned hydrodynamic parameters predetermine each other which impedes a fundamental prediction of gas hold-up and liquid velocity. Several investigators have reported work on characterising an ALR by liquid velocities, gas hold-ups and reactor geometries for air-water systems.

Onken and Weiland [1], for instance, have measured gas hold-ups for an 0.12 m³ ALR with external loop (height: 10 m) and found the gas hold-up in the reactor to be independent of the initial bubble size generated by the gas sparger. In contrast to Onken and Weiland, Merchuk and Stein [2] found that even in tall columns, the measured values of the local gas hold-up in an ALR with external loop depend on the geometry of the gassparger (single orifice or multiple orifices) and on the friction in the reactor. Mercer [3] mentioned diminishing average bubble sizes in a pilot-scale ALR with increasing aeration rates which enhances gas hold-up. In contrast McManamey et al. [4] reported an increasing bubble size due to coalescence when the reactor was operated at high aeration rates. However, Mercer determined the gas hold-up photographically and it is possible that only bubbles at the wall-side were observed which were not necessarily representative for the whole reactor. The results of McManamey et al. were obtained by visual observations. Merchuk and Stein [2] did not observe bubble coalescence or bubble dispersion in their reactor. Bello et al. [5] investigated gas hold-ups in both an external and internal loop airlift reactor with various diameter ratios for the upflow and downflow regions and presented empirical relations for gas fractions in relation to the gas input rate, the liquid velocity and the ratio of downcomer and riser tube cross-area. The discrepant interpretations in literature of gas hold-up characteristics in an ALR hamper a more perspicacious view.

A similar trend is observed for liquid flow behaviour in ALRs which, in

contrast to the gas hold-up measurements, is due mainly to the application of different experimental techniques. Mercer [3] investigated flow characteristics of a pilot-scale airlift (working volume: 0.55 m^3), using a flow follower technique. Because of this technique, the results were affected by secondary flow patterns in the upward flowpath; as a result the velocity gradient of the riser and downcomer appeared to be of opposite sign for increasing gas injection rate. The same method was also applied by Clark and Flemmer [6] in a two-phase bubble upflow and downflow. They reported secondary circulation patterns which disturbed experiments in such a way that the circulation rate could not be measured accurately. Onken and Weiland [1] measured liquid velocity using an inductive flow meter which enables an accurate estimation of the flow velocity in a tube; Merchuk and Stein [2] used a liquid flow meter. Both teams [1,2] found an exponential correlation between the liquid flow and the gas velocity in the riser.

Several models have been proposed in order to describe flow behaviour in an ALR but in most cases these models have been based on empirical correlations specific to the particular ALR used. Hatch [7] for instance, applied the drift-flux model of Zuber and Findlay [8], supplemented with empirical correlations for an internal loop ALR with a working volume of 0.2 m^3 , in order to calculate liquid velocities and gas hold-up fractions in both the riser (draft) and the downcomer (annulus). The semi-empirical model which did not take into account pressure effects, predicted the hydrodynamic parameters to within 10%. Van der Lans [9] and Kubota et al. [10] have studied and modelled hydrodynamics in pilot-plant deep shaft reactors with an external loop and working volumes of 0.6 m^3 and 0.2 m^3 respectively. In both models the rise velocity of the gas bubbles was obtained experimentally. Kubota et al. also included in their model gas exchange by biological activity but did not verify their calculations experimentally. Van der Lans predicted deep-shaft hydrodynamics for his experimental set up, within the experimental accuracy. Jones [11] introduced a simple model on the basis of an energy balance in the upflow region, but gas hold-up in the downflow region was neglected. In this model it was assumed that the work performed by the ascending air bubbles is equal to the work performed in accomplishing liquid circulation. Nevertheless, a discrepancy occurred between the model and the experiments in a concentric tube airlift with a working volume of 0.06 m^3 (about 33%), especially for large draft diameters. No friction calculations were included.

Clearly, some data, correlations and empirical hydrodynamical models concerning air-water systems are available but a more general description of hydrodynamics does not exist, while some authors even present contradictory findings. The present work concerns hydrodynamic properties of an ALR aiming at a more general description and understanding. A simple model based on the drift-flux model of Zuber and Findlay [8] for a two-phase flow is introduced, on the basis of which the liquid velocity and the local gas hold-up in both the riser and downcomer can be predicted in relation to the gas input rate and the reactor dimensions, taking into account non-uniform flow profiles. An iterative procedure is necessary since the liquid velocity and the gas hold up are not independent. The model is non-isobaric and has been used to predict the liquid velocities and local gas hold-ups in external loop reactors of various sizes (0.004 m^3 - 0.6 m^3).

MATERIALS AND METHODS

Two different pilot-plant ALR's have been used for the evaluation of the hydrodynamic model one with a height of 3.23 m and another with a height of 10.5 m. The smaller ALR has a reactor volume of 0.165 m^3 and a riser and downcomer constructed of borosilicate glass pipe sections with diameters of 0.2 m and 0.1 m respectively. The top of this reactor consists of a stainless steel cistern which has a length of 0.7 m and a width of 0.22 m thus allowing for a certain amount of foaming (Figure 1). It was designed to obtain complete deaeration without gas entrainment into the downcomer. The liquid level was kept at 0.13 m above the bottom of the cistern in the absence of gas in order to maintain about the same liquid velocity in the riser and in the topsection. The funnel shaped top of the downcomer accomplishes a smooth diameter change. A gas sparger has been designed which produces bubbles of about the equilibrium diameter ($d_b = 6 \text{ mm}$) of air bubbles in water [12]. At the bottom of the reactor air and water can be supplied. Temperature control is provided by a contact-element heater fixed on the stainless-steel pipe element of the top section.

The larger ALR has a working volume of 0.6 m^3 and a riser and downcomer diameter of 0.225 m and 0.1 m respectively. The whole reactor consists of borosilicate glass pipe sections and has the same geometry as the 0.165 m^3 ALR except for the topsection which, in this case, consists of a glass pipe

section with a length of 0.85 m and diameter of 0.15 m. In this reactor, temperature control is performed by a heater positioned in the riser liquid flow. The ALR is provided with a vacuum pump by which the pressure at the top of the reactor can be lowered to a value of 3-5 kPa, depending on the gas input rate. This reactor is situated at the Delft University of Technology and more details about this reactor have been reported by van der Lans [9].

In both reactors the liquid flow in the downcomer was measured by means of an inductive flow meter. A reversed U-tube manometer was used to measure the pressure difference over the length of interest. For this purpose the riser is equipped with various pressure points (Figure 1). The gas fraction in the riser was estimated from the pressure difference between two points which is represented by the following equation:

$$\Delta p = \rho g L (1 - \alpha) \quad (1)$$

Here, α is the mean gas volume fraction in the relevant part of the tube with length L , ρ is the liquid density and g the gravitational constant. Friction and acceleration terms were assumed to contribute negligibly to the changes in gas hold-up along the column. From eq (1) the mean gas hold up over a tube length L can be calculated.

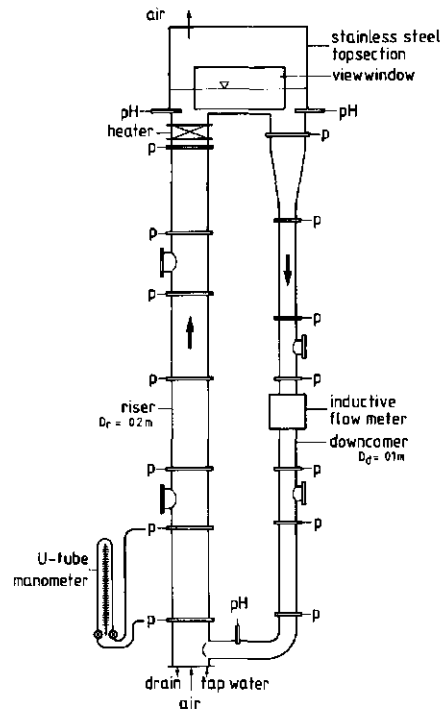


Fig. 1 The airlift-loop reactor

THE MODEL

As stated above, the liquid velocity and the gas hold-up have to be estimated in relation to the main input parameter of an ALR, the injected gas flow. The density differences due to a gas hold-up α_r in the riser and α_d in the downcomer result in a liquid flow in the ALR. In a stationary situation the driving force has to be equal to the friction losses in the ALR:

$$\int_0^L \alpha_r(z) dz - \int_0^L \alpha_d(z) dz = K_f / (2g) \cdot v_{1s}^2 \quad (2)$$

where K_f is the friction coefficient and v_{1s} the superficial liquid velocity. Thus the liquid velocity can be calculated when both the riser and the downcomer gas hold-up are known. However, the gas hold-up is a function of the liquid velocity. Therefore an iterative procedure has been used for this calculation, which is shown in Figure 2 and explained below.

The local gas fraction is expressed by the following equation:

$$\alpha(z) = v_{gs}(z) / v_g(z) \quad (3)$$

In this equation $v_g(z)$ is the local gas velocity and $v_{gs}(z)$ the local superficial gas velocity:

$$v_{gs}(z) = \Phi_{vg}(z) / A \quad (4)$$

with $\Phi_{vg}(z)$ equal to the local volumetric gas flow rate and A is the tube cross-sectional area. The gas velocity, v_g , is a function of the liquid velocity, the superficial gas velocity and the local relative velocity between the bubble and the liquid phase.

In the present research the two-phase drift-flux model of Zuber and Findlay [8], taking into account non-uniform flow and hold-up distributions across the duct, has been used in order to calculate the gas hold-up in the column. Zuber and Findlay made the initial assumption that the drift velocity is independent of the void fraction and proposed the drift velocity term to be equal to the terminal rise velocity of a single bubble in an infinite medium. Wallis [13] reviewed the influence of column diameters on the bubble

rise velocity and found the rise velocity to reach the terminal rise velocity of a bubble in an infinite medium if $d_b < 0.125D_{\text{column}}$. From the above-mentioned model Zuber and Findlay obtained

$$v_g = C \cdot \{ v_{gs} + v_{ls} \} + v_{b,\infty} \quad (5)$$

where C is a distribution parameter for non-uniform radial flow. The flatter the flow profiles the closer C approaches unity. Hatch [7] determined the C -value experimentally in the draft of an internal loop airlift (206 mm). The resulting value was: $C = 1.065$. Clark and Flemmer [6] investigated the distribution parameter C in up- and downflow regions and concluded that as pipe diameter increases bubble behaviour may become less symmetrical and less predictable. They reported a mean value of $C = 1.07$ for the upflow region (100 mm pipe) and revealed a strong trend for C to vary linearly with voidage. These values are in agreement with the calculations of Zuber and Findlay [8] who reported a theoretical value of

$C = 1.07$ provided that $\alpha_{\text{wall}}/\alpha_{\text{centre}} = 0.5$ and the radial distributions in the duct are given by:

$$\frac{v_{gs} + v_{ls}}{(v_{gs} + v_{ls})_{\text{centre}}} = 1 - (r/R)^2 \quad \frac{\alpha - \alpha_{\text{wall}}}{\alpha_{\text{centre}} - \alpha_{\text{wall}}} = 1 - (r/R)^7 \quad (6)$$

Equations (6) agree with the results of Menzel et al. [14] who investigated flow profiles in a loop reactor. Serizawa et al. [15] pointed out from their

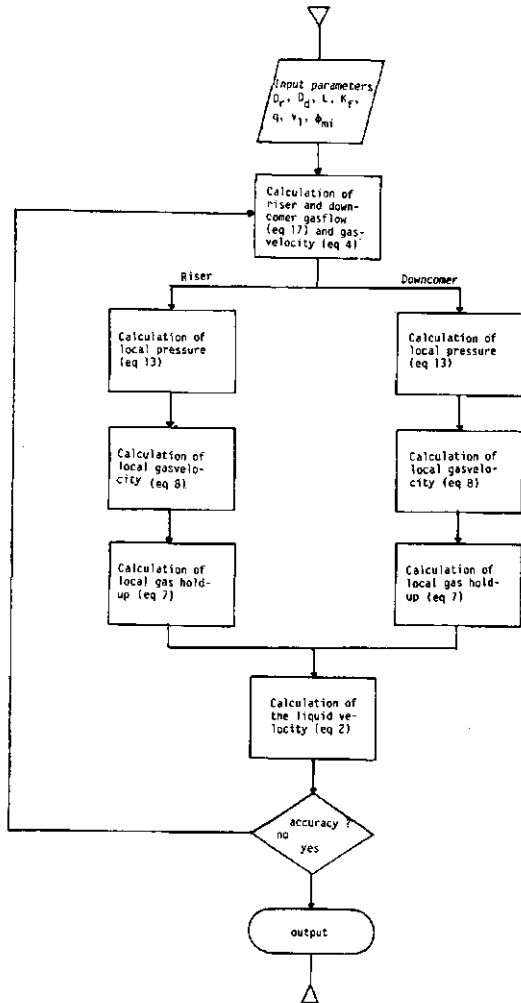


Fig. 2 Schematic presentation of the calculation of the hydrodynamic model

experiments that the gas hold-up profiles in a 60 mm vertical tube were fairly flat, confirming the high value of the exponent in eqns (6). From this work the plausability of the condition $\alpha_{\text{wall}}/\alpha_{\text{centre}} = 0.5$ is also confirmed.

Substitution of eqn(5) into eqn(3) yields:

$$\alpha(z) = v_{gs}(z) / \{ C.(v_{ls}(z) + v_{gs}(z)) + v_{b,\infty} \} \quad (7)$$

Owing to pressure effects, the superficial gasvelocity varies in the ALR. Assuming one-dimensional isothermal flow, steady state and negligible mass transfer effects between the phases, the gasvelocity can be expressed as follows:

$$v_{gs}(z) = v_{gs}(0) \cdot p(0) / p(z) \quad (8)$$

where $v_{gs}(0)$ and $p(0)$ are the superficial gas velocity and the pressure at the bottom of the reactor respectively. The local pressure in the ALR is represented by:

$$p(z) = p(0) - \rho \cdot g \cdot \left\{ z - \int_0^z \alpha(z) dz \right\} \quad (9)$$

Substitution of eqn (9) and (8) into eqn (7) shows that eqn (7) is implicit for $\alpha(z)$. To overcome this problem an approximation for $\alpha(z)$ in eq (9) is employed as is proposed by van der Lans [9] and which will be denoted by $\alpha'(z)$:

$$\alpha'(z) = \alpha(0) \cdot p_h(0) / p_h(z) \quad (10)$$

In this equation, p_h is the hydrostatic pressure which seems a reasonable approximation for the real pressure if $\alpha(z) \ll 1$. The hydrostatic pressure is defined as:

$$p_h(z) = p(0) - \rho g z \quad (11)$$

Substitution of eqns (11) and (10) into eqn (9) gives:

$$p(z) = p_h(z) - p(0)\alpha(0) \int_0^{p_h(z)} \frac{1}{p_h(z)} \cdot d(p_h(z)) \quad (12)$$

Integration of eq (12) yields:

$$p(z) = p(0) - \rho g z - p(0) \cdot \alpha(0) \cdot \ln\{1 - \rho g z / p(0)\} \quad (13)$$

With this approximation for the local pressure instead of eqn (9), the implicitness for $\alpha(z)$, (eqn 7), has disappeared. Substitution of eqn (13) together with eqn (8) into eqn (7) gives an expression by which the local gas hold up in the riser of the ALR can be calculated if the liquid velocity is known and gas is absent from the downcomer. In practice, gas hold-up in the downflow region is present in most cases and will contribute to the total hydrodynamic behaviour of the ALR.

Gas hold-up in the downcomer

Gas hold-up in the downcomer may result from incomplete deaeration at the top of the reactor or it can be accomplished deliberately by forced gas injection into this section. Assuming no influence of turbulence on the rise velocity of a bubble, the condition for complete deaeration at the top of the ALR is:

$$\Phi_{v1} / (L \cdot B \cdot v_s) > 1 \quad (14)$$

Here, Φ_{v1} is the liquid flow rate, L and B the length and width respectively of the topsection and v_s the bubble rise velocity. Equation (14) shows that the rate of deaeration at the top is independent of the liquid level in the topsection.

The mass flow rate of gas in the riser is defined as:

$$\Phi_{mgr} = \Phi_{mgi} + \Phi_{mgd} \quad (15)$$

where Φ_{mgi} is the injected mass flow of air in the sparger and Φ_{mgd} is the mass flow of air in the downcomer. If the gas flow in the downcomer is given as a fraction q of the riser gas flow:

$$\phi_{mgd} = q \cdot \phi_{mgr} \quad (16)$$

substitution of eqn (16) into eqn (15) yields:

$$\phi_{mgr} = \phi_{mgi} / (1 - q) \quad \text{and} \quad \phi_{mgd} = \phi_{mgi} \cdot q / (1 - q) \quad (17)$$

ϕ_{mgr} and ϕ_{mgd} are used to calculate the superficial gasvelocity in the riser and downcomer (eqn (4)) which enables the use of eqn(7) to derive the local gas hold-up in the pertinent reactor part, taking into account the sign of the bubble rise velocity $v_{b,\infty}$ and the proper superficial liquid velocity v_{ls} .

Clark and Flemmer [6] showed in their literature review that there exists a discrepancy in published values for the distribution parameter, C, for different flow regimes. Some authors assumed the profile constant to have the same value in both the riser and downcomer. Others assumed C to differ between the two sections. Although Clark and Flemmer report contradictory results in their own work, for the downcomer they observe consistent values for C. In downcomers with diameters of 50 mm and 100 mm, almost the same values for C were found: C= 1.16 and C= 1.17 respectively.

Calculation of the friction coefficient

The steady-state pressure drop in the ALR consists of the pressure drop along the length of the riser, P_r , and along the downcomer tube, P_d , and its appendages. When the pressure drop due to acceleration in the flow is neglected (its contribution to the total pressure drop in a pipe element will be less than 1% [13]) the frictional pressure drop in the airlift will be:

$$\Delta P_f = \Delta P_r + \Delta P_d + 4\Delta P_{f_{bend}} + \Delta P_{f_{r \rightarrow d}} + \Delta P_{f_{d \rightarrow r}} \quad (18)$$

In eqn (18), the pressure drop in the appendages consists of six different contributions: four times a 90° bend and two changes in flowed cross section area of riser-downcomer and vice versa.

If the two-phase mixture has a gasfraction of less than 10% the influence of the gasphase on the total friction is negligible [13]. In most cases the gas

fraction in airlift-loop reactors will be below this value. The total frictional pressure drop through the turnaround referred to the superficial downcomer liquid velocity can now be written as:

$$\Delta P_f = \frac{1}{2} K_f \rho_m \cdot v_{ld}^2 \quad (19)$$

where ρ_m is the average density of the gas-liquid mixture in the riser and downcomer. K_f can be divided into eight contributions according to eqn (18):

$$K_f = A_d^2/A_r^2 \cdot \{K_{fr} + 3K_{fbend} + K_{fd-r}\} + K_{fbend} + K_{fr-d} + K_{fd} \quad (20)$$

The expressions used to calculate the friction coefficients of the pipe elements and the appendages are mentioned in the appendix. Use of eqn (20) to calculate the total friction coefficient of the two pertinent ALRs yields the following values: $K_f = 1.8$ for the smaller ALR and $K_f = 4.75$ for the larger ALR. When K_f is known, the liquid velocity and the (local) gas hold-up can be predicted on the basis of eqn(7) with the superficial gas velocity as the sole input parameter.

working volume	K_{fr}	K_{fd}	K_{fbend}	K_{fr-d}	K_{ftot}	K_{fexp}
0.165 m ³	0.1	0.7	0.38	0.62	1.8	1.84
0.6 m ³	0.4	2.0	1.5	1.1	4.75	4.43
0.004 m ³	0.32	0.12	4.5*	-	4.95	4.5
Weiland [21]	0.1	4.0	0.55	0.9	5.55	4.9
Merchuk [2]	0.58	0.58	5.2	6.0**	11.36	11.2

Table 1 Calculated and experimental friction coefficients

* Revealed from Blenke [16]

** Estimated

RESULTS AND DISCUSSION

In figure 3, the measured square of the liquid velocity is plotted against the gas hold-up in the riser for both ALRs. From the slope of these lines the friction coefficient can be derived according to eqn (2). In tabel 1 the calculated values are compared with the experimental values and as is shown they agree very well. From

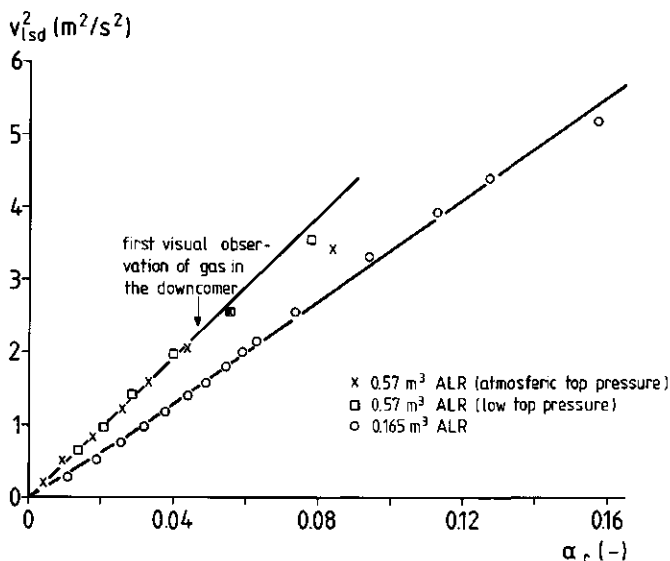


Fig. 3 The gas hold-up in the riser as a function of the square liquid velocity in the downcomer

the graph it appears that the friction coefficient is independent of the liquid velocity and of changes in gas hold-up. Only for the larger ALR, under atmospheric conditions, does a deviation from the straight line occur at large gas injection rates. The deviation coincides with visual observations of air entrainment into the downcomer which is a result of incomplete deaeration at the top of the ALR. In the vacuum the flow at the top was deaerated completely. For the smaller ALR, eqn(14) holds and no significant amount of air was entrained into the downcomer. It can be concluded that the total friction in an ALR can be derived from simple one-phase flow calculations based on known data for the friction factor.

A model evaluation is shown in figure 4 together with the experimental results of the 0.165 m³ pilot-plant ALR for the liquid velocity in the downcomer as well as the gas hold-up in the riser. For low gas input rates the liquid velocities and the gas hold-ups are very sensitive to changes in the gas input rate. For high input rates, however, only a minor increment of

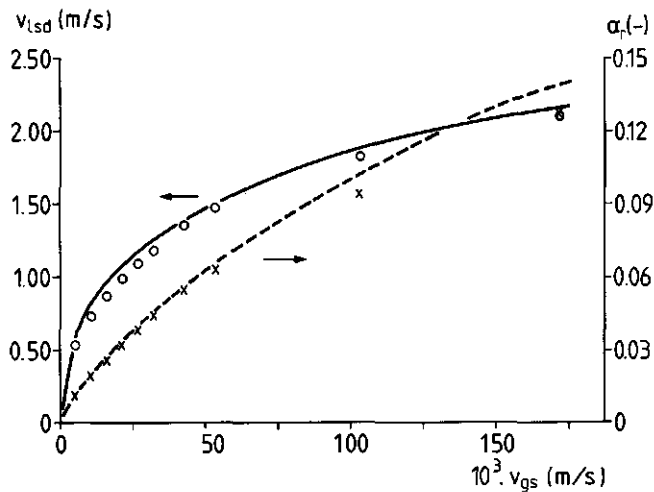


Fig. 4 The liquid velocity in the downcomer and the gas hold-up in the riser as a function of the superficial gas-velocity in the riser (0.165 m^3 , o,x: experimental; —, ---: model predictions)

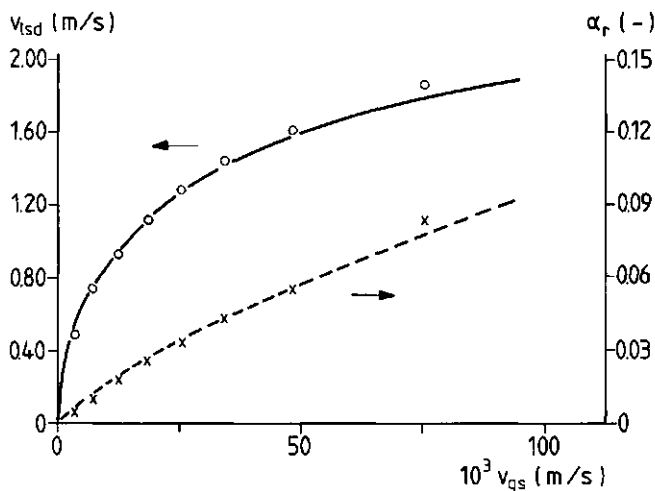


Fig. 5 The liquid velocity in the downcomer and the gas hold-up in the riser as a function of the superficial gas-velocity in the riser (0.6 m^3 , atmospheric conditions, o,x: experimental; —, ---: model predictions)

liquid velocity or gas hold-up is observed when the gas velocity is increased. The model gives an adequate prediction of the flow behaviour in the ALR with an accuracy of better than 10%.

The liquid velocity in the downflow region of the 0.6 m^3 ALR and the riser

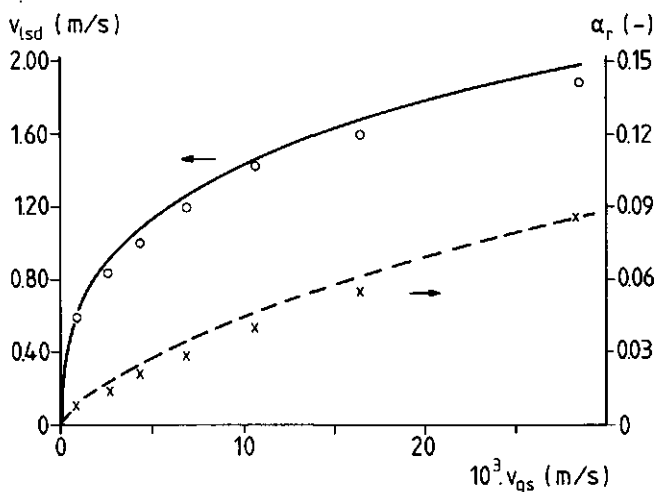


Fig. 6 The liquid velocity in the downcomer and the gas hold-up in the riser as a function of the superficial gas-velocity in the riser (0.6 m^3 , low top pressure, o, x: experimental; —, ---: model predictions)

gas hold up are presented in figures 5 and 6 for both the atmospheric and the low-top pressure ("vacuum") situation. For the latter, the pressure ratio between the top and the bottom of the reactor is altered by a factor 30 for a low gas input rate and by a factor 10 for high input rates. Thus a scale-up factor of 10 to 30 times was achieved, simulating a tower-loop fermentor of 100-300 m high. For atmospheric condition and large gas injection rates, the gas-hold up in the downcomer could not be measured directly because there was no manometer connected to the downcomer. Therefore the mean gas hold up in the downcomer was derived from figure 3; for large gas velocities and in the steady state situation (liquid velocity remains constant) the deviation from the straight line is a direct measure of the mean gas hold-up in the downcomer. The resulting gas fraction in the riser will increase because the downcomer gas hold-up counterbalances the liquid velocity. In the steady state the increment in the riser will be equal to the mean gas fraction in the downcomer. When the reactor was operated at liquid velocities of 1.61 m/s and 1.86 m/s in the atmospheric case, mean downcomer gas hold-ups of 0.1% and 1.5% respectively were generated. The corresponding rates of carry over were approximately 1% and 8.5% of the riser gas flow. Again, the model fits the experiments (accurate to within 5%) for both cases, even at high gas flow rates (See the relevant points in figure 5).

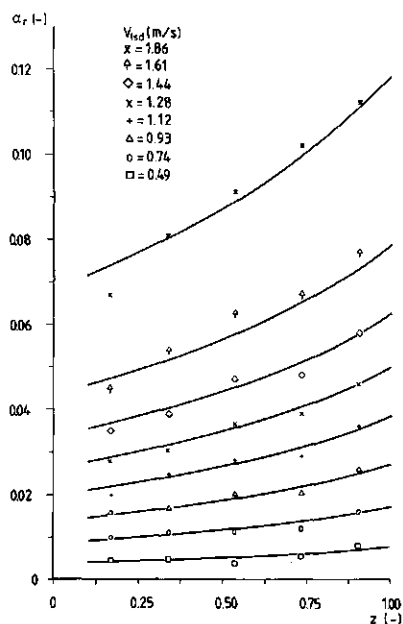


Fig. 7 Local gas hold-up in the 0.6 m³ ALR (atmospheric top pressure). Experiments compared with model calculations

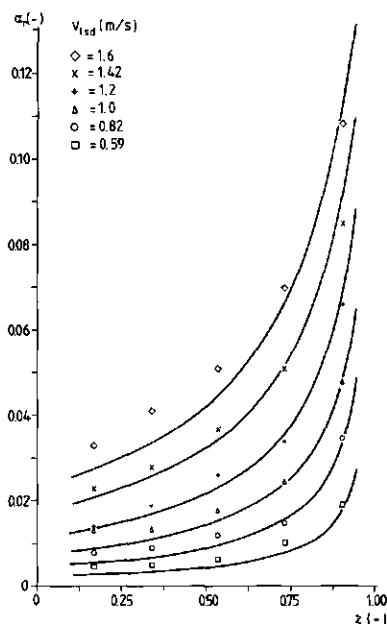


Fig. 8 Local gas hold-up in the 0.6 m³ ALR (low top pressure). Experiments compared with model calculations

The results of model simulations and experiments are shown in figures 7 and 8 for the local gas hold-up in the 0.6 m³ ALR at atmospheric and low top pressure. In this reactor the effect of bubble expansion can be demonstrated fairly well when the ALR is operated under vacuum. The validity of the model and its assumptions, in particular the assumption that there is no mutual interaction of the bubbles, is evident from these graphs. Figure 8 demonstrates the high expansion rate, in particular for the last part of the riser i.e. between $z=0.75$ and $z=1.0$. This phenomenon is very important for the hydrodynamic stability of large deep-shaft reactors [9,10], where gas is injected at elevated locations in the downflow region. Merchuk and Stein [2] observed the same trend for the gas fraction in the riser as that shown in figure 7, but also discovered that if the resistance in the downcomer was increased, a maximum for the gas fraction was observed as a result of increasing coalescence in the riser.

The good fit of the model to the experimental data shows that coalescence is not an important factor in this reactor. The bubbles ascend almost without collision and the growing hold up along the axis is dependent on the

increasing volume of the bubbles owing to the decrease in pressure, according to eqn(7). For the bubble sizes of interest, this effect prevails over the increment in bubble rise velocity associated with the expanded volume. An enlargement of the bubble diameter with 50% induces a positive contribution to the ascending velocity of only 20%. The effect of coalescence on the gas hold up was investigated by adding KCl to the 0.165 m³ reactor. A salt solution is a non coalescing medium and the bubble size is dependent on the geometry of the gas sparger. As

pointed out in a previous section, the bubble size generated at the gassparger is equal to the equilibrium bubble size in tap water. If there is no interaction between the bubbles, the mean bubble diameter is only influenced by the decrease in pressure.

The gas hold-up in the riser was recorded as a function of the ionic strength of the salt solution (in this case the ionic strength was equal to the molar concentration) with the results shown in figure 9. As can be seen there was no effect of ionic strength on the gas hold-up. This is in agreement with the results of Weiland [21] who found that the gas hold-up values for a 1.0 M sodium chloride solution were equal to those for tap-water. McManamey et al. [4] reported a similar result for sodium chloride and sodium sulphate solutions up to 1 M. This result confirms the assumption of a low collision frequency in the tap-water-air system. Lee and Ssali [17] and Miller [18] investigated bubble collision frequencies in a bubble column and found the frequency factor to be of the order 0.02-0.07 s⁻¹ for air-water systems, if bubble coalescence is considered to be a first order process in the number of bubbles. This means that for large gas input rates, e.g. $v_{gs} = 0.1$ m/s, 30% of the bubbles will coalesce into larger bubbles which will, according to what is mentioned above, have very little effect on the gas hold-up. Mishima and Ishi [19] pointed out that a transition from bubbly flow to slug flow occurred at a gas hold-up value of $\alpha = 0.3$ and that coalescence below this value was not serious, which also agrees with the

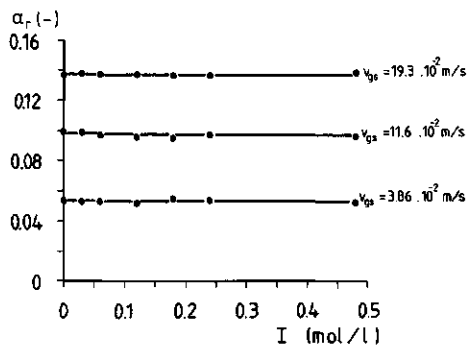


Fig. 9 Gas hold-up in the riser (0.165 m³ ALR) as a function of the ionic strength for different gas input rates

present results.

In figure 10 the predicted liquid velocities are compared with experimental data for three ALRs, the third one being a 0.004 m³ laboratory scale ALR with internal loop as described by Kiese et al. [20]. The model has also been tested on literature values of Weiland [21] and Merchuk and Stein [2]. Weiland's work concerned a 0.09 m³ ALR with external loop, an aerated altitude of 8.5 m and a ratio of flowed areas of $A_d/A_r=0.25$. The ALR of Merchuk and Stein had a volume of

0.2 m³, a height of 2 m and an area-ratio $A_d/A_r=1$. The friction coefficient of both reactors was calculated as is described in the previous section (table 1). As is shown in this plot the hydrodynamic model, in which the only parameters are the superficial gas velocity, the reactor dimensions and its geometry, fits reality fairly well for the five different cases.

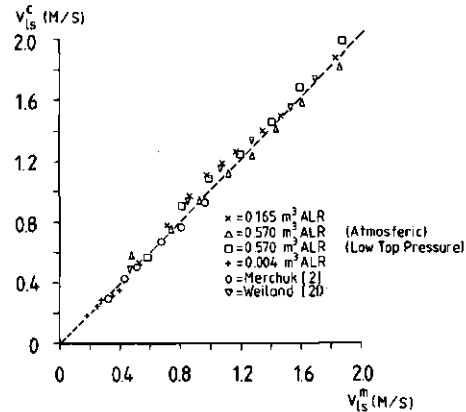


Fig. 10 Comparison of the experimental and calculated liquid velocities in airlift-loop reactors

CONCLUSIONS

Liquid velocities and gas hold-ups in an external loop airlift on different scales were modelled on the basis of a simple equation (eqn(2)). The model was adapted for non isobaric conditions and takes into account non-uniform flow profiles and gas hold-up distributions across the duct. The drift-flux model of Zuber and Findlay [8] was incorporated in the model. As the friction coefficient together with the reactor dimensions are input parameters, it is necessary to estimate this friction coefficient in the ALR. It has been shown that this can be obtained from simple one-phase flow calculations based on known friction factors, taken from data-books, of separate reactor parts. The model predicts liquid velocities and (local) gas hold-ups in an ALR to within 10%. The validity of the model arises from the controlled flow and the low bubble-collision frequency characteristic of tube reactors. The model can also be easily applied to an internal loop reactor.

ACKNOWLEDGEMENT

The authors are grateful to prof J.M. Smith, Laboratory of Physical Technology, Delft University of Technology, for the use of the pilot plant (0.6 m³) airlift-loop reactor.

REFERENCES

- [1] U. Onken and P. Weiland. Hydrodynamics and mass transfer in an airlift loop fermenter. *Eur. J. Appl. Microbiol. Biotechnol.*, 10 (1980) 31-40.
- [2] J.C. Merchuk and Y. Stein. Local hold up and liquid velocity in airlift reactors. *AIChE J.*, 27 (1981) 377-388.
- [3] D.G. Mercer. Flow characteristics of a pilot-scale airlift fermenter. *Biotechnol. & Bioeng.*, 23 (1981) 2421.
- [4] W.J. McManamey, D.A.J. Wase, S. Raymahasay and K. Thayamithy. The influence of gas inlet design on gas hold-up values for water and various solutions in a loop-type air-lift fermenter. *J. Chem. Technol. Biotechnol.*, 34B (1984) 151-164.
- [5] R.A. Bello, C.W. Robinson and M. Moo-Young. Gas hold up and overall volumetric oxygen transfer coefficient in airlift contactors *Biotechnol. & Bioeng.*, 27 (1985) 369-381.
- [6] N.N. Clark and R.L. Flemmer. Predicting the hold up in two-phase bubble upflow and downflow using the Zuber and Findlay drift-flux model. *AIChE J.*, 31 (1985) 500-503.
- [7] R.T. Hatch. Experimental and theoretical studies of oxygen transfer in the airlift fermentor, Thesis, M.I.T., Cambridge, 1973.
- [8] N. Zuber and J.A. Findlay. Average volumetric concentration in two-phase flow systems. *J. Heat Transfer*, Nov. (1965) 453-468.
- [9] R.G.J.M. van der Lans. Hydrodynamics of a bubble column loop reactor, Dissertation, Delft University of Technology, Delft, 1985.
- [10] H. Kubota, Y. Hosono and K. Fujie. Characteristic evaluations of ICI air-lift type deep shaft aerator. *J. Chem. Eng. Jap.*, 11 (1978) 319-325.
- [11] A.G. Jones. Liquid circulation in a draft-tube bubble column. *Chem. Eng. Sci.*, 40 (1985) 449-462.
- [12] J.J. Heynen and K. van 't Riet. Mass transfer, mixing and heat transfer phenomena in low viscous bubble column reactors. *Proc. 4th Eur. Conf. Mixing, Noordwijkerhout*, 1982.
- [13] G.B. Wallis. *One dimensional two phase flow*, McGraw-Hill, New York, 1969.
- [14] T. Menzel, H.J. Kantorek, K. Franz, R. Buchholz and U. Onken. Zur strömungsstruktur in Airlift-Schlaufenreaktoren. *Chem. Ing. Tech.*, 57 (1985) 139-141.
- [15] A. Serizawa, I. Kataoka and I. Michiyoshi. Turbulence structure of air-water bubbly flow-II. Local properties. *Int. J. Multiphase Flow*, 2 (1975) 235-246.
- [16] H. Blenke. *Biochemical loop reactors*, VCH, Weinheim, 1985.
- [17] J.C. Lee and G.W.K. Suali. Bubble transport and coalescence in a vertical pipe, VDI, Berlin, 1973, S1-6.1 S1-6.6.
- [18] D.N. Miller. Interfacial area, bubble coalescence and mass transfer in bubble column reactors. *AIChE J.*, 29 (1983) 312-319.
- [19] K. Mishima and M. Ishii. Flow regime transition criteria for upward two-phase flow in vertical tubes. *Int. J. Heat Mass Transfer*, 27 (1984) 723-737.
- [20] S. Kiese, H.G. Ebner and U. Onken. A simple laboratory airlift fermentor. *Biotechnol. Letters*, 8 (1980) 345-350.
- [21] P. Weiland. Untersuchung eines Airliftreaktors mit Äußerem Umlauf im Hinblick auf seine Anwendung als Bioreaktor, Dissertation, University of Dortmund, Dortmund, 1978.

APPENDIX A

Standard "one-phase flow" equations were used to calculate the friction coefficients in specific parts of the ALR, i.e. both reactor tubes, the bends and diameter changes as it is proposed in eqn (20). A distinction was made between a rectangular 90° bend and a smooth 90° bend which has been used in the 0.165 m³ ALR at the bottom of the downcomer.

Diameter change ($A_2 > A_1$):

$$K_{f_{A_1 \rightarrow A_2}} = (A_2/A_1 - 1)^2 \quad (\text{A.1})$$

$$K_{f_{A_2 \rightarrow A_1}} = (1 - A_1/A_2) \cdot q \quad (\text{A.2})$$

In eqn (A.2) the constant q has a value of $q=0.45$ for a sudden change in diameter and a value of $q=0.16$ for the funnel used in the 0.165 m³ ALR.

Bends:

$$90^\circ \text{ rectangular} \quad K_{f_{\text{bend}}} = 1.3 \quad (\text{A.3})$$

$$90^\circ \text{ smooth} \quad K_{f_{\text{bend}}} = 0.163(D/R)^{3.5} + 0.131 \quad (\text{A.4})$$

In eqn (A.4) D is the diameter of the tube and R the radius of the bend.

pipe-flow:

$$K_{f_{r,d}} = 4C_f L/D \quad (\text{A.5})$$

In eqn (A.5), L is the length of the pipe section and D its diameter. C_f is the friction factor. Wallis [13] proposed the use of a constant friction factor for all conditions. In turbulent flow this value is: $C_f=0.005$.

The friction factor depends on the Reynolds number and the roughness of the pipe and taking this into account the above-mentioned value for C_f seems very acceptable. Tabel 1 gives the results for the calculated and experimental values of the friction coefficient in the specific parts of the ALR.

NOMENCLATURE

A	area	[m ²]
B	width	[m]
C	distribution parameter	[-]
D, d	diameter	[m]
K	friction coefficient	[-]
L	length	[m]
P, p	pressure	[Pa]
R	radius of the bend	[m]
g	gravitational constant	[m/s ²]
q	constant	[-]
v	velocity	[m/s]
z	coordinate	[m]

Greek symbols

α	gas hold up	[-]
α'	approximation of the gas hold-up	[-]
Δ	difference	[-]
ρ	density	[kg/m ³]
ϕ	flow	[m ³ /s]

Subscripts

b	bubble
d	downcomer
f	friction
g	gas
h	hydrostatic
l	liquid
m	mass, mixture
r	riser
s	slip, superficial
v	volumetric

CHAPTER THREE

ESTIMATION OF AXIAL DISPERSION IN INDIVIDUAL SECTIONS
OF AN AIRLIFT-LOOP REACTOR

P. Verlaan, A.M.M. van Eijs, J. Tramper and K. van 't Riet,
Department of Food Science, Food and Bioengineering Group,
Agricultural University,
De Dreyen 12, 6703 BC Wageningen, The Netherlands.

K.Ch.A.M. Luyben, Department of Biochemical Engineering,
Delft University of Technology,
Julianalaan 67, 2628 BC Delft.

ABSTRACT

Axial dispersion in the riser, downcomer and gas-disengagement section of an airlift-loop reactor (ALR) with external loop was estimated and expressed by the Bodenstein number. In contrast to existing methods, the new developed procedure yields reliable results for the individual sections. Values of $Bo = 30-40$ for the riser, $40-50$ for the downcomer and 10 for the gas-disengagement section show that, except for this last section, the flow behaves like plug flow with superimposed dispersion. Depending on the Bodenstein number, the pertinent ALR is fully mixed within 4-7 circulations. This complete mixing time is used as a characteristic time in the presented parameter-estimation method.

Submitted for publication.

INTRODUCTION

In biotechnological processes different types of bioreactors are presently used, e.g. the conventional stirred tank reactors, bubble columns and the more modern airlift-loop reactors. In an airlift-loop reactor (ALR), due to the high circulation flow rate, efficient mixing is combined with a controlled liquid flow. In such an ALR, axial dispersion has an influence on oxygen and other substrate profiles, effecting the kinetics of (immobilized) biocatalysts and thus the design of the ALR. Fields and Slater [1] for instance, investigated the influence of liquid mixing in an ALR on the respiration of micro-organisms and found that respiratory quotients are affected by the local mixing behaviour. For such reasons it is important to characterize liquid mixing in an ALR. Moreover, knowledge of the mixing behaviour in a bioreactor is required for adequate modelling of biotechnological processes.

Several investigators reported results on the characterization of axial dispersion in bubble columns [2-4]. However, in contrast to bubble columns there is a lack of knowledge on the mixing behaviour in ALRs, especially in the separate parts of these loop reactors, i.e. the up and downflow region and the gasdisengagement section. Weiland [5] and van der Lans [6] for instance, presented axial dispersion coefficients in an individual section of an ALR, viz. the riser [5] and the downcomer [6]. The mathematical method they applied to assess these values (moment analysis and Laplace transformed transfer functions) entailed serious problems due to the liquid circulation in the ALR [6]. From their results it can be derived that the liquid flow in these reactor sections behaves more or less like plug flow. The same authors also determined dispersion coefficients for the reactor as a whole. Pulse response techniques were applied to determine the overall dispersion parameters. Using this technique in an ALR with a plug flow character, the results were severely influenced by the "quality" of the initial Dirac pulse. Fields and Slater [7] who investigated axial dispersion in the head section of a laboratory scale ALR with internal loop (working volume: 0.019-0.037 m³), also distinguished the problems mentioned above. Hatch [8] used a method of moments for the estimation of axial dispersion coefficients in the upflow section of an 0.2 m³ ALR with internal loop, for both the liquid and gas phase. However, the author did not report on serious problems in determining liquid phase dispersion coefficients due to liquid circulation. Verlaan et

al. [9] characterized axial dispersion in a laboratory-scale ALR (working volume 0.004 m³) based on a pulse response technique and found a large scatter in their results. Warnecke et al. [10,11] considered axial dispersion and residence time distribution in a laboratory-scale liquid jet-loop reactor. The authors discriminated between sections of different mixing behaviour and developed a procedure to determine the main model parameters of the reactor as a whole and of the individual sections. However for a high degree of axial dispersion (small Bodenstein numbers) this method showed a considerable scatter. From these references it can be concluded that the initial tracer distribution and the circulating flow in an ALR impedes the use of existing parameter estimation methods, especially for individual sections of such a reactor.

In view of biological processes in which small characteristic times (time constants) are of importance, it is essential to investigate axial dispersion for the different sections of the ALR: riser, topsection (gasdisengagement section) and downcomer. In the present work the mixing performances of these three sections of a pilot plant ALR are presented. In contrast to the above-mentioned mathematical methods, the parameter estimation method we developed is not affected by the shape of the tracer nor by the circulation flow of the loop reactor. It will be shown that axial dispersion for the reactor as a whole can be calculated from the contributions of the individual sections.

THEORY

An axial dispersion model has been used to estimate the axial dispersion coefficient in our loop reactor. The model assumes plug flow with disturbances caused by molecular diffusion, small eddies, dead zones and the liquid-velocity profile (radial velocity gradients) lumped in an axial dispersion coefficient. A mass balance over a liquid volume part in the reactor neglecting radial concentration gradients, gives:

$$\partial \hat{c} / \partial \theta = 1/Bo \cdot \partial^2 \hat{c} / \partial x^2 - \partial \hat{c} / \partial x \quad (1)$$

In this equation, \hat{c} is the dimensionless concentration $(c-c_0)/(c_\infty-c_0)$, θ the dimensionless time t/t_C , x the dimensionless axial coordinate z/L and Bo the dimensionless mixing parameter (Bodenstein number):

$$Bo = (v.L)/D \quad (2)$$

where v is the liquid velocity [m/s], L the length of interest [m] and D the dispersion coefficient [m²/s]. The value of the Bodenstein number expresses the degree of axial mixing. If Bodenstein is equal to zero mixing is complete, whilst for very large Bodenstein numbers conditions approach plug flow.

The solution of eqn(1) for an initial Dirac pulse in the ALR, taking into account the circulating flow, is represented by [12]:

$$\hat{c} = \left(\frac{Bo}{4\pi\theta} \right)^{\frac{1}{2}} \cdot \sum_{x=1}^{\infty} \exp\left(\frac{-(x-\theta)^2 Bo}{4\theta} \right) \quad (3)$$

Fitting the model to an experimental response on an initial Dirac pulse yields the Bodenstein number for the reactor. For large Bo -numbers the time delay between the peaks of the response curve can be used as good approximation for the circulation time [12]. This pulse response technique has been commonly used in the literature [5-9]. However, since it is not possible to create an ideal Dirac pulse, an experimental error is already included when using this technique.

The Fourier transformed transfer function

When dispersion in an individual section of the reactor is considered the circulation flow severely impedes the use of existing estimation methods because the tail of a response is influenced by the sequential character of the response. From this it is clear that characterization of axial dispersion by the Bodenstein number in specific parts of an ALR requires a more sophisticated approach.

The dispersion characteristics of a given linear system, such as in one dimensional flow, are represented by the following convolution-product [13]:

$$z(\theta) = \int_0^{\infty} h(\theta) \cdot y(\theta - \tau) d\tau \quad (4)$$

This means that for an arbitrary input signal $y(t)$ the output signal $z(t)$ can be calculated when the transfer function $h(t)$ is known. In case of the

axial dispersion model, this transfer function is the response on an initial Dirac pulse and can be analytically derived from eqn(1).

When eqn(4) is transformed to the Laplace domain defined by:

$$H(p) = \int_0^{\infty} h(\theta) \cdot \exp(-p \cdot \theta) d\theta \quad (5)$$

the convolution becomes a mathematical product:

$$Z(p) = H(p) \cdot Y(p) \quad (6)$$

In this equation, $Z(p)$ and $Y(p)$ are the Laplace transformed output and input functions, respectively. $H(p)$ is the Laplace transformed transfer function and p the dimensionless Laplace operator. From eqn(5) the transfer function in the Fourier domain can be calculated (see the appendix) when the imaginary part, $i\omega$, of the Laplace operator is considered:

$$H(i\omega, x) = \text{Re}(H(i\omega)) + i \cdot \text{Im}(H(i\omega)) \quad (7)$$

Combination of eqns (6) and (7) yields the Fourier transformed output function, calculated from the (experimental) input function.

Time domain analysis

As pointed out by Fahim and Wakao [14] time domain analysis is in favour of other existing parameter estimation methods; with this method the most reliable values are obtained. Therefore the Fourier transformed output function calculated from eqn(6), is transferred by an inverse Fourier transformation to the time domain, defined by:

$$h(\theta) = \int_{-\infty}^{\infty} H(p) \cdot \exp(p \cdot \theta) dp \quad (8)$$

The calculated output signal is fitted to the experimental output signal according to the least square criterium. This method yields a

reliable parameter estimation for the ALR. In contrast to the existing methods, the input function comprises the complete mixing time, i.e. 4-7 circulations. The method is represented schematically in Figure 1.

In practice the response on a Dirac-like signal was used as input function. However, it should be stressed that any type of continuous function can be used as input function.

When the Bodenstein numbers of individual sections of the ALR, i.e. the riser, topsection and downcomer, have been determined it is possible

to calculate, from these values, the Bodenstein number for the reactor as a whole. As shown by Aris [15] and Bisschof [16] the sum of the variances of a Dirac-response of the specific parts is equal to the variance of the complete reactor:

$$\sigma_r^2 + \sigma_t^2 + \sigma_d^2 = \sigma_s^2 \quad (9)$$

For large Bodenstein numbers ($Bo > 20$) the variance of a system can be approximated by [12]:

$$\sigma^2 = 2 \cdot t^2 / Bo \quad (10)$$

In this equation, t is the mean residence time of the pertinent reactor part. Substitution of eqn (10) in eqn (9) yields:

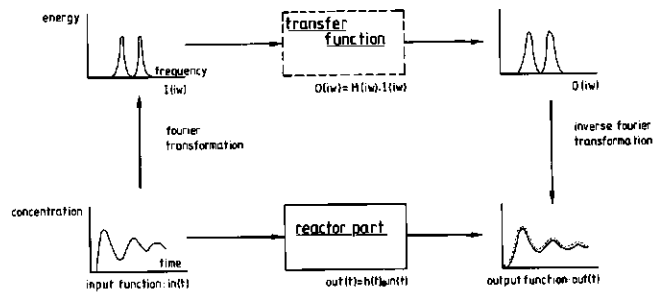


Fig. 1 A schematic representation of the estimation method

$$t_s^2/Bo_s = t_r^2/Bo_r + t_t^2/Bo_t + t_d^2/Bo_d \quad (11)$$

From eqn (11) the Bodenstein number for the ALR is calculated, provided that the mean residence time in the pertinent sections are known and $Bo > 20$ in these sections.

Application of a digital computer for the Fourier transformed transfer function

Non-periodical functions like the damped sinoidal input function we use, can be transformed to the Fourier domain. In this case the function is made periodic by using the mixing time as a period (characteristic time). As a result, the complete response on a Dirac-like pulse is considered as one period.

The Fourier transformation (CFT) gives a continuous spectrum in the frequency domain. A digital computer cannot perform the integration indicated by eqn (5). Thus the CFT has to be approximated at discrete frequencies by a method known as the discrete Fourier transformation (DFT). The DFT is represented mathematically as:

$$H\left(\frac{n}{N \cdot dt}\right) = \sum_{k=0}^{N-1} h(k \cdot dt) \cdot \exp(-i \cdot 2\pi n \frac{k}{N}) \quad (n=0,1,\dots,N-1) \quad (12)$$

The mathematical expression of the inverse DFT is:

$$h(k \cdot dt) = \frac{1}{N} \sum_{n=0}^{N-1} H\left(\frac{n}{N \cdot dt}\right) \cdot \exp(i \cdot 2\pi n \frac{k}{N}) \quad (k=0,1,\dots,N-1) \quad (13)$$

In the equations above, dt and N are the time intervals between two measured points and the total number of points, respectively. The frequency spectrum of the CFT has now been replaced by a number (n) of frequencies:

$$f = n/(N \cdot dt) \quad (14)$$

This means that the time interval between two points, dt , has to be chosen carefully in order not to lose essential information. A condition for this is that the function to be transferred must be sampled at a rate greater than twice the highest frequency component of interest in the function.

The DFT we applied was a special variant namely the Fast-Fourier transformation (FFT) [17]. The FFT provides an efficient means of numerically approximating analytical or continuous Fourier transforms. When a FFT or a DFT is used one has to take into account that in fact the product of three functions are transferred to the Fourier domain: the continuous function, the discretisation function and in the case of a FFT, the boundary function.

MATERIALS AND METHODS

The pilot-plant ALR used in the experiments has a working volume of 0.165 m^3 and a height of 3.23 m. Figure 2 gives a schematic representation of the reactor that has been described in more detail elsewhere [18]. The liquid level in the topsection was kept at 0.13 m above the bottom of the cistern in the absence of gas in order to maintain about the same liquid velocity in the riser and in the topsection. Temperature was maintained at a constant value of 30°C . The gas sparger produced bubbles with the same diameter as the equilibrium diameter of air bubbles in water [19].

Acid and base were used as tracers because detection of these tracers by pH-electrodes was not disturbed by the presence of air bubbles. This in contrast to a conductivity measurement system by which we found it impossible to carry out these experiments

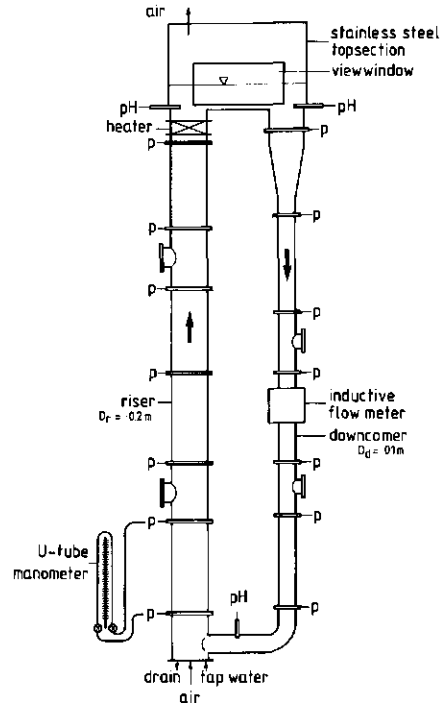
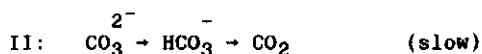
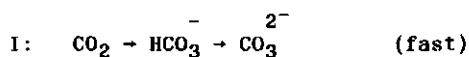


Fig. 2 The experimental set up

in a two-phase flow, though several investigators reported results on axial dispersion in two phase flows based on conductivity measurements [2,6,7]. The advantage of the conductivity system is that responses are linear with the amount of tracer which is not the case for the pH-method. However, a more important advantage of the pH-method is that the total amount of tracer which is added to the ALR is two orders of magnitude below that in the case of conductivity measurements. In case of pulse response measurements this is a very important advantage because the initial Dirac pulse can thus be approximated very close.

The pH-electrodes used, have a low membrane resistance ($R_m \approx 40 \text{ M}\Omega$) and were provided with short connecting cables ($\pm 1 \text{ m}$) to the pH-meters in order to keep the time of response as low as possible. This response time of the measuring system was: $\tau = 0.1 (\pm 0.05) \text{ s}$.

Einsele [20] pointed out that only restricted pH-trajectories are suitable for measurement purposes because of carbondioxide equilibrium reactions:



Another condition for accurate pulse response measurements with acid and base tracers is that a small amount of tracer causes a large change in pH. Therefore, as a result of the above-mentioned conditions, a pH-trajectory of $3.5 < \text{pH} < 6.2$ was selected as a suitable trajectory for the experiments.

The ALR contained a 50 mM potassium-chloride solution in tap water in order to create an adequate salt buffer for the pH-measurements. It was experimentally shown that a salt solution of potassium-chloride with molar concentrations up to 0.17 M does not show a significant reduction of coalescence [21]. Moreover, potassium chloride was chosen as a salt buffer since it modifies the properties of the air-water mixture less than other salts [21]. The amount of tracer (about $1 \text{ cm}^3 \text{ HCl}$) was injected within 0.1 s. The response of both electrodes was recorded on line by a micro-computer with time intervals of 0.15 s until the response of the pulse was completely damped. The liquid velocity in the downcomer was recorded simultaneously by an inductive flowmeter.

A polynomial was fitted to the titration curve and used to transfer the

measured response (pH) of the system into a linear response curve (ion concentrations). Each experiment was carried out in triplo. The first peak of a response was not taken into account because of the incomplete radial distribution of the pulse across the duct during the first circulation. The trajectory of $4.3 < \text{pH} < 5.5$ proved to be a stable trajectory which confirms the results of Einsele [20]. However, the first two titrations did not yield reproducible results, but succeeding titrations were stable; a titration could be performed 10-20 times without a significant change in the curve. We have no plausible explanation for this phenomenon. Consequently, the first two titrations were not used for the experiments.

Figure 3 shows a titration curve for a 50 mM potassium chloride solution together with the curve of the polynome regression. The tracers were injected at different locations in the ALR dependent on which reactor part was subject to investigation: at the bottom of the riser or at the top of the downcomer. In figure 2 these locations are indicated.

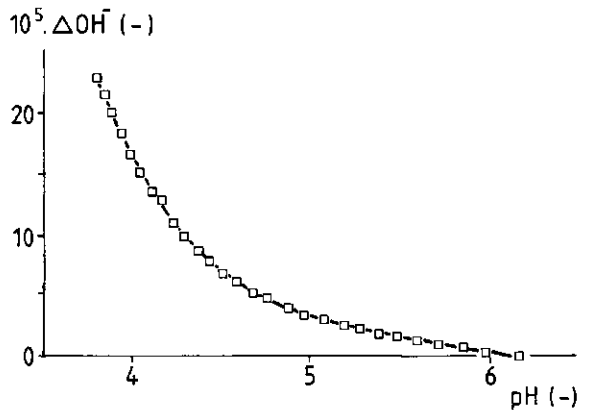


Fig. 3 Titration curve of a 50 mM potassium-chloride solution fitted by a polynome (□ experimental, — polynome fit).

RESULTS AND DISCUSSION

The model was tested by means of a theoretical input and output curve, both generated by eqn (3), the solution of the axial dispersion model. The Bodenstein value was fixed on $Bo = 60$ which is a representative value for this system. The response was simulated for an arbitrary dimensionless retention time of $\hat{t} = 0.25$. The simulated signal was exactly treated as the experimental response, as shown schematically in figure 1. The sample frequency numbered $f = 0.15 \text{ s}^{-1}$. The results are shown in figure 4 where both

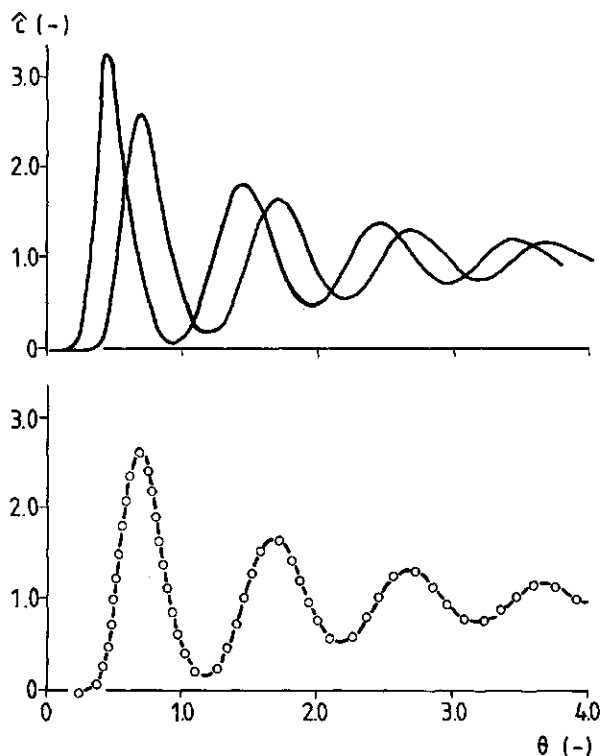


Fig. 4 (A) Simulated input and output curve for $Bo = 60$ and (B) a comparison of the calculated output curve (o) with the simulated output curve (—)

the input and output signals are shown as well as the calculated output signal. The latter signal is fitted to the actual output signal which is also demonstrated in figure 4. The sensitivity to changes in the Bodenstein number is clearly displayed by figure 5. Here the relative deviation between the actual and the calculated curve is plotted as a function of Bodenstein. As can be seen, according to the optimal value of Bodenstein, the estimation method is less sensitive at high Bodenstein numbers.

An experimental example of such a

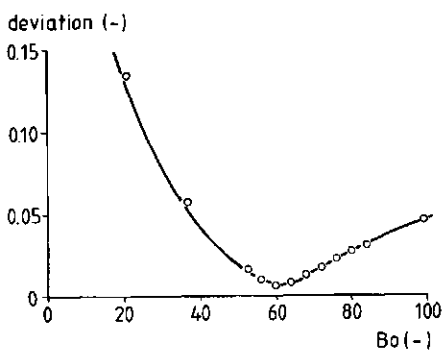


Fig. 5 Sensitivity of the Bodenstein number in the estimation procedure shown in figure 3

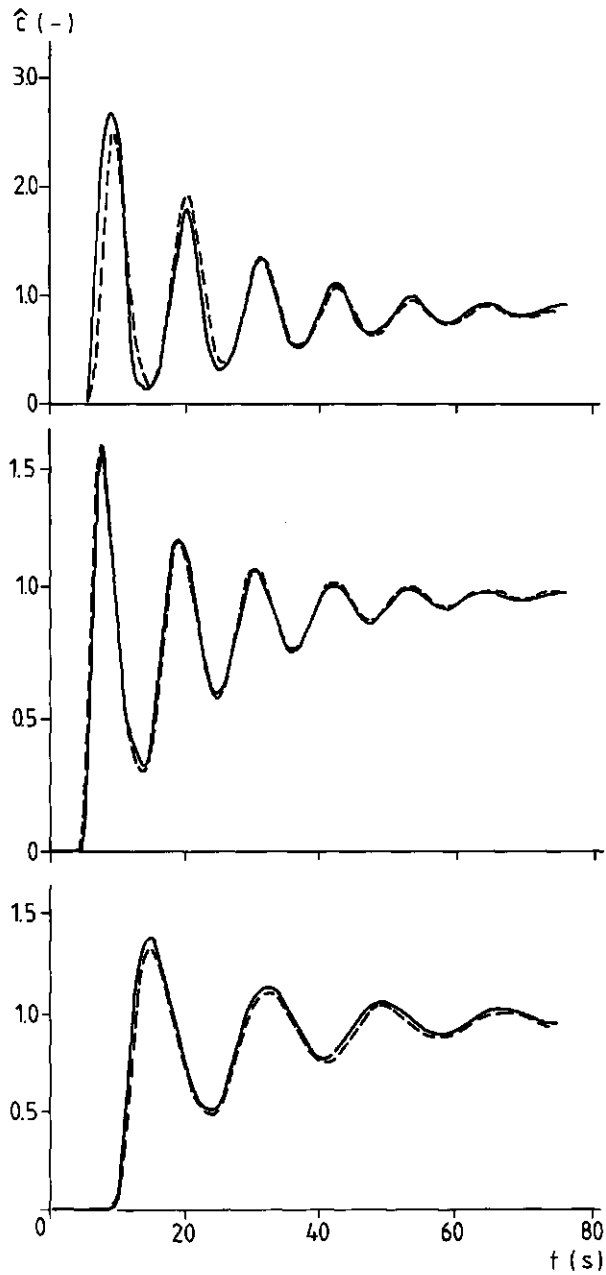


Fig. 6 Comparison of a typical output response curve (—) compared with the estimated curve (---) for the riser (A), the topsection (B) and the downcomer (C).

response on an initial signal at the outlet of each section of the ALR i.e. the riser, downcomer and topsection is represented by figure 6. In this figure the calculated output signals are also shown, featuring the estimated Bodenstein number. The calculated signals approximate the experimental functions very close for the complete mixing time, therefore an accurate estimation of the Bodenstein number could be made for each section.

Figure 7 shows the Bodenstein numbers for the various reactor sections and the calculated and experimental Bodenstein numbers for the reactor as a whole as a function of the superficial gas velocity. The latter Bodenstein

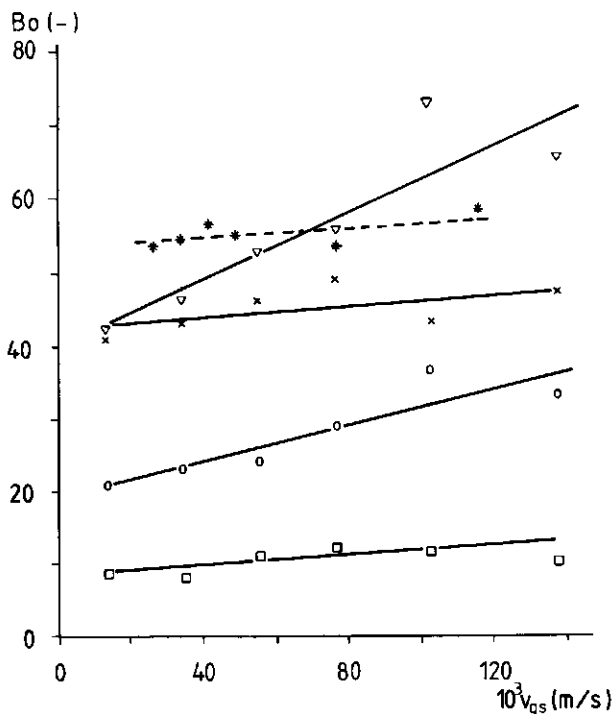


Fig. 7 The Bodenstein number as a function of the superficial gas velocity. (*) ALR experimental, (∇) ALR calculated (eq(11)), (x) downcomer, (o) riser, (\square) topsection.

numbers were obtained by the pulse-response method, based on equation (3). The downcomer shows the highest Bodenstein number due to the single phase flow in this part. The riser has a somewhat better mixing performance as a result of the presence of the gas phase which induces flow patterns on a

small scale. Axial dispersion is most significant in the topsection where disengagement of bubbles and reversion of the flow-direction from the riser to the downcomer create considerable turbulence resulting in a low Bodenstein number.

Longitudinal mixing can also be represented by the tanks in series model provided that $Bo > 8$ [22]:

$$n_{eq} \approx 1 + Bo/2 \quad (17)$$

where n_{eq} represents the number of CSTR's in cascade, giving an equivalent residence time distribution to plug flow with dispersion model for the pertinent Bodenstein parameter. This means that the riser, downcomer and top-

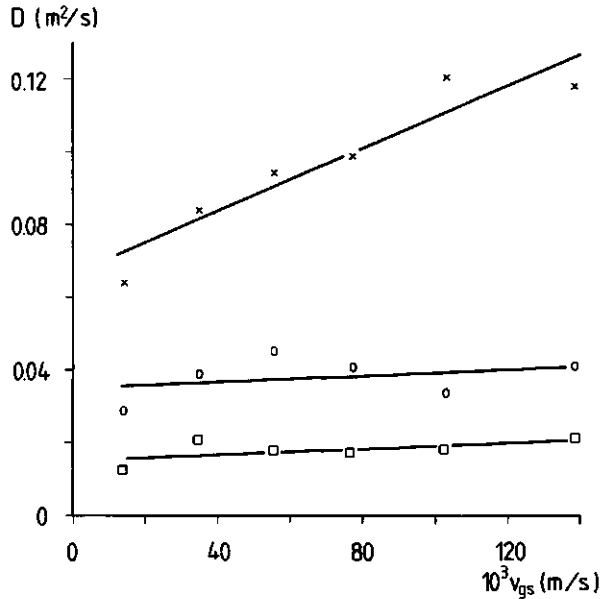


Fig. 8 The dispersion coefficient as a function of the superficial gasvelocity. (x) downcomer, (o) riser, (\square) topsection.

section can be replaced, according to the results in figure 7, by 15, 25 and

4-6 STRs in series, respectively. It is concluded therefore that the plugflow with dispersion model in the ALR is suitable for the riser and the downcomer but not for the topsection. The mixing performance of the latter section obviously lies in between ideally mixed and plug flow.

Figure 8 shows the dispersion coefficients of the three sections, calculated using eqn(2). The downcomer exhibits a maximum of absolute dispersion due to the relative high liquid velocity thus a high turbulence intensity. A smaller dispersion coefficient was obtained in the two phase-riser where the liquid velocity is four times less than in the downcomer. The presence of air bubbles apparently has a minor influence. This result demonstrates that turbulence induced by the liquid velocity forms the main contribution to dispersion in the reactor tubes. The results of the topsection are not in contradiction with this assumption. When the ALR is completely deaerated, the liquid level in this part of the ALR is such that the cross sectional area in the topsection is equal to that of the riser. When the ALR is in operation, the gas phase causes a rise of the liquid level in the topsection which reduces the local liquid velocity. For high gas velocities this effect will be more significant. As a result of this phenomenon turbulence induced by the liquid flow will decrease while turbulence induced by gas disengagement will be enhanced. Apparently these effects counterbalance dispersion in the topsection, as the dispersion coefficient in this section remains about constant through the range of gas flows that were usual.

Equation (3) predicts that response around the extreme values in figure 3 is not symmetrical. For high Bodenstein numbers, however, the mean circulation time, t_c , could yet be obtained with negligible error from the distance between the peaks. In figure 9 the liquid velocity in the downcomer calculated from the mean circulation time thus obtained, the cross sectional area of the downcomer and the reactor liquid volume is com-

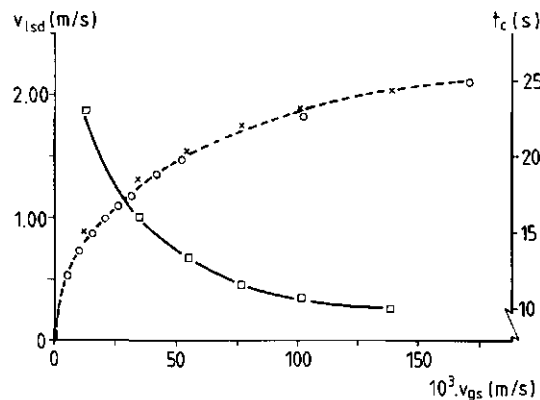


Fig. 9 The measured (o) and calculated (x) superficial liquid velocity in the downcomer and the circulation time (□) as a function of the superficial gas velocity.

pared with the measured liquid velocity in the downcomer at various gas-velocities [18]. As is shown in this figure, both curves agree well.

The mixing behaviour of the ALR can also be classified according to the dimensionless mixing time (circulation number), \hat{t}_m , required to achieve a certain degree of mixing throughout the reactor. The degree of mixing is described in terms of the homogeneity h defined as:

$$h = \frac{C - C_{end}}{C_{end}} \quad (17)$$

The homogeneity h can be obtained from the envelope of the extremi of the response curve (eq.(3)). When the dimensionless mixing time, \hat{t}_m , for a homogeneity $h=0.05$ is correlated with the Bodenstein number, the following emperic equation results:

$$\hat{t}_m = 0.093 * Bo \quad (18)$$

Equation (18) agrees with the results of Blenke [22] and with the results of Murakami et al. [23] who derived a general expression for the dimensionless mixing time, \hat{t}_m , in relation to the Bodenstein number for loop reactors. The real mixing time, t_m , is calculated from the dimensionless mixing time by:

$$t_m = t_c * \hat{t}_m \quad (19)$$

From equation (18) it is derived that, depending on the Bodenstein number, it takes about 4-7 circulations for the ALR to be mixed ($h < 0.05$). Accordingly, from eq (19) it follows that the mixing time, t_m , varies from 93 to 61 seconds, respectively.

The experimental results are in agreement with the values found by Hatch [8] who investigated axial dispersion in the draft tube of an internal loop ALR and reported values of $Bo=30-60$ for a gas velocity in the range of $0.05 < v_{gs} < 0.3$ m/s. Weiland [5] reported values of $Bo=60-80$ for the upflow region in an external loop ALR ($0.005 < v_{gs} < 0.05$ m/s). These values represent a fully established flow in a tall ALR (8.5 m) and are somewhat higher than the values obtained in our study which represent the riser and its lower appendages (90° bend plus a diameter change). Van der Lans [6] reported values of $Bo=70-80$ for an ALR as a whole ($0.005 < v_{gs} < 0.03$ m/s). The ALR

used, consisted of tall columns (10.5 m) with diameters of 0.225 m (riser) and 0.1 m (downcomer). Because of its length the flow was better established than in the present one, resulting in higher Bodenstein values.

CONCLUSIONS

The newly developed parameter estimation procedure has proven to be reliable for determining the mixing behaviour in individual sections of an ALR. From the results it can be concluded that in an ALR the liquid flow behaves like plug flow with superimposed dispersion. This is expressed by the Bodenstein number which reaches values of $Bo=40-60$ for the reactor as a whole, $Bo=30-40$ for the riser, $Bo=40-50$ for the downcomer and $Bo=10$ for the topsection. From the latter result it follows that it is not reasonable to assume plug flow in this last section. According to the mixing performance and the tank in series model the topsection can be described by 4-6 tanks in series.

ACKNOWLEDGEMENT

The authors wish to thank Dr. H.N.J. Poullisse for his helpful discussions during the preparation of the manuscript.

REFERENCES

- [1] P.R. Fields and N.K.H. Slater. The influence of fluid mixing upon respiratory patterns for extended growth of a methylotroph in an air-lift fermentor. *Biotechnol. & Bioengng.* 26 (1984) 719-726.
- [2] R.W. Field and J.F. Davidson. Axial dispersion in bubble columns. *Trans. I. Chem. Eng.* 58 (1980) 228-235.
- [3] K.H. Mangartz and Th. Pilhofer. Interpretation of mass transfer measurements in bubble columns considering dispersion of both phases. *Chem. Engng. Sci.* 36 (1981) 1069-1077.
- [4] J.B. Joshi and Y.T. Shah. Hydrodynamic and mixing models for bubble column reactors. *Chem. Engng. Commun.* 11 (1981) 165-199.
- [5] P. Weiland. Untersuchung eines Airliftreaktors mit Außerem Umlauf im Hinblick auf seine Anwendung als Bioreaktor, Thesis, University of Dortmund, Dortmund GDR 1978.
- [6] R.G.J.M. van der Lans. Hydrodynamics of a bubble column loop reactor, Thesis, Delft University of Technology, Delft the Netherlands 1986.
- [7] P.R. Fields and N.K.H. Slater. Tracer dispersion in a laboratory air-lift reactor. *Chem. Engng. Sci.* 38 (1983) 647-653.
- [8] R.T. Hatch. Experimental and theoretical studies of oxygen transfer in the airlift fermentor. Thesis, M.I.T., Cambridge, Massachusetts 1973.

- [9] P. Verlaan, A.C. Hulst, J. Tramper, K. van 't Riet and K.Ch.A.M. Luyben. Immobilization of plant cells and some aspects of the application in an airlift fermentor. Proc. 3rd Europ. Congress on Biotechnol., vol. 1, München, GDR, 10-14 sept. 1984, 151-157.
- [10] H.-J. Warnecke, J. Prüss and H. Langemann. On a mathematical model for loop reactors - I. Residence time distribution, moments and eigenvalues. Chem. Engng. Sci. 40 (1985) 2321-2326.
- [11] H.-J. Warnecke, J. Prüss, L. Leber and H. Langemann. On a mathematical model for loop reactors - II. Estimation of parameters. Chem. Engng. Sci. 40 (1985) 2327-2331.
- [12] O. Levenspiel. Chemical reaction engineering. John Wiley & Sons Inc., New York 1972.
- [13] J.S. Bendat and A.G. Piersol. Random data: analysis and measurements procedures, Wiley-Interscience, New York 1971.
- [14] M.A. Fahim and N. Wakao. Parameter estimation from tracer response measurements. Chem. Engng. J. 25 (1982) 1-8.
- [15] R. Aris. Notes on the diffusion-type model for longitudinal mixing in flow. Chem. Engng. Sci. 9 (1959) 266-267.
- [16] K.B. Bisschof. Notes on the diffusion-type model for longitudinal mixing in flow. Chem. Engng. Sci. 12 (1960) 69-70.
- [17] Subroutine FFT, version 1.2, Programmers Reference Manual, Laboratory Subroutine Package, DEC, Marlboro, Massachusetts 1982.
- [18] P. Verlaan, J. Tramper, K. van 't Riet and K.Ch.A.M. Luyben. A Hydrodynamic model for an airlift-loop bioreactor with external loop. Chem. Engng. J., 33 (1986) B43-B53 (Chapter two of this thesis).
- [19] J.J. Heynen and K. van 't Riet. Mass transfer, mixing and heat transfer phenomena in low viscous bubble column reactors. Proc. 4th Europ. Conf. on Mixing, 1982 Noordwijkerhout, The Netherlands.
- [20] A. Einsele. Charakterisierung von Bioreaktoren durch Mischzeiten. Chem. Rundschau, 29 (1978) 53-55.
- [21] R.R. Lessard and S.A.Z. Zieminski. Bubble coalescence and gas transfer in aqueous electrolytic solutions. Ind. Eng. Chem. Fundam. 10 (1971) 260-269.
- [22] H. Blenke. Loop reactors, Adv. Biochem. Eng. 13 (1979) 121-214.
- [23] Y. Murakami, T. Hirose, S. Ono, and T. Nishyima. Mixing properties in loop reactors. J. Chem. Engng. Japan., 15 (1982) 121-125.

APPENDIX

The Fourier transformed transfer function

Laplace transformation of equation (1) by means of equation (5) yields:

$$p.C(x,p) - C(x,0) + \frac{dC(x,p)}{dx} - \frac{1}{Bo} \frac{d^2C(x,p)}{dx^2} = 0 \quad (A.1)$$

where p is the dimensionless Laplace variable. The solution of equation (A.1) is expressed by:

$$C(x,p) = A(p) \cdot \exp(a(p) \cdot x) + B(p) \cdot \exp(b(p) \cdot x) \quad (A.2)$$

where the coefficients $a(p)$ and $b(p)$ are defined by:

$$a(p) = \frac{1}{2}Bo + \frac{1}{2}(Bo^2 + 4Bo.p)^{\frac{1}{2}} \quad (A.3.1)$$

$$b(p) = \frac{1}{2}Bo - \frac{1}{2}(Bo^2 + 4Bo.p)^{\frac{1}{2}} \quad (A.3.2)$$

When axial dispersion in an infinite tube is considered, the following boundary conditions for equation (A.1) are valid:

$$C(0, p) = C_i \quad (A.4.1)$$

$$\lim_{x \rightarrow \infty} C(x, p) = 0 \quad (A.4.2)$$

where c_i is the amount of tracer injected at the beginning of the tube. The complex coefficients $a(p)$ and $b(p)$ can be divided into a real and an imaginary part. Together with the conditions for the present system: $Bo > 0$ and $p > 0$ it is derived that:

$$\text{Re } a(p) > 0 \quad (A.5.1)$$

$$\text{Re } b(p) > 0 \quad (A.5.2)$$

From equation (A.5) and the condition (A.4.2) it is concluded that the solution (A.2) is valid if $A(p) = 0$. As a result the final solution of the Laplace transformed axial dispersion equation (eq(1)) is:

$$C(x, p) = C_i \cdot \exp(b(p) \cdot x) \quad (A.6)$$

where C_i and C are the input and output functions of a given system, respectively. Therefore the Laplace transformed transfer function is defined by:

$$F(p) = \frac{C}{C_i} = \exp(b(p) \cdot x) \quad (A.7)$$

By substituting $p = i\omega \cdot \tau$ we obtain the Fourier transform. Together with the condition: $x = 1$, equation (A.7) gives in the Fourier domain the following transfer function:

$$H(i\omega) = \exp\left\{\frac{1}{2}Bo(1 - (1 + 4i\tau\omega/Bo)^{\frac{1}{2}})\right\} \quad (A.8)$$

In order to divide equation (A.8) into a real and imaginary part the following complex parameter is introduced:

$$z = |z| \cdot (\cos\phi + i \cdot \sin\phi) \quad (\text{A.9})$$

with:

$$|z| = (1 + (4 \cdot \tau \cdot \omega / B_0)^2)^{1/2} \quad (\text{A.10.1})$$

$$\phi = \arctg(4 \cdot \tau \cdot \omega / B_0) \quad (\text{A.10.2})$$

As a result, equation (A.8) can be formulated as:

$$H(i\omega) = \text{Re}(i\omega) + i \cdot \text{Im}(i\omega) \quad (\text{A.11})$$

with the following specifications:

$$\text{Re}(i\omega) = \exp(d) \cdot \cos(f \cdot \sin(g)) \quad (\text{A.12.1})$$

$$\text{Im}(i\omega) = -\exp(d) \cdot \sin(f \cdot \sin(g)) \quad (\text{A.12.2})$$

$$d = B_0/2 - f \cdot \cos(g) \quad (\text{A.12.3})$$

$$f = B_0/2 \cdot z^{1/2} \quad (\text{A.12.4})$$

$$g = \frac{1}{2} \cdot \phi \quad (\text{A.13.5})$$

NOMENCLATURE

A	complex integration parameter	[-]
B	complex integration parameter	[-]
D	dispersion coefficient	[m ² /s]
F	Laplace transformed transfer function	
H	Fourier transformed transfer function	
L	length	[m]
N	summation number	[-]
Y	input function	
Z	output function	
a	complex integration parameter	[-]
b	complex integration parameter	[-]
c	concentration	[kg/m ³]
\hat{c}	dimensionless concentration	[-]
d	constant	[-]
f	constant	[-]
g	constant	[-]

h	transfer function in time domain	
h	homogeneity	[-]
i	$i^2 = -1$	[-]
k	summation index	[-]
n	number	[-]
p	Laplace variable	[-]
t	time	[s]
x	coordinate	[-]
y	input function in time domain	
z	coordinate	[m]
z	complex variable	[-]
z	output function in time domain	

Subscripts

r	riser
t	topsection
d	downcomer
s	system (i.e. ALR)
i	initial
m	mixing
c	circulation
eq	equal

Greek symbols

ϕ	angle	[rad]
θ	time	[-]
τ	characteristic time	[s]
$\hat{\tau}$	characteristic time	[-]
ω	circle frequency	[rad/s]
σ	deviation from mean	[-]

Abbreviations

Bo	Bodenstein
STR	Ideally stirred tank reactor

CHAPTER FOUR

ISOBARIC AND NON-ISOBARIC MODELLING OF DYNAMIC GAS-LIQUID
OXYGEN TRANSFER IN AN AIRLIFT-LOOP BIOREACTOR

P. Verlaan and M.A.F. Hermans.

Department of Food Science, Food and Bioengineering Group,
Agricultural University,
De Dreyen 12, 6703 BC Wageningen, The Netherlands.

R.G.J.M. van der Lans.

Department of Biochemical Engineering,
Delft University of Technology,
Julianalaan 67, 2628 BC Delft, the Netherlands.

ABSTRACT

Oxygen transfer in an airlift-loop reactor with external loop has been modelled in two different ways. An isobaric model on the basis of a continuous stirred tank reactor and a non-isobaric model on the basis of plug-flow characteristics of the reactor produced consistent results in relation to the overall volumetric oxygen transfer coefficient k_{1a} . The non-isobaric model predicts k_{1a} -values and steady-state dissolved oxygen concentrations in the individual sections of the pilot-plant ALR and includes oxygen depletion of the gas phase. In contrast to what is stated in the literature, the local k_{1a} -value of the gas-sparger region does not necessarily have to differ from the overall k_{1a} -value of the ALR.

It is shown that injection of a relative small amount of gas in the down-comer up to 5% of the riser gas injection enhances the overall volumetric k_{1a} with 16%. This effect will be reduced when the gas injection rate in the riser is enlarged.

Submitted for publication.

INTRODUCTION

At present, different types of bioreactors are used for aerobic processes of which the airlift-loop reactor (ALR) is a recent development. In an ALR, due to the high circulation flow rate, economic oxygen transfer is combined with a controlled liquid flow and efficient mixing. Because of the controlled liquid flow and the geometry of the reactor intolerable variations in the dissolved oxygen concentration (DOC) may however occur during a fermentation. Numerous investigations have been carried out on the mass transfer capability of airlift contactors [1-4] but the results so far do not yield much more than empirical correlations.

Merchuk and Stein [5] introduced a stationary mathematical model for the oxygen mass transfer in an ALR. They regarded the flow in the ALR as a plug flow except for the topsection which was assumed to be well mixed. The downflow region was considered as a one phase flow. The fundamental parameters were obtained from experimental correlations making large scale predictions doubtful. Ho et al. [6] presented an ALR with internal loop having a number of interconnected compartments, each assumed to be well mixed. In this way, the mixing behaviour of the column determines the number of stages in the model whilst axial dispersion for both the liquid and the gas phase is approximated to the same extent. The topsection was considered to be well mixed. The model was used to simulate steady state oxygen transfer in an ALR. The aeration constant, k_1a , was assumed to be pressure invariant. The work was based mostly on experimental data and information provided by Hatch [3] and the results were not experimentally verified.

A real theoretical basis for the description of mass transfer and the estimation of mass transfer coefficients in an ALR is thus actually lacking in the literature. On the basis of earlier research [7-9] a steady state, non-isobaric gas-liquid oxygen transfer model was developed and is presented here. With this model, the aeration constant, k_1a , in a pilot-plant ALR can be estimated by a dynamic measurement procedure. The model was also used to investigate the influence of the air sparger region on the overall oxygen transfer. Carbondioxide and nitrogen transport are included in the model as mass transfer of these components between the gas and the liquid phase is able to severely influence the DOC and the mole fraction of oxygen in the gas phase. Moreover, large carbondioxide concentrations in the liquid phase can influence the metabolism of biomass [10]. The model predicts stationary

oxygen concentration profiles through the entire column (riser and downcomer). The results of the dynamic measurement procedure are compared with the results of an isobaric and quite simple STR-model [11] which has been adapted to the ALR.

THEORY

Estimation of the volumetric oxygen transfer coefficient, k_1a , in the ALR by a dynamic method requires modelling of the complete system dynamics. In the present work the liquid and gas-phase dynamics were investigated for a stationary and non-stationary situation. Typical ALR characteristics allowed us to treat the modelling of mass transfer in two different ways. On the one hand the ALR behaves like a loop reactor with relative high circulation rates. From this point of view the reactor can be modelled as a STR. On the other hand the ALR is a tube reactor in which the liquid phase as well as the gas phase behave like plug-flow which has been experimentally verified earlier [8]. Of course, the real flow pattern of the ALR is intermediate. The first estimation method, based on ideal mixing, considers an isobaric situation while the second method, based on plug flow, takes into account pressure variations in the ALR. Both methods utilize a step change in the inlet oxygen pressure in order to induce a time varying DOC in the batch liquid phase.

Isobaric model

The STR-method is a generally known estimation method which is quite simple to handle with, under the proper circumstances, acceptable accuracy [12]. The unsteady-state oxygen balance for the liquid phase is

$$\frac{dc(t)}{dt} = k_1a(c_s - c(t)) \quad (1)$$

where $c(t)$ is the actual DOC, c_s the saturation DOC and k_1a the volumetric oxygen transfer coefficient. In this isobaric model, the liquid phase is assumed to be well mixed and not exposed to any local gas and pressure variation. The gas phase composition is assumed to remain constant during

the aeration process. As a result, the change of the inlet oxygen pressure accomplishes a change of the DOC which can be described by an exponential function.

Non-isobaric model

The non-isobaric plug-flow estimation of (oxygen) mass transfer in the ALR is more complicated. In this model the gas-phase composition dynamics, axial pressure and gas hold-up distributions are incorporated. In contrast to the STR method, the plug flow model is extended with nitrogen (N_2) and carbon-dioxide (CO_2) dynamics.

Desorption of CO_2 in the gas phase is proportional to the dissolved CO_2 concentration in the liquid phase. If $pH < 6.4$, CO_2 reacts with water in such a way, that the equilibrium in the water stabilizes in the advantage of carbondioxide. According to the reaction rate of the CO_2 equilibrium reaction the amount of carbon-dioxide calculated by the model which does not take into account CO_2 reaction, should be corrected with a factor of 0.96 in order to obtain the actual value.

In developing a plug-flow, mass transfer model it is also necessary to consider the hydrodynamics of gas-liquid operations in the ALR, which has been reported elsewhere [7]. The influence of gas liquid interfacial mass transfer on the hydrodynamic behaviour of the ALR has here however been neglected. The here presented mass transfer model can be incorporated in a

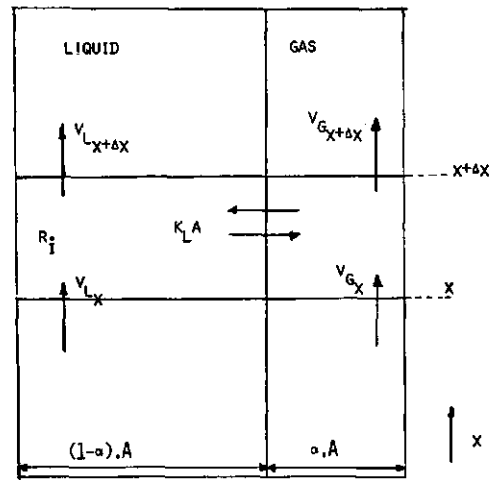


Fig. 1 Schematic representation of the plug flow model

hydrodynamic model for very large ALRs.

When a cross sectional volume element of the reactor tube is considered, a mass balance can be drawn over the element for the liquid and the gas phase (Figure 1). The volume element is chosen with a length Δx and a cross-sectional area of the local tube, A . Mass transfer of O_2 and N_2 is characterized by an overall volumetric mass transfer coefficient, $k_1 a$. As the diffusion coefficients of N_2 and O_2 in water approximately have the same values, it is assumed in this model that the actual transfer coefficient k for each component, will be equal to the liquid side mass transfer coefficient, k_1 , due to the low solubility of the components in the liquid phase. According to the Higbie model [13], a value of $0.83.k_1$ has been used for the CO_2 component as the diffusion coefficient of CO_2 has a value of about 30% below that of N_2 and O_2 .

For the gas phase in a stationary situation the mass balance for each component yields:

$$\frac{d}{dx} (v_{gs} \cdot \rho_i) = - k_1 a (c_{s_i} - c_i) \quad (2)$$

where v_{gs} is the superficial gas velocity and ρ the density; i denotes the specific component i.e. O_2 , N_2 or CO_2 . For the liquid phase the mass balance is:

$$\frac{d}{dx} (v_{ls} \cdot c_i) = k_1 a (c_{s_i} - c_i) - r_i \quad (3)$$

where v_{ls} is the superficial liquid velocity and r_i a respiration contribution of the micro-organisms which is assumed not to contribute in the nitrogen mass balance. As x is the only spatial variable, no radial gradients are incorporated. The contribution of axial dispersion is neglected in the present model because both the liquid and gas phase behave like plug flow [3,8].

The gas phase concentration is related to the mole fraction, y_i , of component i in the gas phase:

$$\rho_i = \frac{M_i}{RT} \cdot p(x) \cdot y_i \quad (4)$$

where M_i is the molar mass of component i , T its temperature and R the gas constant. Substitution of eq(4) in eq(2) and enumerating eq(2) over the components i yields an expression for the local superficial gas velocity, provided that $\sum y_{i=1}$:

$$\frac{d}{dx} [v_{gs} \cdot p(x)] = \frac{RT \sum k_{1a} (c_{s_i} - c_i)}{M_i} \quad (5)$$

In eq.(5), the superficial gas velocity, v_{gs} , is given as a function of the local pressure and interfacial mass transfer of the components.

Combination of eq(2), eq(4) and eq(5) yields a system of differential equations for the mole fraction of a component i in the gas phase:

$$\frac{v_{gs} \cdot p(x)}{RT \cdot k_{1a}} \begin{bmatrix} \dot{y}_{O_2} \\ \dot{y}_{N_2} \\ \dot{y}_{CO_2} \end{bmatrix} = \begin{bmatrix} -\frac{(y_{N_2} + y_{CO_2})}{M_{O_2}} & \frac{y_{O_2}}{M_{N_2}} & \frac{y_{O_2}}{M_{CO_2}} \\ \frac{y_{N_2}}{M_{O_2}} & -\frac{(y_{O_2} + y_{N_2})}{M_{N_2}} & \frac{y_{N_2}}{M_{CO_2}} \\ \frac{y_{CO_2}}{M_{O_2}} & \frac{y_{CO_2}}{M_{N_2}} & -\frac{(y_{N_2} + y_{O_2})}{M_{CO_2}} \end{bmatrix} \cdot \begin{bmatrix} c_{s_{O_2}} - c_{O_2} \\ c_{s_{N_2}} - c_{N_2} \\ c_{s_{CO_2}} - c_{CO_2} \end{bmatrix} \quad (6)$$

where \dot{y} denotes the derivative of y to x . As a result, 7 coupled linear differential equations are generated, expressed by eq.(3) for each component, eq(5) and eq(6). These equations are integrated simultaneously by a numeric procedure.

According to Henry's law, the partial pressure of the component i in the gas phase at equilibrium with liquid is proportional to the concentration of oxygen in the liquid film:

$$c_{s_i} = \frac{p(x) \cdot \rho_i}{H_{e_i}} \quad (7)$$

where ρ_i and H_{e_i} are the gas phase concentration and the Henry constant of component i , respectively.

As the model is non-isobaric the local pressure is defined by

$$p(x) = p(0) - \rho_l g(x - \int_0^L \alpha(x) dx) \quad (8)$$

where $\alpha(x)$ is the local gas fraction which is integrated over the specific reactor part (riser or downcomer) with a length L . The non-isobaric condition in the reactor will involve an axial dependency of the specific interfacial area, a ,

$$a(x) = \frac{6 \cdot \alpha(x)}{d_b(x)} \quad (9)$$

where $d_b(x)$ is the local bubble diameter defined by:

$$d_b(x) = \frac{d_b(0) \cdot p(0)^{1/3}}{p(x)^{1/3}} \quad (10)$$

where $d_b(0)$ and $p(0)$ are the local bubble diameter and pressure at the bottom of the reactor, respectively. In order to calculate the local pressure by eq.(8), the local gas hold up is approximated by $\alpha(x)$ as otherwise eq(8) becomes implicit for the gas hold-up [7,9]:

$$\alpha(x) = \frac{\alpha(0) \cdot p(0)}{p(x)} \quad (11)$$

In the model, the respirative contribution, r_{O_2} , is represented by the Michaelis-Menten model with the O_2 rate limiting substrate:

$$r_{O_2} = V_m \cdot \frac{c_{O_2}}{c_{O_2} + K_m} \quad (12)$$

where V_m and K_m are the intrinsic Michaelis-Menten parameters. The CO_2 production term is deduced from eq(12) provided that glucose is totally oxidized to CO_2 and H_2O .

The model assumes no interaction of the bubbles during their stay in the column. It was experimentally proved in previous work [7] that this is a reasonable assumption in the present ALR.

MATERIALS & METHODS

The pilot plant ALR used for the experiments has a working volume of 0.165 m^3 , an aerated height of 3.23 m (Figure 2) and has been described in more detail elsewhere [7,8]. The gas disengagement section has a length of 0.7 m and a width of 0.22 m , thus allowing a certain rate of foaming. It was designed such that complete deaeration occurs and no gas entrains into the downcomer during normal operation. The liquid level was kept at 0.13 m above the bottom of the cistern in the absence of gas in order to maintain about the same liquid velocity in the riser and in the topsection. The gas sparger produces bubbles with the same diameter as the equilibrium diameter of air

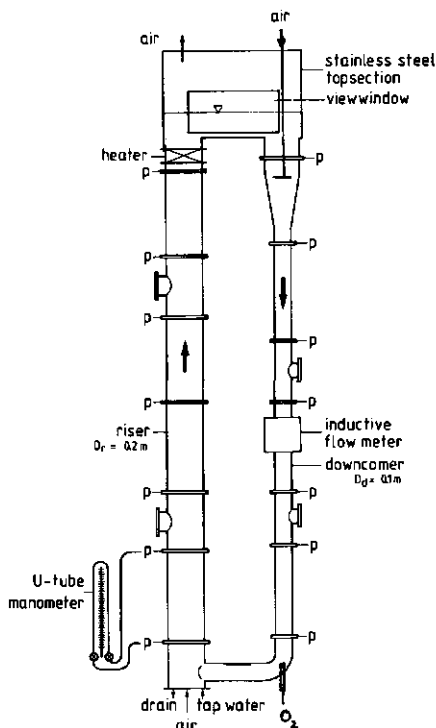


Fig. 2 The airlift loop reactor

bubbles in water. Forced gas injection in the downcomer is made possible by a small perspex tube (length: 0.1 m , diameter: 0.05 m) with 10 holes of 0.3 mm , positioned in the upper part of the funnel where axial and radial velocity gradients were present. This location prevents the creation of an air lock which is unavoidable during normal downflow air injection [9]. The temperature was kept at a constant value of 30° C . The ALR was filled with local tap water. This tap-water is ground water with quite consistent properties. Typical concentrations are: nitrates $< 1 \text{ g/m}^3$, sulphates 7 g/m^3 , total hardness 0.74 mol/m^3 , CO_2 : 2 g/m^3 .

A polarographic DOC electrode was positioned at the bottom of the downcomer in such a way that a sufficient flow towards the electrode membrane was ensured. A second DOC-probe could be located all over the axis of the riser

in order to measure local DOCs. This probe had a small propellor stirrer in front of the membrane to ensure a sufficiently high liquid approach velocity [11]. The time constant of both electrodes was about 4.5 s. Probe dynamics were not influenced by the pressure variations. Each electrode was connected to a DOC-meter which in turn was connected to a transmitter. The transmitter was coupled to a micro-computer by which data-sampling was performed.

As the present ALR has a limited height, the DOC profile was not very pronounced. Moreover, the accuracy of the steady state DOC experiments was very poor. Nevertheless an attempt has been made to measure the steady state DOC profiles by monitoring the local DOC on line for several minutes. The time averaged value thus obtained, was used as the final result. A valve, positioned at the bottom of the reactor, between the downcomer and the riser, was used to control the liquid velocity independent of the gas injection rate in order to enhance the maximum DOC difference over the length of the column [21].

A gas-analyzer was connected to the inlet and outlet gasflow of the reactor in order to monitor the gas phase composition. For this purpose, the outlet gas phase was dried by a countercurrent membrane tube before its composition was analysed.

Isobaric method

The isobaric k_1a -estimation method consisted of the STR-method which was applied to an ALR. For that several assumptions and simplifications have been introduced [11]. An oxygen mass balance over the the liquid in the riser of the ALR yields:

$$(1-\alpha) \cdot V_r \cdot \frac{dc}{dt} = \phi_v \cdot c(t-t_d) - \phi_v \cdot c(t) + k_1 A (c_s - c(t)) \quad (13)$$

Here, t_d is the mean residence time of the liquid in the downcomer, ϕ_v the liquid volume flow through the reactor tubes and A the absolute interfacial area. If the mean residence time in the downcomer, t_d , is relatively small in relation to the total circulation time, t_c , the first two terms of the right hand-side of eq(13) can be approximated by:

$$\lim_{t_d \rightarrow 0} \left[\phi_v \cdot t_d \cdot \frac{-((c(t) - c(t - t_d)))}{t_d} \right] = -v_d \cdot \frac{dc(t)}{dt} \quad (14)$$

where V_d is the volume of the downcomer tube. Combination of eq.(14) and eq.(13) results into eq(1) where the specific interfacial area, a , is concerned to the total liquid volume V of the ALR. Integration of eq(1) yields:

$$\frac{c_s - c(t)}{c_s - c(0)} = \exp(-k_1 a \cdot t) \quad (15)$$

where $c(0)$ is the initial concentration. With a non linear regression method based on the least square criterium according to c_0 , c_s and $k_1 a$ [14] it is possible to determine $k_1 a$ without the need of knowing the initial and saturation concentration. Moreover the method provides a weighing for the measured response curve in the essential part. A starting concentration of about $0.3c_s$ is used to avoid any lingering effects of the deoxygenation technique [15]. This method can also be applied with a respirative system in the ALR.

Non-isobaric method

The non-isobaric $k_1 a$ -estimation method consists of a stationary plug-flow model which is used to predict steady-state DOC-profiles through the column. This model has also been used to characterize the gas-liquid mass transfer by estimating $k_1 a$ values with the dynamic method. For this purpose the steady state model defined by equations 3, 5 and 6, has been adapted to predict dynamic mass transfer. As time and place in the present plug flow reactor are unambiguously related to each other, the following time-place transformation is introduced:

$$dt = \frac{dx}{v_{1s}} (1 - \alpha(x)) \quad (16a)$$

where $\alpha(x)$ is the local gas hold-up. An analogous transformation exists for the gas phase:

$$dt' = \frac{dx}{v_g} \quad (16b)$$

Since equation (3) and equation (6), in combination with equation (5) are solved simultaneously by the numeric procedure and the mass transfer process is mainly determined by the liquid properties, equation 16a is used as the time-place transformation in as well the liquid phase mass balance (equation 3) as the gas phase mass balance (equation 5 and 6). As a result, the liquid phase and the gas phase composition can be calculated as a function of the time.

Consequently, the use of equation 16a in equations 5 and 6 will cause a systematic error in the outlet gas phase composition during the instationary aeration process. This will result in a value of the oxygen concentration in the gas phase being 80% of the actual value which will introduce a systematic underestimation of the DOC. The k_{1a} -value calculated by this way will therefore have a progressive value which however differs less than 1% of the actual value.

For the liquid phase, each time a circulation has accomplished, the end value of the DOC is the initial value of the sequential iteration. This process continues until the steady state situation has been reached and the end

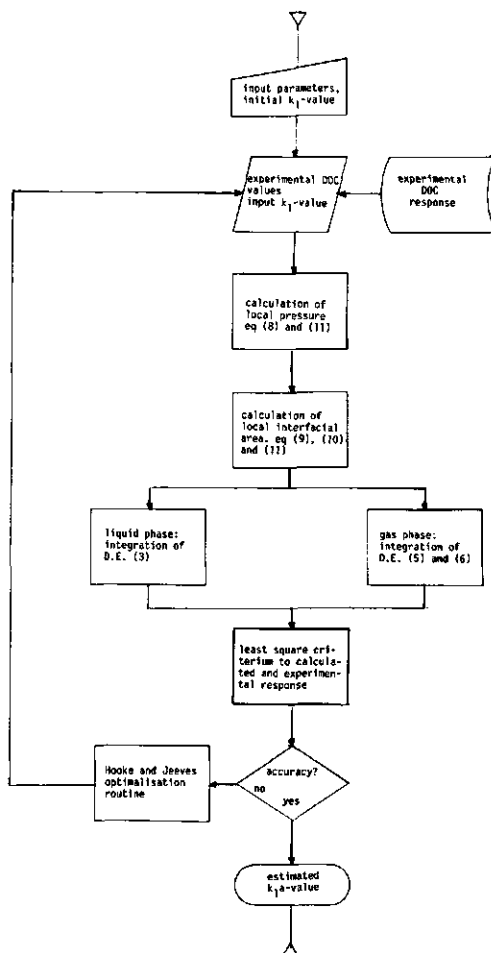


Fig. 3 Schematic representation of the k_{1a} -estimation procedure by the non isobaric plug flow model

and begin values of sequential circulations both have the same values. As a result, the iteration can also be used to calculate steady state concentration profiles in case of unknown boundary values. Essentially, the pertinent iteration can be regarded as a fluidum element with a length dx travelling through the turnaround with a velocity defined by equation 16a.

The non-isobaric method was realised experimentally by a step change in the inlet gas composition. The DOC was measured with the polarographic electrode. Probe dynamics in relation to the system dynamics were neglected which in this case is allowed [12,17] as the minimum reciprocal k_1a value was about 20 s. The interface nitrogen transport will interfere with the oxygen transport. This effect however is negligible [18].

The same calculation procedure is applied to the downcomer section. For the topsection the calculation procedure could be simplified as this reactor part is operated under isobaric conditions. Deaeration in the topsection is described as proposed by Verlaan et al.[7]. However, in practise an accurate estimation of k_1a could be obtained when the topsection was incorporated in the riser section thus obtaining two different reactor parts of length L : the riser and the downcomer.

The model was fitted to the experimental dynamic response curve by an optimisation routine based on the Hooke and Jeeves method [19]. A schematic representation of the non-isobaric method is given in Figure 3.

As the plug flow model calculates local k_1a -values based on the total dispersion volume (i.e. gas-liquid volume) and the STR model calculates a mean volumetric k_1a -value concerned on the total liquid volume, the estimated volumetric k_1a -values according to the plug flow model have been adapted and are also concerned on the total liquid volume. The overall k_1a -value for the ALR is defined by:

$$\overline{k_1a} = \frac{(1-\alpha_d)\overline{k_1a_d} + A_r/A_d(1-\alpha_r)\overline{k_1a_r}}{(1-\alpha_d) + A_r/A_d(1-\alpha_r)} \quad (17)$$

Equation (17) is based on the residence time distribution in each reactor part. The mean volumetric mass transfer coefficient in the riser or downcomer concerned on the liquid volume and averaged for pressure variations over the column is defined by:

$$\overline{k_1 a_{r,d}} = \frac{\int k_1 a_{r,d}(x)/(1-\alpha(x)) dx}{\int x dx} \quad (18)$$

$k_1 a$ -estimation in a yeast suspension

The estimation of the volumetric oxygen transfer coefficient by the STR-model could be performed directly from the response curve. In order to apply the plug flow model for this purpose, the oxygen consumption rate of the yeast and the dynamic DOC response curve were measured as described below. In the absence of gas (no aeration) the decrease of the DOC was monitored as a function of time. As the airlift was out of operation then, a sufficient liquid flow to the electrode-membrane was ensured by a small propeller stirrer positioned in front of the electrode. When the DOC decreased to 10% of the saturation value, airlift operation was started and the DOC response monitored. From the experimental data the oxygen consumption rate

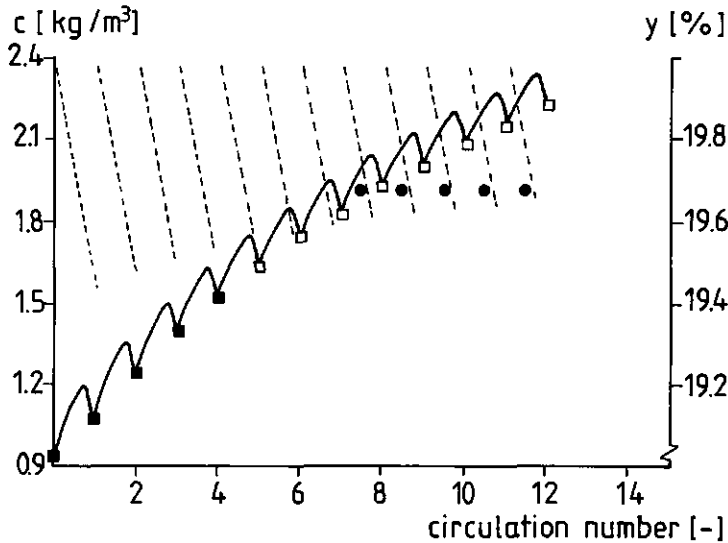


Fig. 4 Comparison of experimental values and calculated values in a yeast suspension. ■ and □ experimental DOC values (■ used for $k_1 a$ -estimation), ● experimental gas concentration values. — calculated DOC profile, ---- calculated oxygen concentration in the gas phase

of the yeast (Fermipan) was calculated. Thereupon the volumetric oxygen transfer coefficient was estimated as described in the previous section. For maintaining viability of yeast cells 1 mM KH_2PO_4 , 0.8 mM MgSO_4 and 0.05 g/l glucose was added to the ALR. Moreover, $3 \cdot 10^{-3}$ volume percent of soya oil was added as anti-foam agent.

During the experiment samples were taken from the batch in order to determine the oxygen saturation concentration as described by Robinson and Cooper [20]. The activity of the yeast in the reactor remained constant for 3 to 4 hours which was sufficient to carry out our experiments. The experimental results thus obtained were well reproducible.

RESULTS AND DISCUSSION

Figure 4 shows a simulated response of the dimensionless concentration of a respirative system in the ALR on a step change in the gas inlet composition, combined with experimental results of aeration in a yeast suspension. As the model calculates the DOC in a fluid-element which travels through the ALR, pressure variations are clearly shown. Figure 5 shows the experimental results plotted semilogarithmic. A good agreement with the STR model, expressed by equation (13) is demonstrated by figure 5. From both results it can be concluded that the aeration process in the ALR can be very accurately modelled by the plug flow model as well as by the STR-model.

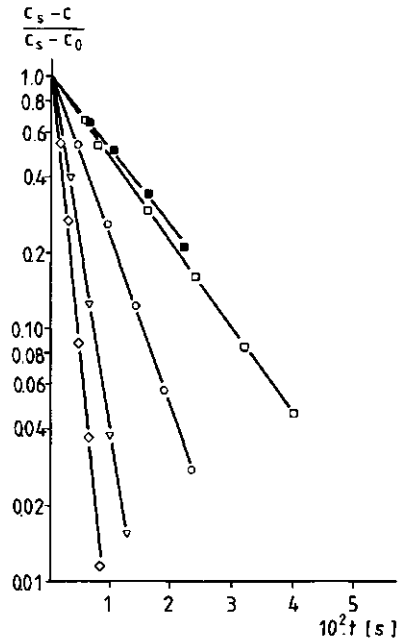


Fig. 5 Experimental DOC values as a function of time for tap water ($v_{ga} = \square -0.0194$; $\circ -0.0383$; $\nabla -0.0771$; $\diamond -0.193$ m/s) and a yeast suspension (\blacksquare) for the situation mentioned in fig. 4

In Figure 6 the results of both methods are compared for tap water and yeast suspension. The overall volumetric mass transfer coefficient, k_1a , is presented in relation to the barometric superficial gas velocity. The mean k_1a -

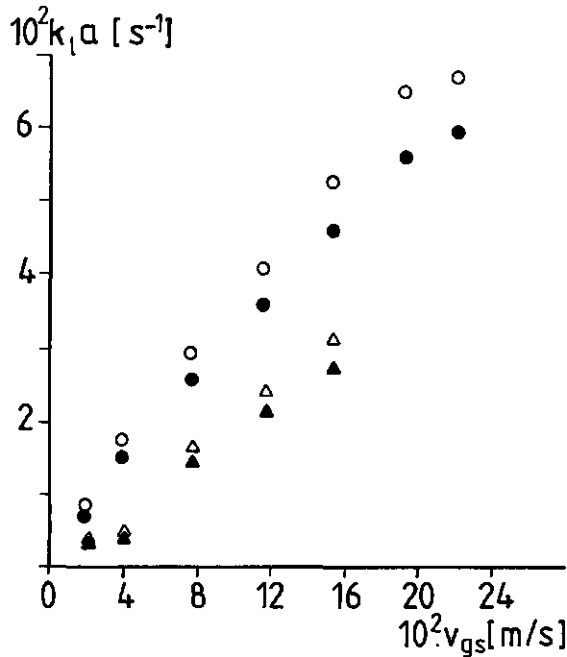


Fig. 6 The volumetric oxygen transfer coefficient as a function of the barometric superficial gas velocity. \circ tap water, plug flow model, \bullet tap water, STR model, Δ yeast suspension, plug flow model, \blacktriangle yeast suspension, STR model.

values of the non-isobaric plug-flow model are 10% higher than those predicted by the isobaric STR model. This is caused by the assumption of a well mixed liquid phase in the STR model, leading to values that are too low [9]. Figure 7 shows an example of the axial dependency of the volumetric oxygen transfer coefficient according to the plug flow model. As a result of the decreased hydrostatic pressure in the riser, the bubbles expand thus increasing the gas hold-up and the interfacial area, a , as has been experimentally verified by Verlaan et al. [7].

Figure 8 shows an example of a steady-state DOC profile for tap water in the

Gas injection rate [g/s]	0.83	1.53	3.05	3.05	3.05
Riser liquid velocity [m/s]	0.1	0.16	0.23	0.34	0.49
Δc_{\max} in riser: simulation [mg/l]	0.55	0.35	0.24	0.15	0.12
Δc_{\max} in riser: experimental [mg/l]	0.26	0.34	0.26	0.34	0.17
location of c_{\max} in riser: simulation [-]	0.45	0.5	0.5	0.5	0.5
location of c_{\max} in riser experimental [-]	0.55	0.55	0.5	0.5	0.55

Table 1 Comparison of the simulated and experimental axial DOC profile in the ALR at different gas injection rates

The k_{1a} -value of the gassparger region relative to the actual k_{1a} -value	Location of c_{\max} [-]	
	volume gassparger region relative to the riser volume	
	10%	1%
0.1	0.554	-
1.0	0.508	0.508
1.1	0.504	0.508
2.0	0.468	0.503
10.0	0.289	0.468

Table 2 The effect of the k_{1a} -value of the gassparger region on the location of the maximum DOC-value in the column

riser in combination with the local saturation concentration according to Henry's law, eq(4). As can be seen, due to the relative high pressure and driving force at the lower part of the column the DOC increases until equilibrium occurs. This is the point (the maximum DOC value) where the local DOC is equal to the saturation concentration. In the upper part of the column the supersaturated liquid is deaerated as the pressure decreases. This process continues for sequential circulations. Because of the limited height of the ALR used (3.23 m), the DOC profiles were fairly flat. Consequently we were not able to reveal the entire stationary DOC curve with acceptable accuracy. Therefore we only determined the value and the location of the maximum of the DOC curve. In order to obtain a more pronounced DOC profile, a valve was placed in between the riser and the downcomer at the bottom of the reactor. By gradually closing down this valve, the liquid velocity could be reduced independent of the gas input rate, as has been described elsewhere [21]. In table 1, the results of the model calculations, predicting the maxima, are compared with the experimental revealed maxima. The predicted values coincide with the experimental values. From these results it can be concluded that the local k_1a value is fairly well predicted by the model and that the maximum DOC concentration in the ALR is located halfway the riser.

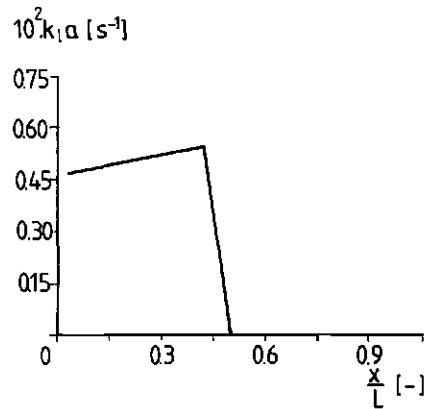


Fig. 7 Local k_1a -values in a yeast suspension for the situation mentioned in Figure 4

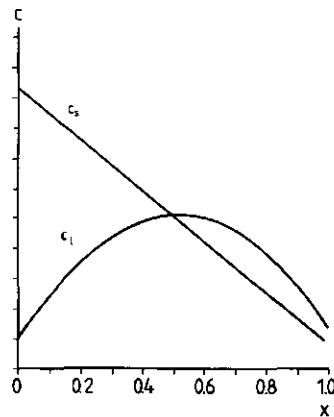


Fig. 8 Example of a DOC-value in the ALR compared with the local DOC-saturation curve

The steady state profiles measured by Weiland [2] show a significant shift of the maximum to the bottom of the reactor which can be attributed to the relative high mass transfer in the neighbourhood of the air-sparger, effecuated by a special geometry of the sparger region [2]. Alvarez-Cuenca et al. [22] claimed that up to 95% of the total mass transfer takes place in the sparger region, dependent on sparger design and relative volume of that region. In contrast to these findings in our case no significant shift of the steady-state profile is noticed as has been demonstrated above. From this appearance it is concluded that there is no distinct influence of the sparger region on oxygen transfer. This conclusion agrees with the fact that the sparger was designed to create bubbles of equilibrium size thus keeping entrance-effects as low as possible. This conclusion can be supported by a model simulation demonstrating the influence of a varying sparger- k_{1a} on the overall k_{1a} . For this purpose the riser is divided into arbitrary sparger regions of 1% and 10% of the total riser volume. In the sparger region, the values for the volumetric oxygen transfer coefficient are varied from 0.1 to 10 times of the k_{1a} values in the riser part of the reactor. Table 2 shows the results of the model

simulations. The maximum of the steady-state profile shows a shift from $x=0.5$ to $x=0.3$, depending on the variation of k_{1a} and the dimension of the sparger region. From these calculations it can be concluded that the sparger region can significantly contribute to the aeration process in an ALR.

Moreover, the position of maximum of the steady-state DOC-profile in the riser is a measure for the contribution of the sparger region to the overall aeration.

A small amount of gas injected at the top of the downcomer is able to create a significant rise in k_{1a} as shown in Figure 9. In this figure, the relative

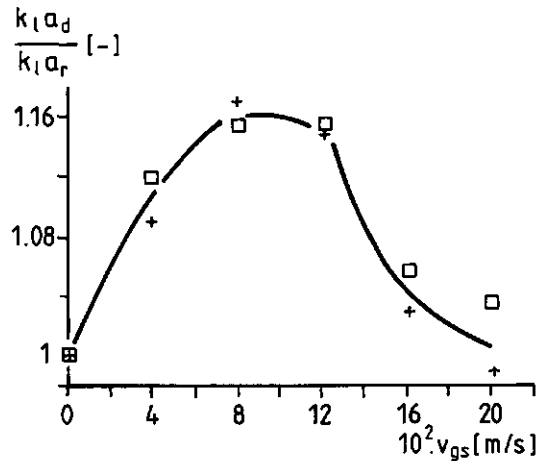


Fig 9 Ratio of the k_{1a} value with downcomer injection and the k_{1a} value without downcomer injection as a function of the barometric superficial gas velocity in the riser

volumetric oxygen transfer coefficient is given in relation to the riser gas input. Figure 10 shows the corresponding contribution of downcomer gas injection to the riser superficial gas velocity.

As shown, the downcomer contribution to the overall k_{1a} shows a maximum and decreases with an increasing riser gas input rate. At low gas input rates the liquid velocity in the upper part of the downcomer is below the bubble rise velocity so that no carry over will occur. At high gas input rates despite the geometry of the topsection, a cer-

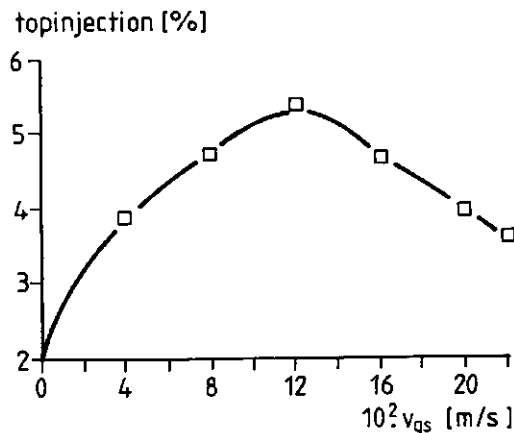


Fig. 10 Topinjection of gas in the downcomer relative to the total gas flow in the riser

tain amount of gas will entrain into the downcomer as a result of the increased liquid velocity and the incomplete gas disengagement. Because of this phenomenon the relative contribution of gas injection into the downcomer is low. Consequently, for high gas input rates it has not much significance to inject gas into the downcomer of the pertinent ALR.

CONCLUSIONS

The newly developed, non-isobaric plug flow model predicts stationary and non-stationary DOC profiles in large scale ALRs and has been applied to estimate dynamic k_{1a} values in a pilot plant ALR. Comparison with the results estimated by an isobaric STR model demonstrates that the STR model yields conservative values. For the present situation deviations between both models did not exceed a relative value of 10%. Therefore, due to its simplicity, it is recommended to use the STR model for a rapid characterisation of the aeration capacity with a satisfactory accuracy of pilot-scale ALRs.

Oxygen depletion of the gas phase, even during a fermentation, was very

little and did not surpass 1 volume-% of oxygen, which was fairly well predicted by the plug flow model. For this reason an ALR is a very suitable reactor for aerobic processes showing a high oxygen demand.

If necessary, the aeration capacity of the ALR can be enhanced by injection of a small amount of gas at the entrance of the downcomer. Injection of 5% of the total riser gas flow enhances the overall k_1a value up to 16%.

It is possible to incorporate the gas sparger contribution to the overall oxygen transfer process into the plug flow model. However, as shown by model calculations, in the present ALR the aeration capacity of the gas sparger did not differ significantly from the main aeration process due to its special geometry.

ACKNOWLEDGEMENTS

The authors wish to thank prof. dr. K. van 't Riet and prof. K.Ch.A.M. Luyben for their helpful discussions during the preparation of the manuscript.

REFERENCES

- [1] R.A. Bello, C.W. Robinson and M. Moo-Young. Gas hold-up and overall volumetric oxygen transfer coefficient in airlift contactors. *Biotechnol. & Bioeng.* 27, (1985) 369-381.
- [2] P. Weiland. Untersuchung eines Airliftreaktors mit äußerem Umlauf im Hinblick auf seine Anwendung als Bioreaktor. Thesis, University of Dortmund, Dortmund, 1978.
- [3] R.T. Hatch. Experimental and theoretical studies of oxygen transfer in the airlift fermenter. Thesis, Massachusetts Institute of Technology, Cambridge, MA, 1973.
- [4] C.H. Lin, B.S. Fang, C.S. Wu, H.Y. Fang, T.F. Kuo and C.Y. Hu. Oxygen transfer and mixing in a tower cycling fermentor. *Biotechnol. & Bioeng.* 18 (1976) 1557-1572.
- [5] J.C. Merchuk and Y. Stein. A distributed parameter model for an airlift fermentor. *Biotechnol. & Bioeng.* 22 (1980) 1189-1211.
- [6] C.S. Ho, L.E. Erickson and L.T. Fan. Modeling and simulation of oxygen transfer in airlift fermentors. *Biotechnol. and Bioeng.* 19 (1977) 1503-1522.
- [7] P. Verlaan J. Tramper, K. van 't Riet and K.Ch.A.M. Luyben. A Hydrodynamic model for an airlift-loop bioreactor with external loop. *Chem. Eng. Journal.* 33 (1986) B43-B53 (Chapter two of this thesis).
- [8] P. Verlaan, A.M.M. van Eijs, J. Tramper, K. van 't Riet and K.Ch.A.M. Luyben. Estimation of axial dispersion in individual sections of an airlift-loop reactor. submitted for publication (Chapter three of this thesis).
- [9] R.G.J.M. van der Lans. Hydrodynamics of a bubble column loop reactor. Thesis, Delft University of Technology, Delft, 1985.
- [10] A.V. Quirk and R.W.H. Plank. The effect of carbondioxide on the production of an extracellular nuclease of staphylococcus aureus. *Biotechnol. & Bioeng.* 25 (1983) 1083-1093.

- [11] J. van de Donk. Water aeration with plunging jets. Thesis, Delft University of Technology, Delft, 1981.
- [12] G. Ruchti, I.J. Dunn and J.R. Bourne. Comparison of dynamic oxygen electrode methods for the measurements of k_{1a} . *Biotechnol. & Bioeng.* 23 (1981) 277-290.
- [13] R. Highie. The rate of absorption of a pure gas into a still liquid during short periods of exposure. *Trans. Am. Inst. Chem. Eng.* 31 (1935) 365-389.
- [14] M.M.C.G. Warmoeskerken. Gas-liquid dispersing characteristics of turbine agitators. Thesis, Delft University of Technology, Delft, 1986.
- [15] L.C. Brown and C.R.J. Baillod. Modeling and interpreting oxygen transfer data. *Proc. ASCE.* (1982).
- [16] Subroutine DVERK (Runge-Kutta method, initial value problem.) IMSL library edition 9.2, Houston, 1984.
- [17] K. van 't Riet. Turbine agitator hydrodynamics and dispersion performance. Thesis, Delft University of Technology, Delft, 1975.
- [18] V. Linek, P. Benes and F. Hovorka. The role of interphase nitrogen transport in the dynamic measurements of the overall volumetric mass transfer coefficient in air-sparged systems. *Biotechnol. & Bioeng.* 23 (1980) 301-319.
- [19] OPTPAC3. Non-linear optimisation package NDV-DSA/SCA/TK/77:054/ap. N.V. Philips Gloeilampen fabrieken, Eindhoven, The Netherlands, 1977.
- [20] J. Robinson and J.M. Cooper. Method of determining oxygen concentrations in biological media, suitable for calibration of the oxygen electrode. *Anal. Biochem.* 33 (1970) 390-399.
- [21] P. Verlaan, J.-C. Vos and K. van 't Riet. From bubble column to airlift-loop reactor. Hydrodynamics of the transition flow regime. Submitted (Chapter five of this thesis).
- [22] M. Alvarez-Cuenca, C.G.J. Baker and M.A. Bergougnou. Oxygen mass transfer in bubble columns. *Chem. Eng. Sci.* 35 (1980) 1121-1127.

NOMENCLATURE

A	(interfacial) area	[m ²]
a	volumetric interfacial area	[m ⁻¹]
c	concentration	[kg/m ³]
d	diameter	[m]
g	gravitational constant	[m/s ²]
He	Henry constant	[pa]
K	Michaelis Menten constant	[kg/m ³]
k	mass transfer coefficient	[m/s]
k_{1a}	volumetric mass transfer coefficient	[s ⁻¹]
k_{1a}	mean volumetric mass transfer coefficient concerning the column length	
k_{1a}	overall, mean volumetric mass transfer coefficient of the ALR	[s ⁻¹]
L	length	[m]
M	molar mass	[kg/mol]
p	pressure	[Pa]

R	gas constant	[J/(mol.K)]
r	respiration coefficient	[kg/(m ³ .s)]
STR	ideally stirred tank reactor	
T	temperature	[K]
t	time	[s]
V	volume	[m ³]
V _m	Michaelis Menten constant	[kg/(m ³ .s)]
v	velocity	[m/s]
x	coordinate	[m]
y	mole fraction	[-]

Greek symbols

α	gas hold up	[-]
α'	approximated gas hold up	[-]
ϕ_v	volume flow	[m ³ /s]
ρ	density	[kg/m ³]

Subscripts

b	bubble
g	gas
i	denoting a specific component
l	liquid
s	saturation, superficial

CHAPTER FIVE

FROM BUBBLE COLUMN TO AIRLIFT-LOOP REACTOR:
HYDRODYNAMICS OF THE TRANSITION FLOW REGIME

P. Verlaan, J.-C. Vos and K. van 't Riet.

Department of Food Science, Food and Bioengineering Group,
Agricultural University,

De Dreyen 12, 6703 BC Wageningen, The Netherlands.

ABSTRACT

The hydrodynamics of an airlift-loop reactor (ALR) and a bubble column (BC) have been studied in the same reactor unit. When the the liquid circulation in the ALR is impeded gradually in order to obtain a BC mode of operation, it appears that there exists a transition flow regime in between that of the ALR-type of flow and the BC-type of flow. In the BC the heterogeneous flow was represented by an instationary circulatory flow pattern and characterised by a liquid circulation velocity according to Joshi and Sharma. The liquid flow in the ALR was represented according to the drift-flux model of Zuber and Findlay. In the transition flow regime, hydrodynamic calculations based on the plug-flow behaviour of an ALR appeared to be valid up to a certain defined value of the total gas-liquid flow rate. The more the liquid flow in the ALR is impeded the lower this value will be. In order to distinguish between BC and ALR flow characteristics, a simple criterium is proposed, qualifying that the distinction between both flow patterns is determined by the superficial liquid velocity and the liquid circulation velocity. If the latter velocity exceeds the superficial liquid velocity a hydrodynamic transition will occur from a uniform ALR type of flow to a heterogeneous BC type of flow. The criterium coincides with an empirical power law function in which the liquid velocity is given as a function of the gas velocity. The values of the power-law coefficients were found to depend on the characteristics of the two-phase flow. The change in value cohered with the onset of a change in the flow pattern.

Submitted for publication.

INTRODUCTION

Various types of bioreactors are presently used in biotechnological processes of which the airlift-loop reactor (ALR) is a recent development. The ALR concept has been evolved from that of the bubble column and was first described by Le François et al. [1]. The special feature of the ALR is the circulation of the liquid through a downcomer which connects the top and the bottom of the main bubbling section (the riser). Due to the high circulation flow rate, efficient mixing is combined with a controlled liquid flow in the absence of mechanical agitators [2]. Moreover, an ALR satisfies a high oxygen demand even at large ALR constructions (50 - 100 m) [3]. For this reasons, an ALR seems an attractive alternative for aerobic processes.

An ALR has a plug flow for both the liquid and the gas phase with the liquid phase circulating through the reactor. If the liquid flow is hampered (e.g. by gas redispersion plates, a small downcomer diameter, monitoring devices etc.) the upflow region can loose its typical plug flow characteristics. Gradually, a transition from plug flow to a BC type of flow will occur when the liquid flow decreases. The intermediate region between an unhampered ALR-flow and an established BC-flow is what we call the transition flow regime.

A major problem in designing and modelling the hydrodynamic characteristics of an ALR is the exact characterization of the flow regime in the column. This problem has been recognized earlier in the literature, though until yet, only a few results have been reported on this topic. Merchuk and Stein [4], for instance, investigated gas hold-ups and liquid velocities as a function of the hydrodynamic resistance in an ALR by partially closing the downcomer. They found the liquid velocity to be a simple power law function of the gas flow rate. The coefficients of the power-law function did depend on the geometry of the ALR and the two-phase flow regime in the riser column and therefore on the resistance in the ALR. However, on the one hand the authors concluded that a change of the exponent in the above-mentioned correlation gives an objective method to recognize the onset of change in the flow pattern. On the other hand they concluded that, in evaluating their results according to the Zuber and Findlay drift-flux model [5], fairly flat velocity and gas hold-up radial profiles exist all along the column, independent of reactor operation under bubble column or ALR conditions. Merchuk [6] investigated gas hold-up and liquid circulation in an ALR with a rec-

tangular cross flow area and compared the results between bubble column and airlift operation in the same unit. The author distinguished between the different flow regimes for the bubble column and that for the ALR and concluded that these flow regimes were typical for both reactors. These findings were in contradiction with the results of Menzel et al. [7] who investigated flow profiles in an ALR and a bubble column. They derived that the radial liquid profiles did not essentially differ between both configurations except for a superimposed liquid velocity in the case of an ALR.

Obviously, the discrepant and diverse interpretations in the literature of the comparison of the gas hold-up characteristics between an ALR and a bubble column hamper a more perspicuous view, while for the transition regime information is lacking.

In this paper we discuss the hydrodynamics of the transition regime. A criterium will be presented by which the transition of bubble column to ALR hydrodynamics can be predicted. The criterium also determines the range of the process variables for which a general hydrodynamic model for an ALR, presented elsewhere [8] is valid. The criterium can also be an important tool in scaling up and designing mass transfer and mixing processes in an ALR.

THEORETICAL BACKGROUND

Density differences between the liquid dispersion in the riser and downcomer induce a liquid circulation which can be mathematically expressed by:

$$\int_0^L g \alpha_r(z) dz - \int_0^L g \alpha_d(z) dz = \frac{1}{2} K_f \cdot v_{1s}^2 \quad (1)$$

where α_r and α_d are the local gas hold-up in the riser and downcomer respectively, v_{1s} the superficial liquid velocity, K_f the friction coefficient and g the gravitational constant.

Liquid velocities and local gas hold-ups in both the riser and downcomer in relation to the gas injection rate can be predicted on the basis of eq(1) and the two phase flow model of Zuber and Findlay [5], as was proposed by Verlaan et al. [8]. The model of Zuber and Findlay however, assumes plug

flow in the liquid phase, taking into account a non-uniform flow and hold-up distribution across the duct. This means that this model is restricted only to an ALR with a high circulation rate because in that regime the plug flow characteristics are reached. From the Zuber and Findlay model the following equation is obtained:

$$v_g = C. \{v_{gs} + v_{ls}\} + v_{b,\infty} \quad (2)$$

where C is a distribution parameter for non-uniform, radial flow and $v_{b,\infty}$ is the rise velocity of a single bubble in an infinite medium. The flatter the flow profiles, the closer C approaches unity. When v_g is plotted as a function of the total flow, $v_{gs}+v_{ls}$, the values of C and $v_{b,\infty}$ can be obtained and the flow is characterized. If the flow regime changes, there will be a non-linear relationship between the gas velocity and the total flow, indicating that C and $v_{b,\infty}$ will depend on the value of the total gas-liquid flow rate.

In the case of a bubble column, the Zuber and Findlay model is not valid. In such a column, the heterogeneous two-phase flow induces instationary circulation cells which cannot be represented by a single distribution parameter. Moreover, radial hold-up and liquid velocity profiles are strongly dependent of the gas input rate [9,10]. Joshi and Sharma [10], introduced a model which predicts the circulation velocity, v_{cl} , of the liquid in the circulation cells. They derived an expression for the liquid circulation velocity at high superficial liquid velocities which can be represented by:

$$v_{cl} = 1.18 \{gDa(v_s - v_{b,\infty})\}^{0.33} \quad (3)$$

where v_s is the slip velocity between the gas and the liquid phase and D is the diameter of the column.

MATERIALS AND METHODS

The pilot plant ALR used for the experiments has a working volume of 0.165 m^3 , an aerated height of 3.23 m and has been described in more detail elsewhere [8]. At the bottom of the reactor in between the riser and downcomer, a butterfly valve was positioned in order to influence the liquid velocity independent of the gas injection rate (figure 1). When the valve was closed totally, the riser functioned as a bubble column. The ALR was filled with Wageningen tap water having quite consistent properties [3]. The liquid level was kept, in the absence of gas, at 0.13 m above the bottom of the cistern in order to maintain the liquid velocity in the riser and in the topsection nearly equal. The gas sparger produces bubbles with the same diameter as the equilibrium diameter of air bubbles in water. The temperature of the water was fixed on a constant value of 30° C . The liquid flow in the downcomer was measured by means of an inductive flow meter. A reversed U-tube manometer was used to determine the gas fraction in the riser as has been described by Verlaan et al. [8].

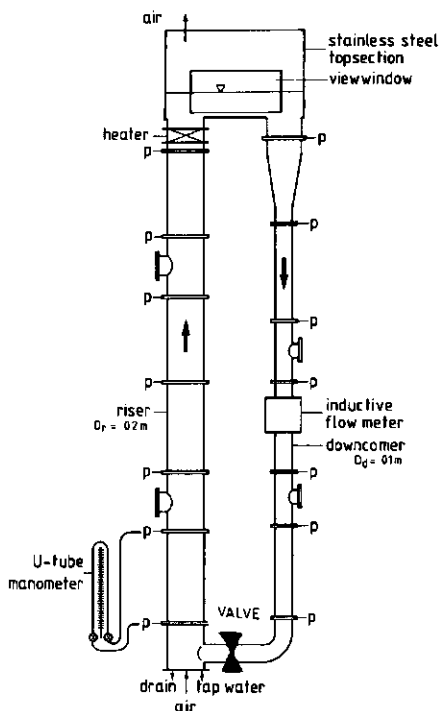


Fig. 1 The airlift loop reactor

Key	Valve position	Friction coefficient (K_f)
□	1	4.62
○	4	8.85
△	5	19.3
+	6	61.5
×	7	409
◇	8	∞

Table 1. The friction coefficient for the different valve positions and the key to the figures 2-9.

key	traject where the the deviation starts according to fig 7	traject where the discontinuity appears according to fig 8
	v_{gs}	v_{gs}
□	0.055 - 0.077	0.053 - 0.073
○	0.028 - 0.048	0.04 - 0.053
△	0.028 - 0.042	0.033 - 0.045
+	0.028 - 0.042	0.025 - 0.045

Table 2. Trajects for the superficial gas velocity where a hydrodynamic transition occurs, obtained from fig. 7 and 8.

RESULTS AND DISCUSSION

Liquid velocity and hold-up

Figure 2 shows the liquid velocity as a function of the normalized superficial gas velocity in the riser. The normalized value is the value at

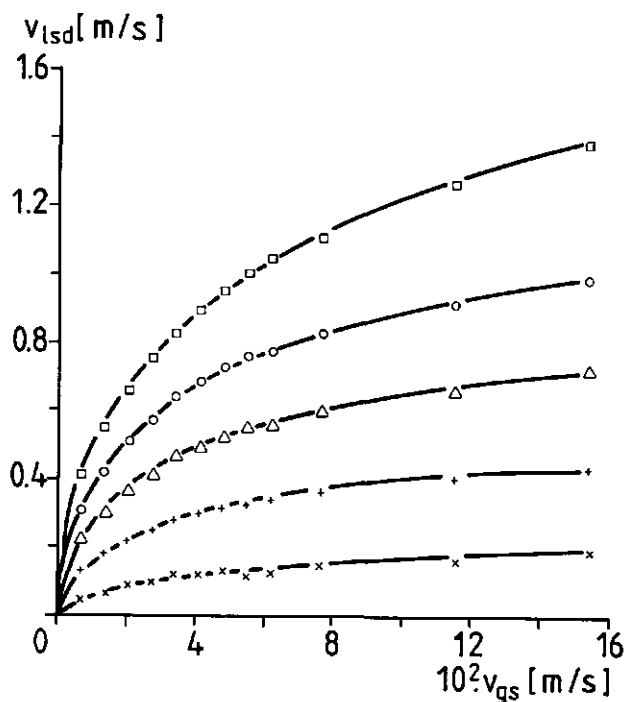


Fig. 2 Superficial liquid velocity in the downcomer as a function of the superficial gas velocity with the valve position as a parameter. (Key given in table 1)

100 kPa and 0 °C. In this figure, the position of the butterfly valve is a parameter. As shown, the position of the butterfly valve determines the liquid circulation and therefore the liquid velocity in the downcomer and riser. As a result, the residence time of the gas phase in the riser

increases with increasing valve closure, thereby enlarging the gas hold-up in the riser. This phenomenon is shown in figure 3. For superficial gas-velocities up to 0.08 m/s the gas hold-up is very sensitive to changes in

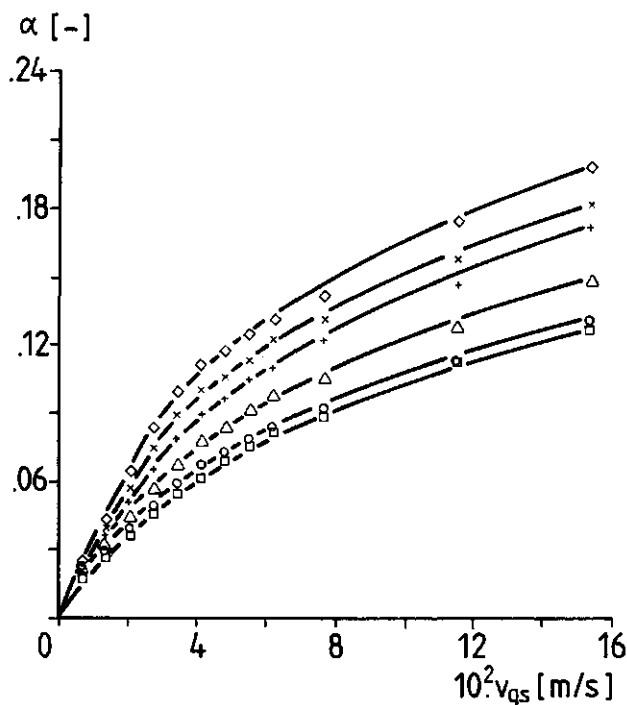


Fig. 3 Gas hold-up in the riser as a function of the superficial gas velocity with the valve position as a parameter. (Key given in table 1)

the gas input rate. For superficial gas velocities above 0.08 m/s, the increment of the gas hold-up is almost linear with that of the superficial gas velocity. The effect of the reduced liquid velocity at various valve positions on the gas hold-up is expressed in figure 4 where the relative gas hold-up is plotted as a function of the relative liquid velocity. Both parameters are related to the values that occur for a totally opened valve position (position 1). Figure 4 shows that at bubble column operation, the gas hold-up in our reactor increases up to 170% from the initial ALR values.

This coincides with the results of Weiland [12], who reported an enhancement during bubble column operation up to 180% of the ALR gas hold-up for an ALR with an aerated height of 8.5 m.

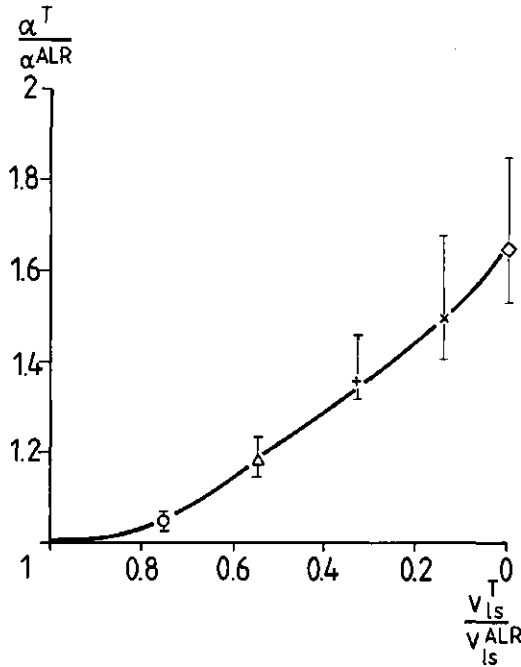


Fig. 4 The ratio of the gas hold-up in the transition flow (α^T) and the gas hold-up in the ALR (α^{ALR}) as a function of the ratio of the liquid velocity in the transition flow (v_{ls}^T) and the liquid velocity in the ALR (v_{ls}^{ALR}). (Key given in table 1).

Friction coefficient

The position of the butterfly valve influences the overall friction in the ALR, resulting in changes of the liquid velocity and the gas hold-up at constant gas input rates. An overall friction coefficient can be obtained according to eq(1) by plotting the measured square of the superficial liquid velocity as a function of the mean gas hold-up in the riser in the absence of gas in the downcomer. From the slope of the lines the friction coef-

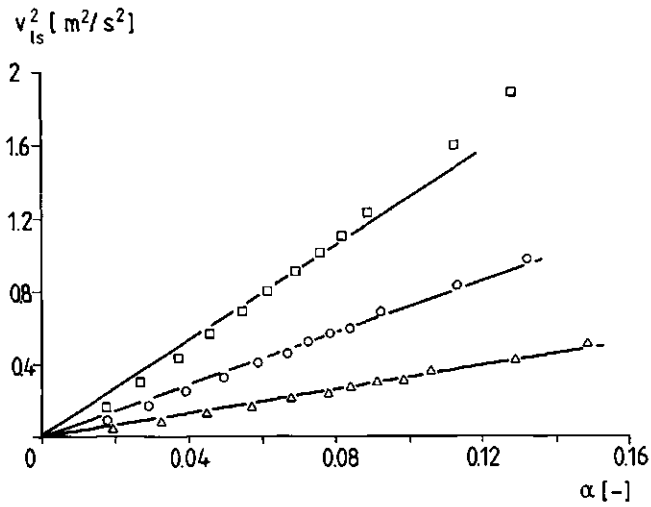


Fig. 5a The square of the liquid velocity in the downcomer as a function of the gas hold-up with the valve position as a parameter (Key given in table 1).

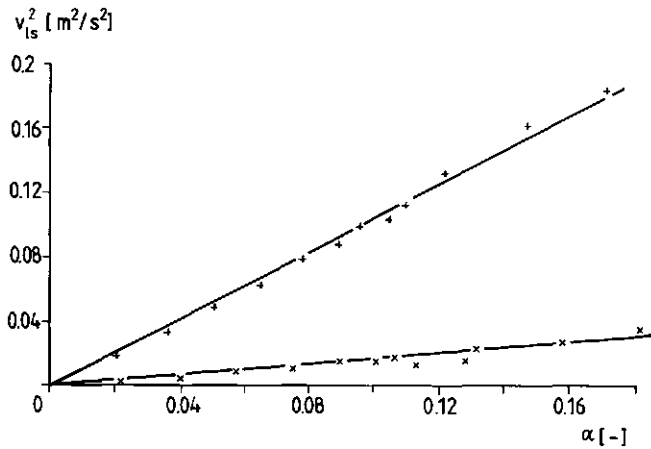


Fig. 5b The square of the liquid velocity in the downcomer as a function of the gas hold-up with the valve position as a parameter (Key given in table 1).

efficient can be obtained [8]. In figure 5a and 5b the results are shown for the five valve positions. From both graphs it appears that for low gas hold-up values the friction coefficient is constant and thus independent of the liquid velocity and of changes in gas hold-up. This establishes the assumption of Verlaan et al. [8] that for an ALR and, in this case for the transition-flow regime, the total friction in an ALR can be derived from simple one-phase flow calculations based on known data for the friction coefficient [11]. This assumption is only valid in a restricted gas input range as will be explained later. A closer look at the friction in the ALR learns that, especially for larger gas input rates, the above-mentioned coefficient decreases when the liquid velocity is increased. This is shown in figure 6 where the friction coefficient, obtained from the individual data points of figure 5, is represented as a function of the Reynolds number in the downcomer with the valve position as a parameter. In the range of operation, the mean friction coefficient can be obtained from figure 6. The results are summarized in table 1 for the different operation conditions.

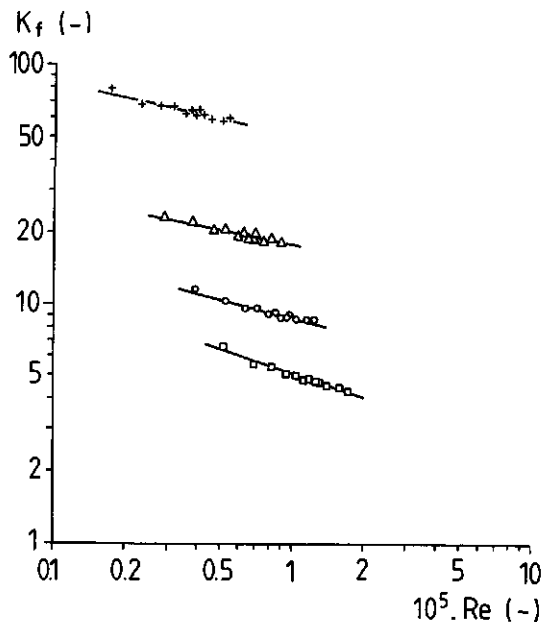


Fig. 6 The friction coefficient as a function of the Reynolds number (Key given in table 1)

The Zuber and Findlay model

In figure 7 the relationship between the total flow rate, averaged for the column length, and the local gas velocity is given for different valve positions. For all valve positions up to a certain defined value of the total

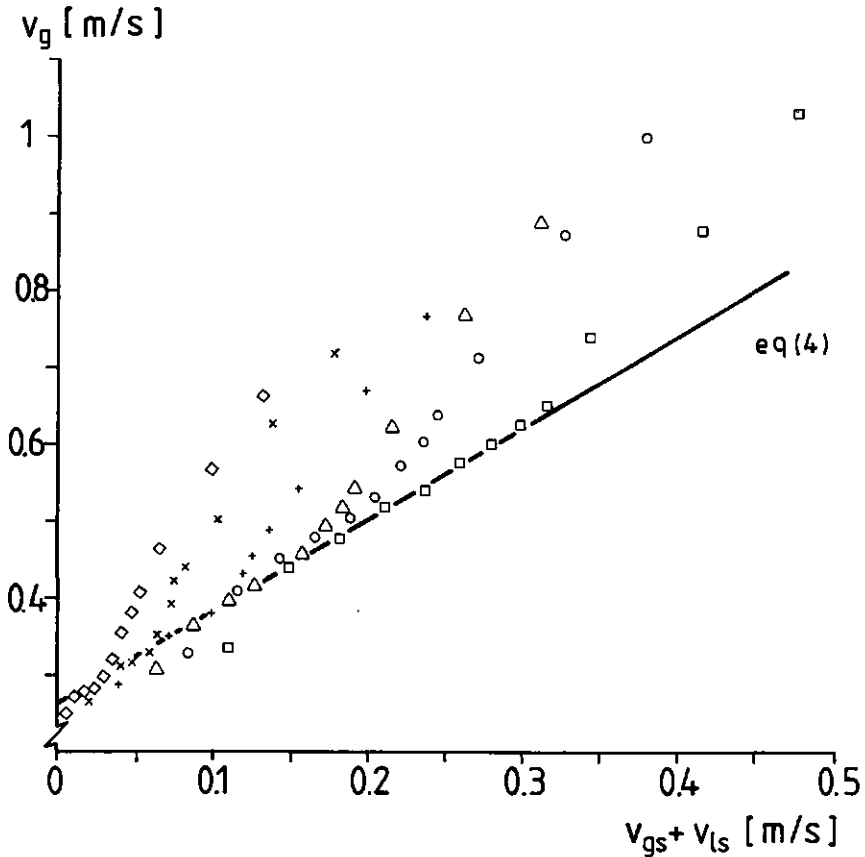


Fig. 7 The gasvelocity as a function of the total flow rate in the riser (Key given in table 1).

gas-liquid flow rate, a straight line can be fitted to the experimental data as shown in figure 7. The points corresponding to the lowest total gas-liquid flow rate are not incorporated in the fit-procedure. The straight line thus obtained represents the linear relationship resulting from the Zuber and Findlay two-phase drift flux model (eq(2)) and can be mathematically expressed by:

$$v_g = 1.2(v_{ls} + v_{gs}) + 0.26 \quad (4)$$

For each sequential valve position the experimental values will obey eq(4) (the drawn line in figure 7), up until a maximum value of the total flow. From this point onward, the results deviate from eq(4). The total-flow value at which the deviation starts decreases with an increasing valve closure indicating that the flow pattern changes at different friction coefficients. This means that hydrodynamic calculations based on the plug flow behaviour of an ALR are only valid up to a maximum value of the total flow. These findings are in contradiction with the results of Merchuk and Stein [4] who concluded from their work that eq(2) is valid for the entire trajectory in the transition-flow regime. However, a closer look to their results learns that the experimental values of the total flow and the gas velocity for each case are below the total gas-liquid flow rate at which a deviation from eq(2) can be expected, according to the criterium to be presented in the next paragraph.

The transition regime

In the literature several empirical correlations are reported describing the liquid velocity in an ALR as a function of the gas velocity [4,12,13] having the general form:

$$v_{ls} = a \cdot v_{gs}^b \quad (5)$$

However, the values of the coefficients a and b are not constant for the entire gas input range at which an airlift can be operated. This is shown in figure 8 where the superficial liquid velocity and the superficial gas-velocity are plotted on a double logarithmical scale. A discontinuity is shown in the curve which appears at lower gas input rates when the valve is further shut. The value of b , in our case, is $b = 0.44 (\pm 0.01)$ for low gas velocities while for high gas velocities b is reduced to values ranging from $b = 0.26-0.31$. Obviously, for high gas velocities and depending on the position of the valve, there exists a spread in results for the coefficient b . For low gas velocities the coefficient is independent of the position of the valve. It can also be concluded from figure 8 that an increment of the

friction diminishes the value of a . Merchuk and Stein [4] also noticed these phenomena and attributed these effects to the transfer of bubble flow to turbulent bubble flow in the column. Onken and Weiland [12] and van der Lans [13] were able to describe their results for an ALR with one single value for the exponent.

The position of the discontinuity for the individual lines in figure 8 coincides with the start of the deviation from the Zuber and Findlay relation (eq(2))

in figure 7, as is shown in table 2. Apparently, a change in flow pattern is responsible for this deviation. The background of this change of flow pattern can be explained when the typical hydrodynamic flow behaviour of a bubble column is considered according to Joshi and Sharma [10] (eqn(3)). From their model it is derived that there exists a heterogeneous circulation flow pattern inside the bubble column when the slip velocity, v_s , is greater than the rise velocity of a single bubble in an infinite medium, $v_{b,\infty}$. When the slip velocity, v_s , is calculated, the circulating velocity can be obtained from the model of Joshi and Sharma. By applying eqn(3) for the present reactor a circulation velocity can be obtained thereby suggesting the appearance of circulation cells. This would imply a heterogeneous flow pattern though the actual flow pattern can be very accurately predicted by the plug-flow model of Zuber and Findlay. Obviously, the relative high liquid flow rates in the upflow region of the ALR suppresses the existence of the circulation cells. In figure 9, the ratio of the superficial liquid velocity in the riser and the calculated liquid circulation velocity from eqn (3) is given as a function of the superficial gas velocity for ALR operation and two intermediate valve positions. From this figure it can be seen that each

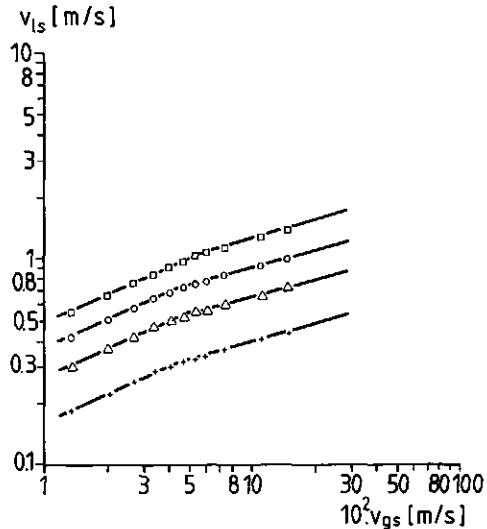


Fig. 8 The superficial downcomer liquid velocity as a function of the superficial gas velocity (Key given in table 1).

relation crosses the line for which v_{ls} equals v_{cl} . As the subtraction, $v_s - v_{b,\infty}$, in equation (3) could not be revealed with a sufficient accuracy in the range of interest, it was impossible to determine the separate tran-

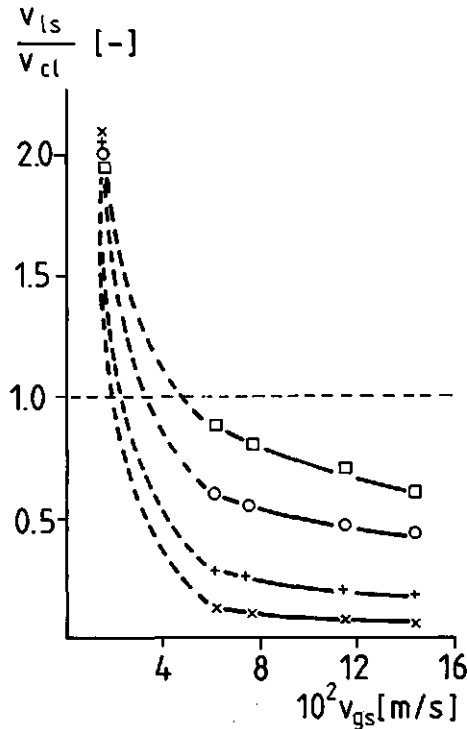


Fig. 9 The ratio of the superficial liquid velocity in the riser and the circulation velocity as a function of the superficial gas velocity (Key given in table 1)

sition gas velocities. Only a range for the gas velocities can be denoted where the circulating velocity equals the superficial liquid velocity. A comparison of the figures 7 and 9 learns that if the circulation velocity in the ALR, calculated from eq(3), significantly exceeds the superficial liquid velocity, the Zuber and Findlay theory is no longer valid as the relevant points in figure 9 correspond with the four points in figure 7 having the highest flow rate. Apparently, the ALR type of flow has been transferred into a BC type of flow which in our case has been represented by the circulation-cell model. From this view, in conclusion, a simple criterium is

postulated leading to a discrimination between both types of flow in the transition regime. The criterium states that the change between an ALR-type of flow and a BC-type of flow can be expected when:

$$v_{ls} \approx v_{cl} \quad (6)$$

If eqn [6] holds for an ALR the flow in such a reactor can be very well modelled by the two phase flow drift flux model of Zuber and Findlay. This conclusion also indicates that the hydrodynamic model of Verlaan et al. [8] only gives an accurate description of liquid velocities and gas hold-ups until a hydrodynamic transition occurs, according to eqn(6). If the superficial liquid velocity obviously exceeds the liquid circulation velocity, the airlift is operated as a bubble column and the above-mentioned hydrodynamic model will calculate progressive values for the gas hold-up and the liquid velocity as the gas velocity is underestimated by the Zuber and Findlay model.

CONCLUSION

The gas hold-up in an ALR is, in contrast to a BC, determined by the liquid velocity. When the friction in an ALR is enhanced, the liquid velocity will be reduced thereby enlarging the gas hold-up. The maximum value will be obtained when the ALR is operated as a BC. For the latter operation mode the gas hold-up in our reactor reaches values of 170% of the initial ALR value. The liquid velocity was found to be a simple power-law function of the gas flow rate for both reactor configurations; the coefficients depending on the flow characteristics of the reactor configuration. The liquid flow in a BC is characterized by the liquid circulation velocity according to the circulation-cell model of Joshi and Sharma. In the ALR the flow was represented according to the drift-flux model of Zuber and Findlay. In the transition flow regime between both reactor configurations the hydrodynamic calculations based on the plug-flow behaviour of an ALR are only valid up to a maximum value of the total gas-liquid flow rate. For greater values, the ALR type of flow will change into a BC type of flow. A simple criterium qualifies the distinction between both flow patterns, determined by the superficial liquid velocity and the liquid circulation velocity.

REFERENCES

- [1] M.L. Lefrançois, C.G. Mariller and J.V. Mejane. Effectonnements aux procedes de cultures Forgiques et de fermentations industrielles. Brevet d'Invention, France, no. 1 102 200 (1955).
- [2] P. Verlaan, A.M.M. van Eijs, J. Tramper, K. van 't Riet and K. Ch. A. M. Luyben. Estimation of axial dispersion in individual sections of an airlift-loop reactor. Submitted for publication. (Chapter three of this thesis).
- [3] P. Verlaan, M.A.F. Hermans, J. Tramper, K. van 't Riet and K.Ch.A.M. Luyben. Isobaric and non-isobaric modelling of dynamic gas-liquid oxygen transfer in an airlift-loop bioreactor. Submitted for publication. (Chapter four of this thesis).
- [4] J.C. Merchuk and Y. Stein. Local hold up and liquid velocity in airlift reactors. *AIChEJ.*, 27 (1981) 377-388.
- [5] N. Zuber and J.A. Findlay. Average volumetric concentration in two-phase flow systems. *J. Heat Transfer*, November (1965) 453-468.
- [6] J.C. Merchuk. Gas hold-up and liquid velocity in a two dimensional air-lift reactor. *Chem. Eng. Sci.*, 41 (1986) 11-16.
- [7] T. Menzel, H.J. Kantorek, K. Franz, R. Buchholz and U. Onken. Zur Strömungsstruktur in Airlift-Schlaufenreaktoren. *Chem. Ing. Techn.*, 57 (1985) 139-141.
- [8] P. Verlaan, J. Tramper, K. van 't Riet and K.Ch.A.M. Luyben. A hydrodynamic model for an airlift-loop bioreactor with external loop. *Chem. Eng. J.*, 33 (1986) B43 (Chapter two of this thesis).
- [9] J.B. Joshi and Y.T. Shah. Hydrodynamic and mixing models for bubble column reactors. *Chem. Eng. Commun.*, 11 (1981) 165-199.
- [10] J.B. Joshi and M.M. Sharma. A circulation cell model for bubble columns. *Trans.I.Chem.E.*, 57 (1979) 244-251.
- [11] G.B. Wallis, *One dimensional two phase flow*, McGraw-Hill, New York, 1969.
- [12] U. Onken and P. Weiland. Hydrodynamics and mass transfer in an airlift loop fermentor. *Eur. J. Appl. Microbiol. Biotechnol.*, 10 (1980) 31-40.
- [13] R.G.J.M. van der Lans, *Hydrodynamics of a bubble column loop reactor*, Thesis, Delft University of Technology, Delft, 1985.

NOMENCLATURE

α	gas hold-up	{-}
ν	viscosity	[m ² /s]
C	flow parameter	{-}
D	diameter	[m]
g	gravitational constant	[m/s ²]
K_f	friction coefficient	{-}
L	length	[m]
Re	Reynolds number:	
	Re= $v.D/\nu$	{-}
v	velocity	[m/s]
$v_{b,\infty}$	rise velocity of a single bubble in an infinite medium	[m/s]
z	coordinate	[m]

Subscripts

cl	according to the liquid circulation
d	downcomer
g	gas
l	liquid
r	riser
s	superficial, slip

CHAPTER SIX

FROM BUBBLE COLUMN TO AIRLIFT-LOOP REACTOR:
AXIAL DISPERSION AND OXYGEN TRANSFER

P. Verlaan, J.-C. Vos and K. van 't Riet
Department of Food Science, Food and Bioengineering Group,
Agricultural University,
De Dreyen 12, 6703 BC Wageningen, The Netherlands.

ABSTRACT

Axial dispersion and oxygen transfer were investigated in a bubble column with a circulation loop. A butterfly valve, situated at the bottom of the loop enabled us to study the above-mentioned physical characteristics in the transition regime between typical airlift-loop-reactor (ALR) flow and bubble-column (BC) flow. The Bodenstein number was found to decrease when the liquid velocity was reduced, implicating a less established plug flow character. The number of circulations required to achieve complete mixing in the reactor was diminished if the liquid circulation was hampered and appeared to be proportional to the Bodenstein number. The volumetric oxygen transfer coefficient was estimated by an ideally-stirred-tank reactor (STR) model and a plug-flow model. The STR model yielded reliable results for the whole range of operation while the plug-flow model only appeared to be appropriate for the ALR operation mode. The k_{1a} values obtained, were included in a generalized correlation for the transition flow regime and were found to increase gradually when the circulation velocity was reduced.

Submitted for publication.

INTRODUCTION

Various types of bioreactors are presently used in biotechnological processes, the airlift-loop reactor (ALR) being a recent development. The ALR concept has been evolved from that of the bubble column (BC) and was first described by Lefrançois et al. [1]. The special feature of the ALR is the recirculation of the liquid through a downcomer, connecting the top and the bottom of the main bubbling section (the riser). Due to the high circulation flow rate, efficient mixing is combined with a controlled liquid flow in the absence of mechanical agitators, as has been reported earlier [2]. Moreover, an ALR satisfies a high oxygen demand, particularly for large ALR configurations (50-100 m).

A major problem in characterizing and modelling mixing and oxygen transfer in an ALR is the characterization of the flow pattern in both reactor columns. In general, a distinction can be made between a heterogeneous liquid flow (typical for a BC reactor), a uniform liquid flow and a transition between both flow phenomena. Each flow pattern has its own responsive chord on reactor performance. This problem has been recognized earlier in the literature, especially in relation to the comparison of experimental data between bubble columns and loop reactors. Weiland [3] and Bello et al. [4] for instance investigated axial dispersion in a pilot plant ALR and compared the results between bubble column and airlift operation in the same unit. Weiland found a decrease of the dispersion coefficient at an increasing liquid velocity. Bello et al. reported an increase of the volumetric oxygen transfer coefficient of 22-75% for the BC, dependent on the gas input rate and relative to the ALR value. Heijnen and van 't Riet [5] reviewed experimental data in the literature for ALRs and BCs and concluded that oxygen transfer in a BC is more convenient than in an ALR due to the relative long residence time of the bubbles in the column. Axial dispersion was found to be dependent of the flow behaviour in the column. They concluded that existing correlations for dispersion coefficients in BCs and ALRs must be regarded critically unless the flow behaviour is characterised.

Clearly, some data and correlations for axial dispersion and oxygen transfer concerning air water systems in BCs and ALRs are available. No information of axial dispersion and oxygen transfer in the transition flow regime between an ALR and a BC is, however, existing. In this paper we shall con-

concentrate on axial dispersion and oxygen transfer in an ALR and a BC and the results will be compared with the criteria for the flow transition between both reactor configurations according to Verlaan et al. [6]. The results of our investigations can be an important tool in scaling-up and designing mass transfer and mixing processes in an ALR.

EXPERIMENTAL SET-UP

The pilot plant ALR used, has a working volume of 0.165 m^3 and a height of 3.23 m and has been described in more detail earlier [2,7]. It was designed such that no gas entrained into the downcomer. The liquid level was kept 0.13 m above the bottom of the cistern in the absence of gas, in order to maintain about the same liquid velocity in the riser and in the topsection. Temperature was fixed on a value of 30° C . The reactor was filled with Wageningen tap water with quite consistent properties. At the bottom of the reactor in between the riser and the downcomer, a butterfly valve was positioned in order to influence the liquid velocity independent of the gas injection rate (figure 1).

When the valve was totally closed, the riser functioned as a bubble column. The dispersion measurements were carried out as described by Verlaan et al. [2]. However in this case, the pH-electrode was positioned in the topsection of the reactor.

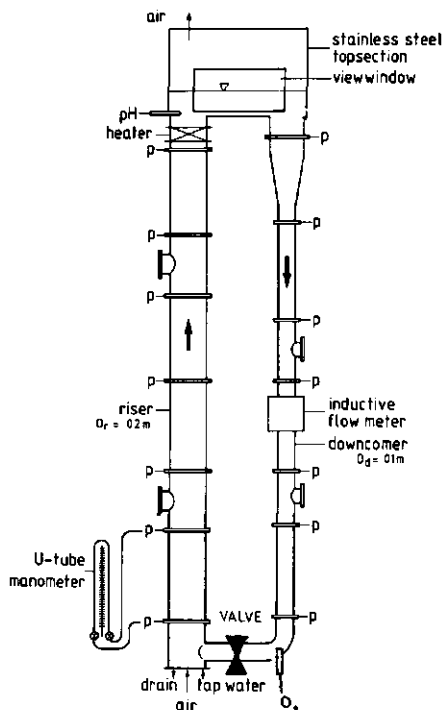


Fig. 1 The airlift-loop reactor.

Key	Valve position
□ ■	(open) 1
○ ●	4
△ ▲	5
+	6
×	7
◇	(closed) 8

Table 1. Key to the figures 2-7

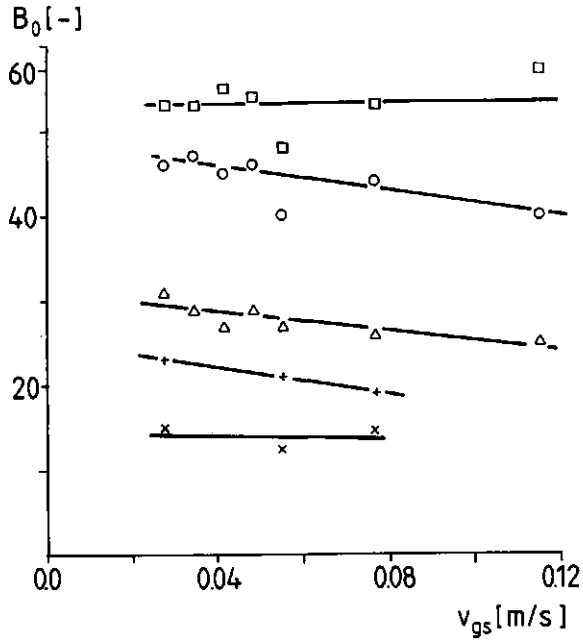


Fig. 2 The Bodenstein number as a function of the superficial gas velocity for different valve positions (Key given in table 1).

The dissolved oxygen concentration (DOC) was monitored by a polarographic electrode, positioned at the bottom of the downcomer and connected to an amplifier and a micro-computer. Detailed information about the experimental procedure is given by Verlaan et al. [7]. The oxygen electrode was positioned at the bottom of the downcomer thus ensuring a sufficient liquid flow at the membrane surface. When the valve was totally closed or when the liquid flow to the electrode was not sufficient, the electrode was positioned at the top of the riser. In this position, the electrode was equipped with a small propellor stirrer in front of the membrane thus keeping a sufficient liquid flow at the membrane surface.

RESULTS AND DISCUSSION

Axial dispersion

Axial dispersion has been expressed by the dispersion coefficient, D , and the dimensionless Bodenstein number defined as:

$$Bo = v.L/D \quad (1)$$

where v and L are the liquid velocity and the length of interest, respectively. The parameter estimation method has been described by Verlaan et al. [2]

Figure 2 shows the Bodenstein number of the ALR at different valve positions. Elsewhere [6] it is reported that the liquid velocity decreases and the gas hold-up increases with increasing valve closure. Combining this with figure 2, it means that the Bodenstein number decreases when the liquid circulation is reduced, implicating a less established plug flow character. When the reactor is operated as an ALR (valve totally open, position 1) the Bodenstein number increases slightly when the gas injection rate is enhanced, coinciding with earlier results [2,8,9]. For other valve positions, when the flow behaviour is intermediate between ALR and bubble column operation, the Bodenstein number decreases when the gas injection rate is increased, being more significant at an increased impediment of the liquid flow. These phenomena are in accordance with the results of Verlaan et al.

[6] who investigated the hydrodynamic properties of the transition flow regime between both reactor configurations. The authors stated that the circulation cell model as introduced by Joshi et al. [10], being typical for bubble columns, can also be applied to the ALR in the transition flow regime. When the liquid velocity in such a circulation cell approaches the superficial liquid velocity in the column, the typical plug flow behaviour of the ALR will be disturbed. For low gas velocities this effect will be less significant than for high gas velocities. For an increased valve closure the effect of the circulation cell will occur at a lower value of the gas velocity [6].

The dispersion coefficient in the ALR is calculated from eq (1) and shown in figure 3. For this purpose, the characteristic length, L , and the characteristic liquid velocity are adopted from Blenke [11]. The values are compared with the dispersion coefficients obtained from the empirical correlation of Joshi [12] for bubble columns. The dispersion coefficients calculated from the Joshi-correlation have lower values than the ALR-values as axial dispersion caused by the superimposed-liquid-induced turbulence is not incorporated in the empirical correlation.

As can be seen the dispersion coefficient increases with an increasing gas velocity. The dispersion coefficient is less sensitive to changes in the liquid velocity than the Bodenstein number. Apparently, the decrease in the Bodenstein number is mainly due to the reduced liquid velocity caused by the increased friction of the valve. This also implicates that the relative contribution of the bubbles and the induced liquid circulation cells to the axial disper-

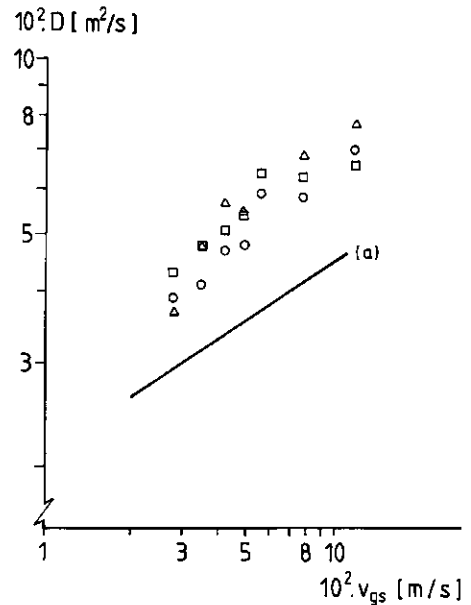


Fig. 3 The dispersion coefficient for different valve positions compared with a literature correlation (a) [12] (Key given in table 1).

sion process becomes more significant. This can be elucidated in terms of a change from plug flow to BC flow which determines the hydrodynamical properties in the reactor [6]. The change in axial dispersion caused by the transition, appears to be gradually.

Figure 4 shows the dimensionless mixing time, i.e. the ratio of the measured mixing time and the circulation time, as a function of the superficial gas velocity. For this purpose, the mixing behaviour of the ALR is classified according to the mixing time required to achieve a degree of mixing throughout the reactor with an inhomogeneity of less than 5% [2]. From figure 4 it is concluded that an increased friction in the reactor reduces the number of circulations required to achieve complete mixing in the reactor. The results are compared with the empirical correlation of Verlaan et al. [2] for an ALR, stating that the dimensionless mixing time is proportional to the Bodenstein number mathematically expressed by:

$$t_m/t_c = 0.093 \cdot Bo \quad (2)$$

As shown in figure 4, the correlation fits the present results for different valve positions, making equation (2) also suitable for the transition flow regime.

Oxygen transfer

The oxygen transfer coefficient in the bubble column was estimated by a non-isobaric plug-flow model and an isobaric stirred-tank-reactor (STR) model as described by Verlaan et al. [7]. Though the ALR is a typical plug-flow reactor, it exhibits a dualistic mixing behaviour due to its high circulation

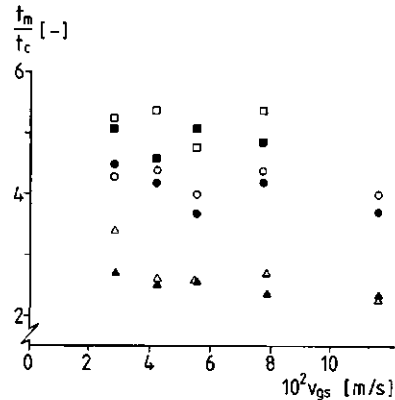


Fig. 4 The dimensionless mixing time as a function of the superficial gas velocity. Measurements (key given in table 1.) compared with calculated values (■, ●, ▲) obtained from eqn (2).

rate. As long as the reciprocal value of the volumetric oxygen transfer coefficient is smaller than the mixing time, the ALR can be modelled with sufficient accuracy as being a STR as discussed earlier [2,7]. In practice, for both reactor configurations, viz the ALR and the bubble column, the mixing is intermediate.

The mean volumetric oxygen transfer coefficient in the reactor, k_1a , is determined at different valve positions. The method given in [7] is applied, assuming plug flow and k_1a is averaged for the pressure variations and corrected for the residence time distribution in each reactor part [7]. The results are shown in figure 5 where the valve position is a parameter.

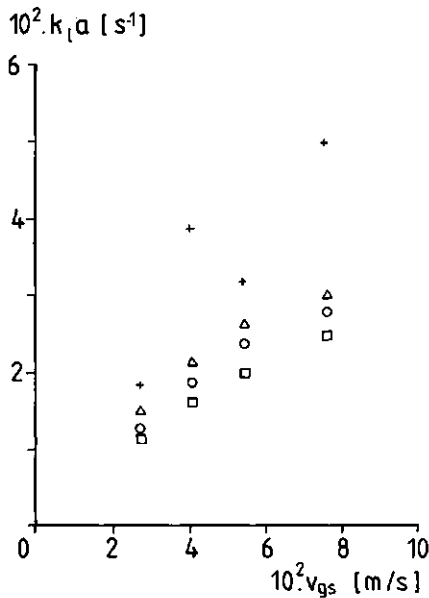


Fig. 5 The volumetric oxygen transfer coefficient, estimated by the plug-flow model, as a function of the superficial gas velocity (Key given in table 1).

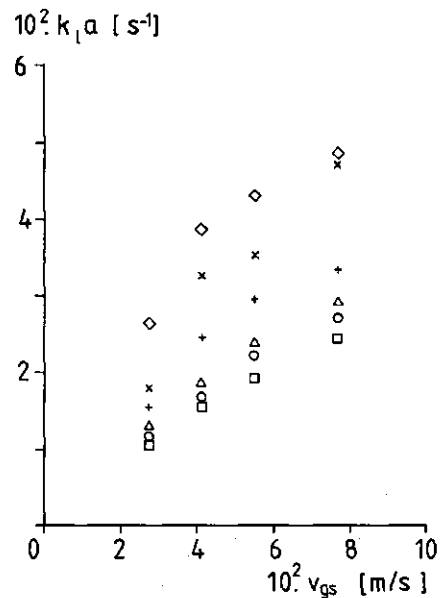


Fig. 6 The volumetric oxygen transfer coefficient, estimated by the STR model, as a function of the superficial gas velocity (Key given in table 1).

Figure 6 shows the k_1a values according to the STR-model. For the valve position 1 (ALR-operation) both results in figure 5 and figure 6 agree though the STR model yields conservative values in relation to the plug flow model, being in accordance with earlier findings [7].

Clearly, an impediment of the liquid flow in an ALR enhances the volumetric oxygen transfer coefficient. This is caused by the reduced liquid velocity

which increases the residence time of the gas phase in the riser of the ALR thus enhancing the gas hold-up. As a result the interfacial area is also increased being the main contribution to the increase of k_{1a} .

As made plausible in the previous section, the transition from ALR flow to BC flow is attended with a transition from plug flow to typical BC flow characteristics. The gas-induced circulation cells, responsible for the typical BC flow, disturb the plug-flow dramatically. As a result the plug-flow model in this case is no longer a suitable model for the estimation of the volumetric oxygen transfer coefficient k_{1a} . This is demonstrated in figure 5 where the results estimated by the plug-flow model for the valve position 6 show a considerable scatter. Apparently, the liquid velocity is hampered in such a way that typical plug flow behaviour has disappeared. This conclusion coincides with the results of Verlaan et al. [6] who studied the hydrodynamical characteristics of an ALR and a BC in the same unit. The

authors reported that in the pertinent range of gas velocities the liquid exhibits plug-flow behaviour for the valve positions 1, 4 and 5. For valve position 6, the typical ALR-plug-flow was found to change into BC-type of flow for the pertinent gas input range. For the same reason, if the liquid flow is reduced, the application of the STR-model for the estimation of k_{1a} becomes more admissible. This can be seen in figure 7, where at a given v_{gs} value, no distinct change of the mixing time is noticed, with reducing liquid flow while the reciprocal value for k_{1a} decreases. The constant mixing-time value is explained by the interaction of an increasing dispersion coefficient as shown in figure 3, and an increasing circulation time, having a neutral result on the mixing time.

Considering the above-mentioned findings, the criterium used for the

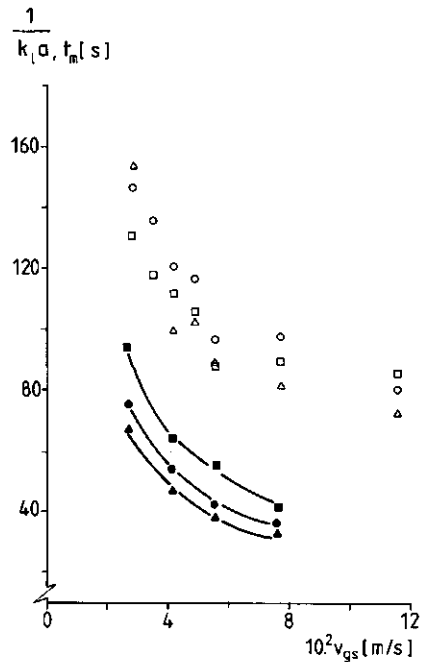


Fig. 7 The reciprocal volumetric oxygen transfer coefficient ($\blacksquare, \bullet, \blacktriangle$), compared with the mixing time ($\square, \circ, \triangle$) (Key given in table 1).

distinction between bubble column-flow and ALR-flow as stated by Verlaan et al. [6], is also recommended to distinguish between the use of typical BC and ALR k_{1a} -estimation methods, in our case being the plug-flow model for the ALR and the STR-model for the BC. For the present reactor, being operated as an ALR as well as for the transition regime, the STR method yields acceptable results for the volumetric oxygen transfer coefficient due to an acceptable ratio of mixing time and reciprocal k_{1a} .

A dimensional analysis of the parameters that, for the scope of this work, may affect the volumetric oxygen transfer coefficient in the reactor, yielded three dimensionless groups: the Stanton number, the Bodenstein number and the ratio of the superficial liquid and gas velocity. The Stanton number gives a measure of the mass transfer rate relative to the convective liquid flow ($St = k_{1a} \cdot L / v_{1s}$), the Bodenstein number represents the ratio of mass transport by dispersion and convection (eq (1)). The effects of viscosity, surface tension, diffusivity, ionic concentration, dimensions and gravitational force also were incorporated in the analysis but were not studied in this work. Hence, a correlation of the form of equation (3) is obtained to describe the Stanton number as a function of the ratio of the superficial liquid and gas velocity and the Bodenstein number:

$$St = 14.5(v_{gs}/v_{1s})^{0.83}Bo^{-0.6} \quad (3)$$

The correlation coefficient belonging to eq (3) amounted to 0.99. Equation (3) is a generalized correlation describing oxygen transfer in an ALR, a BC with a superimposed liquid flow and the transition region between both reactor configurations. The first exponent of the correlation (3) is in good agreement with the results of Bello et al. [4] who reported a value of 0.87. According to the results of Bello et al [4], equation (3) can be extended with a term $(1+A_d/A_r)^{-1}$ to account for different ratios of riser and down-comer diameters, thus obtaining the following equation:

$$St = 18.1(v_{gs}/v_{1s})^{0.83}Bo^{-0.6}(1+A_d/A_r)^{-1} \quad (4)$$

Figure 8 shows the comparison between the present results and results obtained from literature. As shown the results for the BC (valve totally closed) harmonize with the empirical correlation for BCs of Heynen and Van 't Riet [5]. Comparison with literature data for ALRs is less unambiguous as

there exists a considerable scatter in results due to the different geometries and dimensions of the ALRs used. This is shown in figure 8 where the ALR-results are compared with the empirical correlation of Bello et al. [4], the semi-theoretical correlation of Bello et al. [13] and the experimental data of Weiland [3] and van der Lans [14]. These data were all obtained from pilot-plant ALRs having the same geometry as the pertinent reactor. Deviations from our data can possibly be explained by the different dimensions of the ALRs used (height, slenderness) and the use of different gas spargers. The semi-theoretical correlation of Bello et al. [13], based on empirical correlations for the mass transfer coefficient, k_1 , and the local isotropic turbulence theory for the prediction of bubble diameters, fits our results fairly well. This coincides with earlier findings, stating that the gas-sparger region has no distinct influence on the overall volumetric oxygen transfer coefficient [7] and that bubbles in the ALR hardly interact [15].

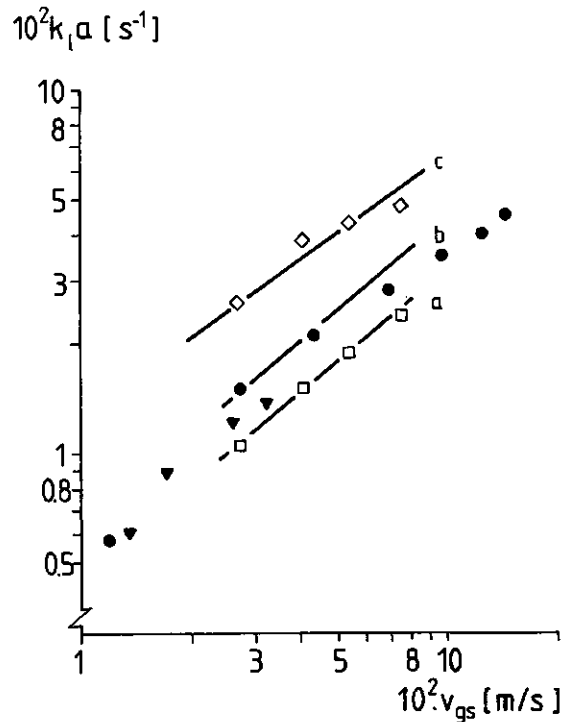


Fig. 8 The volumetric oxygen transfer coefficient compared with literature data. (a): semi-theoretical correlation of Bello et al. [13], (b): empirical correlation of Bello et al. [4], (c) correlation of Heynen and van 't Riet [5]. ● data of Weiland [3], ▼ data of van der Lans [14], □ own results valve position 1, ◇ own results, valve position 8.

CONCLUSIONS

In the transition flow regime between ALR flow and BC flow, the Bodenstein number was found to decrease from $Bo = 55$ to $Bo = 15$ respectively, implicating a less established plug flow for BC type of flows. As the dispersion coef-

ficient remained constant for the entire range of operation, the decrease of the Bodenstein number is mainly attributed to the decreased convective transport as a result of the reduced liquid velocity. The number of circulations required to achieve complete mixing was diminished if the liquid circulation was hampered and appeared to be proportional to the Bodenstein number.

The volumetric oxygen transfer coefficient was estimated by an STR-model and a plug-flow model. The STR model yielded reliable results for the entire range of operation while the plug-flow model only appeared to be appropriate for the ALR operation mode. The k_{1a} -values obtained, were found to increase from 0.01-0.025 s⁻¹ for ALR operation to 0.026-0.05 s⁻¹ for BC operation, the actual value depending on the gas injection rate. A generalized correlation is given for k_{1a} . In this correlation k_{1a} is proportional to the 0.83 power of the ratio of the superficial liquid and gas velocity and proportional to the -0.6 power of the Bodenstein number.

REFERENCES

- [1] M.L. Lefrançois, C.G. Mariller and J.V. Mejane. Effectonnements aux procedes de cultures forgiques et de fermentations industrielles. Brevet d'Invention, France, no. 1 102 200 (1955).
- [2] P. Verlaan, J. Tramper, K. van 't Riet and K.Ch.A.M. Luyben. Estimation of axial dispersion in individual sections of an airlift-loop reactor. Submitted (Chapter three of this thesis).
- [3] P. Weiland, 1978, Untersuchung eines Airliftreaktors mit Aüßerem Umlauf im Hinblick auf seine Anwendung als Bioreaktor, Thesis, University of Dortmund, Dortmund GDR.
- [4] R.A. Bello, C.W. Robinson and M. Moo-Young. Gas Holdup and Overall Volumetric Oxygen Transfer Coefficient in Airlift Contactors. *Biotechnol. Bioeng.*, 27, (1985) pp 369-381.
- [5] J.J. Heijnen, and K. van 't Riet, 1982, Mass transfer, mixing and heat transfer phenomena in low viscous bubble column reactors. Proc. 4th Europ. Conf. on Mixing, Noordwijkerhout, The Netherlands.
- [6] P. Verlaan, J.-C. Vos and K. van 't Riet. From bubble column to airlift-loop reactor. Hydrodynamics of the transition-flow regime. Submitted (Chapter five of this thesis).
- [7] P. Verlaan, M.A.F. Hermans, J. Tramper, K. van 't Riet and K.Ch.A.M. Luyben. Isobaric and non-isobaric modelling of dynamic gas-liquid oxygen transfer in an airlift-loop bioreactor. Submitted (Chapter four of this thesis).
- [8] P. Verlaan, J. Tramper, K. van 't Riet and K.Ch.A.M. Luyben. Hydrodynamics and axial dispersion in an airlift-loop bioreactor with two and three phase flow. Proc. Int. Conf. on Bioreactor Fluid Dynamics (BHRA) Cambridge, England, 15-17 april, 1986.
- [9] P. Verlaan and J. Tramper. Influence of nearly floating particles on the behaviour of a pilot plant airlift-loop bioreactor. Proc. 4th Europ. Congress on Biotechnology, 1987, vol. 1, pp 101-104 (O.N. Neijssel, R.R. van der Meer, K.Ch.A.M. Luyben eds.) Elsevier Science Publishers B.V., Amsterdam.
- [10] J.B. Joshi and M.M. Sharma. A circulation cell model for bubble columns. *Trans. Inst. Chem. Engrs*, 57, 1979, pp 244-251.
- [11] H. Blenke, 1979, Loop reactors, *Adv. Biochem. Eng.* 13, 121-214.
- [12] J.B. Joshi. Axial mixing in multiphase contactors - a unified correlation. *Trans. I. Chem. Eng.* 58 (1983) 155-165.
- [13] R.A. Bello, C.W. Robinson and M. Moo-Young. Prediction of the volumetric mass transfer coefficient in pneumatic contactors. *Chem. Eng.*

- Sci. 40, 1, (1985) pp. 53-58
- [14] R.G.J.M. van der Lans. Hydrodynamics of a bubble column loop reactor, Thesis, Delft University of Technology, Delft, 1985.
- [15] P. Verlaan, J. Tramper, K. van 't Riet and K.Ch.A.M. Luyben, 1986, A Hydrodynamic model for an airlift-loop bioreactor with external loop. Chem. Engng. J., 33, B43-B53 (Chapter two of this thesis).

NOMENCLATURE

A_d	downcomer cross-sectional area	$[m^2]$
A_r	riser cross-sectional area	$[m^2]$
D	dispersion coefficient	$[m^2/s]$
L	length	$[m]$
k_{1a}	volumetric oxygen transfer coefficient	$[s^{-1}]$
t_m	mixing time	$[s]$
t_c	circulation time	$[s]$
v	velocity	$[m/s]$
v_{1s}	superficial liquid velocity	$[m/s]$
v_{gs}	superficial gas velocity	$[m/s]$

Abbreviations

ALR	airlift-loop reactor
BC	bubble column
Bo	Bodenstein number: $Bo = v_{1s} \cdot L / D$
St	Stanton number : $St = k_{1a} \cdot L / v_{1s}$
STR	ideally stirred tank reactor

CHAPTER SEVEN

HYDRODYNAMICS, AXIAL DISPERSION AND GAS-LIQUID OXYGEN TRANSFER
IN AN AIRLIFT-LOOP BIOREACTOR WITH THREE-PHASE FLOW

P. Verlaan and J. Tramper,
Department of Food Science, Food and Bioengineering Group,
Agricultural University,
De Dreijen 12, 6703 BC Wageningen, the Netherlands.

ABSTRACT

Hydrodynamics, axial dispersion and oxygen transfer in a pilot plant airlift-loop bioreactor (0.165 m³) with a three-phase flow have been studied in order to investigate the influence on the physical properties of an airlift-loop reactor (ALR). The third phase consisted of polystyrene or calcium alginate beads both with a density of $\rho = 1050$ kg/m³ and diameters ranging from 2.4 to 2.7 mm, being good representatives for immobilized biocatalysts. It was found that the overall reactor performance is strongly influenced by the presence of the solid phase. The maximum bead loading at which the ALR could be operated was 40 volume-percent. At this loading the liquid velocity declined to 60% of the initial two-phase value independent of the gas injection rate while the gas hold-up decreased from 80% to 20% of the two-phase value depending on the gas injection rate. The essential mixing parameter, the Bodenstein number, tended to a 40% higher value at this loading indicating a better established plug flow. The influence of the solid phase on the volumetric oxygen transfer coefficient k_{1a} was investigated to a maximum bead loading of 20 volume percent. In this case, the k_{1a} -value decreased with 40% compared to the two-phase value.

Published in: Proc. Int. Conf. on Bioreactors and Biotransformations, 9-12 november 1987, Auchterarder, U.K. Elseviers Science Publishers B.V., Amsterdam.

INTRODUCTION

An airlift-loop reactor is a so called second generation type of bioreactor in which efficient oxygen transfer and mixing is combined with a controlled liquid flow while the shear rate can be very low. These properties make the ALR a suitable reactor for shear sensitive organisms requiring a controlled dissolved oxygen concentration. An example of such an application is the production of secondary metabolites by plant cells [1]. In many cases immobilized biocatalysts or micro-organisms growing in aggregates are used in biotechnological production processes. This means that the biophase in the reactor is concentrated in or on beads with diameters up to several millimeters. Also in this case an ALR seems a suitable reactor having excellent suspension characteristics due to the high liquid velocity.

Little research has been reported yet on the influence of relatively large (2-3 mm) particles with a neutral buoyancy, like gel-entrapped biocatalysts, on bioreactor performance. Recently, Frijlink [2] published results on the influence of calcium alginate beads ($\rho = 1050 \text{ kg/m}^3$, $d = 2.2 \text{ mm}$) on oxygen transfer in a stirred-tank reactor. The author found that the volumetric oxygen transfer coefficient decreased proportional with the bead loading. For a bead loading of 37 vol-percent the decrease amounted to 55%-59%, depending on the gas-flow rate. Metz [3] reported results on the influence of yeast pellets on oxygen transfer in a bubble column. A pellet loading of 20% diminished the k_1a -value with 20-30 %.

For ALRs no such data is available. Therefore the aim of this article is to give a concise overview of the physical ALR properties and the interaction with relative large solid particles in order to provide essential information for three phase ALR design. Results are reported on the physical influence of neutral buoyant polystyrene or calcium alginate beads with diameters ranging from 2.4 to 2.7 mm, on ALR performance at pilot plant scale.

MATERIALS AND METHODS

The experiments have been carried out in a pilot plant ALR with external loop as shown in figure 1. The ALR has a reactor volume of 0.165 m^3 and an aerated height of 3.23 m . The upflow and downflow sections, also called riser and downcomer, were constructed of borosilicate glass pipe sections with diameters of 0.2 m and 0.1 m , respectively. The gas sparger, situated at the bottom of the riser, produces bubbles with the same diameter as the equilibrium diameter of air bubbles in tap water. The topsection of the ALR was designed such that complete deaeration occurs during operation and no gas entrains into the downcomer. The ALR was filled with Wageningen tap water and its temperature was maintained on a constant value of 30° C . More details about the ALR and measuring methods of the hydrodynamic parameters are given elsewhere [4].

The mixing performance of the ALR was characterized by estimating the axial dispersion number on the basis of pulse response measurements using acid and base as tracers. Detection of these tracers by pH-electrodes was not disturbed by the presence of air bubbles or solid beads. A mathematical description and detailed information about the experimental method have been published earlier [5,6].

The typical ALR mixing characteristics allowed us to treat the modelling of oxygen transfer in two different ways. On the one hand the ALR behaves like a loop reactor with relative high circulation rates and a short mixing time. From this point of view the reactor can be modelled as an ideally stirred

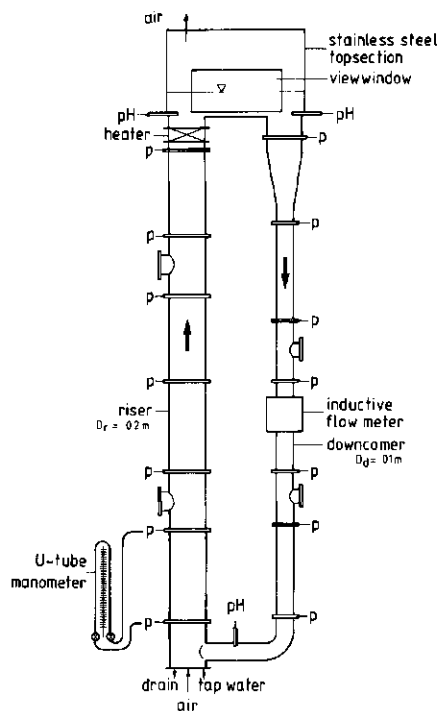


Fig. 1 The airlift-loop reactor

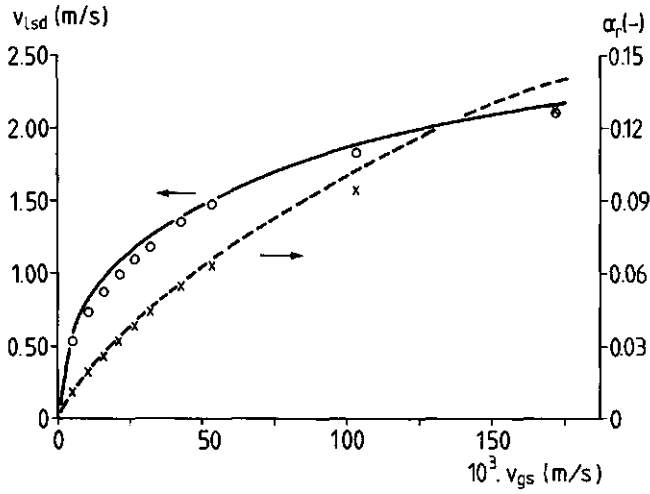


Fig. 2 The downcomer liquid velocity and the riser gas hold-up as a function of the superficial gas velocity in the riser: (o,x) experimental; (—,---) simulation

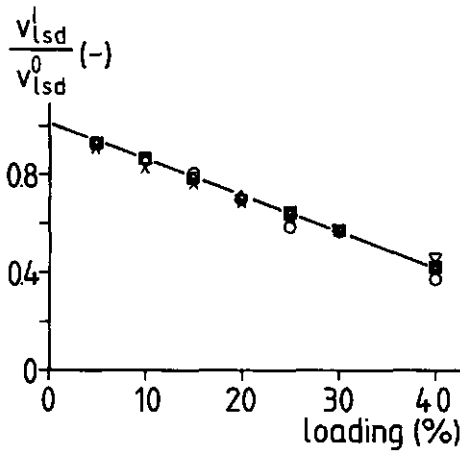


Fig. 3 The relative liquid velocity as a function of the particle loading and the superficial gas velocity as a parameter. (Key given in fig. 4).

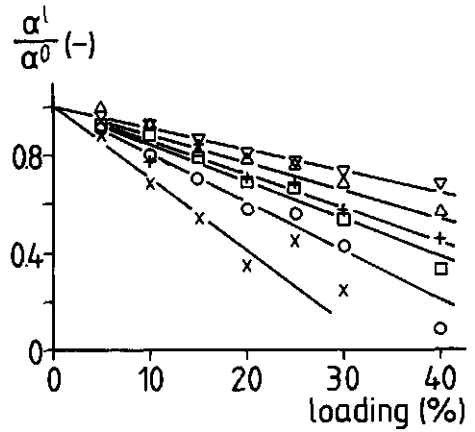


Fig. 4 The relative gas hold-up as a function of the particle loading and the superficial gas velocity as a parameter. (Key: $10^3 v_{gs}$ [m/s]: X 0.54; O 1.07; □ 2.14; + 3.75; Δ 6.88; ▽ 17.2)

tank reactor (STR) [7]. On the other hand the ALR is a tube reactor in which the liquid phase as well as the gas phase behaves like plug flow which has been experimentally verified earlier [5]. In this work, k_1a -experiments in the three phase flow have been carried out by the STR-method for reasons of simplicity.

The solid phase used consisted of calcium alginate or polystyrene spheres with a particle density and diameter of $\rho = 1050 \text{ kg/m}^3$ and $d = 2.35 - 2.7 \text{ mm}$, respectively. The polystyrene spheres have been used in the hydrodynamic and axial dispersion measurements. Both the polystyrene and the calcium alginate spheres have been used in the oxygen transfer experiments. The calcium alginate spheres were produced by a new method described by Hulst et al. [8] which makes it possible to produce large quantities of beads in a relative short time.

RESULTS AND DISCUSSION

Hydrodynamics

Figure 2 shows the results of the hydrodynamic experiments together with model evaluations for both the liquid velocity in the downcomer and the gas hold-up in the riser. The model calculations were derived from an iterative procedure which has been described by Verlaan et al. [4].

For low gas input rates the liquid velocity and gas hold-up are very sensitive to changes in the gas input rate. For high input rates on the other hand only a minor increment of the liquid velocity or the gas hold-up is observed when the gas velocity is increased. The model gives an adequate prediction of the flow behaviour in the ALR with an accuracy of at least 5-10%.

When the polystyrene particles were added to the ALR up to a loading of 40% the liquid velocity decreased gradually to 40% of the initial two phase value as is shown in figure 3. This was also the maximum loading at which the ALR could be operated. When the reactor was stopped it was not possible to restart the liquid circulation at this loading mainly due to the fact that the packed bed volume of the particles approximated the aerated riser volume. The decrease in velocity is caused by a decrease in gas hold-up and

an increased friction. The decrease in gas hold-up is clearly shown in figure 4 and, in contrast to the liquid velocity, strongly affected by the gas injection rate. Obviously, the presence of the particles increases the collision frequency due to the diminished flowed area for the air-water mixture. As a result the coalescence process will be stimulated which on its turn reduces the gas hold-up. For high gas velocities and gas hold-ups, when bubbles already interact, this effect will be of less importance than for low gas velocities. Hence, for low gas velocities a reduction of 60% is achieved at a bead loading of 20% while for high gas input rates the gas hold-up is reduced about 20% at a bead loading of 40%.

Of course, the coalescence process also depends on the local solids concentration and the particle size. Epstein [9] reviewed the mechanisms reported in literature which could be responsible for bubble characteristics and therefore on gas hold-up in a three-phase system. Agreement exists on the assumption that small particles increase the bubble coalescence rate due to the enhanced viscosity of the pseudohomogeneous three-phase medium. For large particles on the contrary several theories are introduced to account for bubble disintegration. As in our case the particles are neutral buoyant and easily follow the liquid motion, the effect of turbulence induced by the particles on bubbles will be of minor importance. We believe that in our system bubbles will break up if the solid particles have sufficient inertia to penetrate the surface of a bubble, when the Weber number $We = \rho v^2 d / \sigma$, the numerical criterium for break-up, exceeds about 3 [9,10]. As in our system the Weber number is about three, it is assumed that neither the bubble coalescence nor the bubble disruption according to the above theories, contribute significantly. These findings are in accordance with the results of Brück and Hammer [11] who concluded that solid beads with densities less than 1050 kg/m³ and diameters ranging from $d=0.06$ to $d=4.35$ mm, cause a decrease in gas hold-up. The authors explained this by the increased solid hold-up and the increased suspension viscosity while they also support the criterium for bubble break-up mentioned above.

As the liquid velocity and the gas hold-up are unambiguously related to each other according to Verlaan et al. [4], the results in figure 3 and figure 4 might at first view seem discrepant in relation to the context mentioned above. The relationship between the liquid velocity and the gas hold-up can be mathematically formulated by:

$$\rho g \alpha L = \frac{1}{2} K_f \rho v^2 \quad (1)$$

where ρ is the liquid density, g the gravitational constant, α the gas hold-up in the riser, L the aerated length, v the superficial liquid velocity and K_f the overall friction coefficient. From equation 1 it should be expected that the dependency of the gas hold-up, shown in figure 4 also should occur in the results shown in figure 3. However, figure 5 demonstrates that in contrast to gas-liquid flow [4],

friction in a three phase flow is severely influenced by the gas injection rate. This happens in such a way that for high gas velocities the increased friction counterbalances the decrease in the relative influence of the gas injection rate on the liquid velocity. As is also shown in figure 5 friction increases with an increasing particle loading. Both phenomena can be explained by the fact that for an increased gas injection rate or an increased bead loading, bubbles tend to concentrate in the middle of the column which has been verified by visual observation. As a result the solid phase concentration at the wall of the column will increase, thus enlarging friction. This phenomenon has been experimentally demonstrated by Linnenweber and Blaß [12] in a bubble column. They found that the solid hold-up at the tube wall of a bubble column with gas hold-ups ranging from $\alpha=0.05$ to $\alpha=0.1$, is twice as high as the solid hold-up in the centre of the tube. The authors also report that this effect becomes less significant at high gas injection rates which in our case corresponds to the results in figure 5.

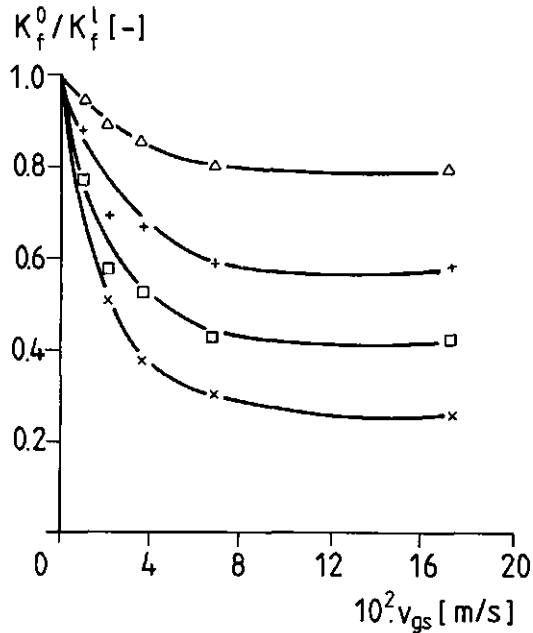


Fig. 5 The friction coefficient of the three phase flow relative to the friction coefficient of the two phase flow as a function of the superficial gas velocity and the bead loading as a parameter (x 40%, □ 30%, + 20%, Δ 5%)

Mixing

An important parameter to quantify axial dispersion characteristics in a tubular reactor is the dimensionless Bodenstein number (Bo) which represents the ratio of convective mass transport and mass transport by axial dispersion. Results for gas-liquid flow in the pertinent ALR are shown in figure 6 which are obtained from the results of Verlaan et al. [6]. As is shown in figure 6, the Bodenstein values lie in between $50 < Bo < 60$ depending on the gas injection rate and indicating a plug flow character.

Addition of a solid phase consisting of polystyrene spheres significantly enhances the Bodenstein number up to 50% for a bead loading of 40% (figure 7). Obviously, the presence of polystyrene spheres in the gas-liquid flow damps the small eddies which are, apart from other mechanisms, responsible for the axial dispersion. In the literature, there is no agreement on this subject. In his literature overview,

Frijlink [2] concludes that sometimes particles are said to dampen the turbulence in the continuous liquid phase while

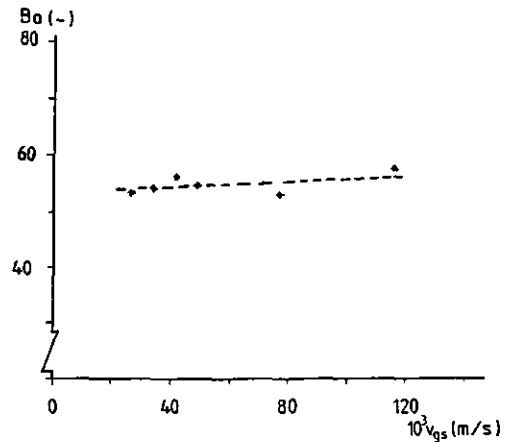


Figure 6. The Bodenstein number as a function of the superficial gas velocity

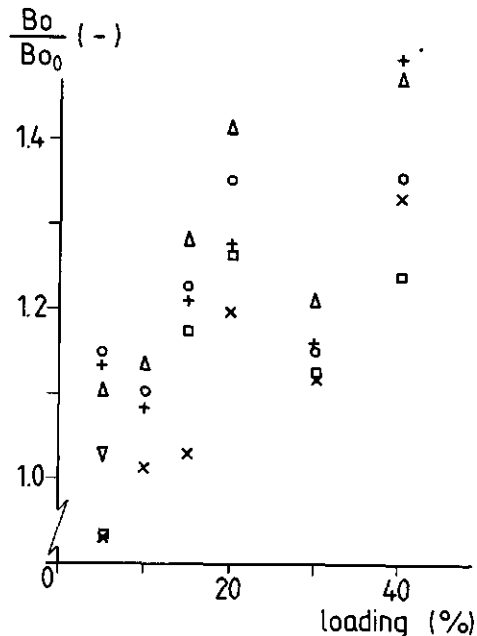


Fig. 7 The relative Bodenstein number as a function of the relative bead loading. (Key: $10^3 v_{gs}$ [m/s]: ∇ 2.08; \times 3.47; \square 5.54; Δ 7.71; $+$ 10.22; \circ 13.76)

in other cases they are supposed to increase turbulence intensities, depending on particle size and particle density. Epstein [9] and Kelkar [14] conclude that small particles in a three phase flow do not significantly influence axial dispersion as solid dispersion is mainly determined by the liquid dispersion. When particle sizes become larger solid and liquid phase dispersion start to differ. Kato et al. [13] gives an empirical correlation by which solid dispersion can be calculated from liquid dispersion. Epstein [9] stated that it is not unreasonable to assume that when particle size or density increase up to the point where the liquid and solid dispersion start to differ, the flow regime in effect is moving from a regime of slurry-column operation to three-phase fluidisation.

In the present case obviously three-phase fluidisation is involved and we propose that two mechanisms are responsible for the three-phase mixing behaviour of the ALR. On the one hand as bubble size grows, as explained in the previous section, the bubble rise velocity increases and the amount of liquid which can be transported in the form of liquid wakes decreases. This phenomenon results in a decrease in the axial dispersion coefficient [14]. On the other hand the ratio of particle diameter to scale of turbulence is considered as a measure for assessing fluid-particle interaction. The strongest mutual influence is to be expected if the size of the phase elements are of the same order. As the particle diameter lies in between 2-3 mm, turbulence on this scale and even on a smaller scale will be damped, which makes the explanation given above a plausible one.

Another conclusion which can be drawn from figure 4 and figure 7 is the fact that axial dispersion decreases more than proportional to the Bodenstein number ($Bo = v.L/D$) at an increasing gas injection rate as the liquid velocity simultaneously decreases (figure 4) thus effecting the ratio of mass transport by convection and mass transport by dispersion.

Oxygen transfer

The results for the volumetric oxygen transfer coefficient, k_{ja} , estimated by three different methods are shown in figure 8. Two methods are based on the plug flow characteristics of the ALR for both the liquid and the gas phase, the first method being a non isobaric, steady-state, plug-flow model [7], the second method being a dynamic, non-isobaric, plug-flow model on the

basis of which also the dissolved oxygen concentration control was performed [15]. The third method consists of an isobaric model predicting the dissolved oxygen concentration in the liquid phase of an ideally-stirred-tank reactor [7]. For the present ALR, the k_{1a} -values obtained by all three methods harmonize rather well notwithstanding both different ways of approximating the (gas-) liquid flow in the ALR. However, as already stated in the previous section, it is allowed within certain restrictions, to model the ALR as being a STR due to its high circulation rate. The following results were obtained by the STR method as this method appeared to be a reliable and fast response estimation method requiring little computing time.

The presence of the solid phase negatively influences aeration for both the polystyrene and calcium alginate particles as shown in figure 9 and figure 10. In literature many results are reported on the influence of small particles on aeration [10,11,16-18] and agreement exists on the mechanism responsible for the change in k_{1a} . It is reported that for low particle loadings a slight enhancement for k_{1a} occurs and that no dramatic change in k_{1a} can be expected until a bead loading of 20 vol-%. It is proposed that for these low concentrations the small particles do not change the viscosity of the water but enhance the surface renewal and mobility thereby increasing the value of k_{1a} . Higher concentrations increase the viscosity of the slurry thereby increasing coalescence as a result of which k_{1a} decreases. This has been experimentally verified in the literature mentioned and a sharp decrease in k_{1a} for particle loadings greater than 20 vol-% is reported. In our case, for large particles, the sharp reduction in k_{1a} is probably due to

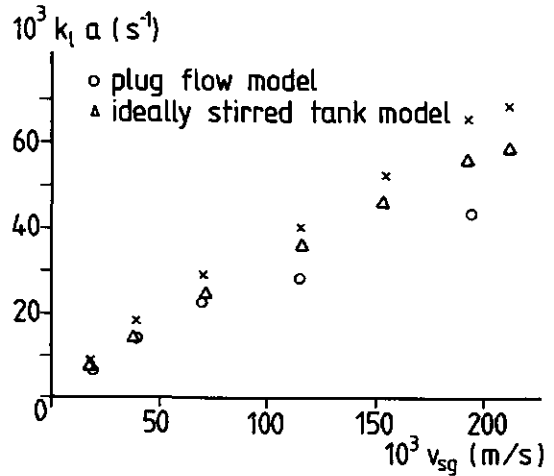


Fig. 8 The volumetric oxygen transfer coefficient as a function of the superficial gas velocity (x plug flow model 1, o plug flow model 2, ΔSTR model)

a larger extent to a reduction in the specific area a , as a result of the coalescence process which has been discussed in the first section of this

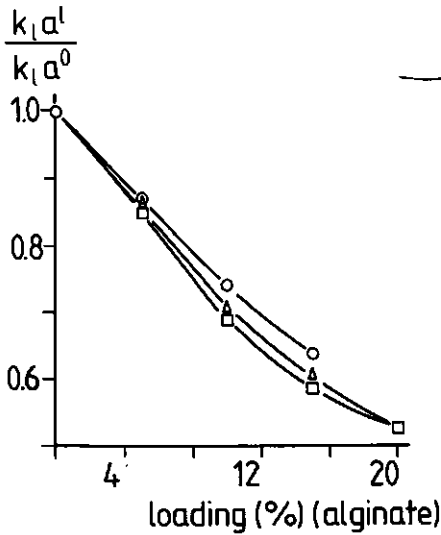


Fig. 9 The relative volumetric oxygen transfer coefficient as a function of the bead loading (Key: $10^2 v_{gs}$ [m/s]: □ 3.86; △ 11.6; ○ 15.4)

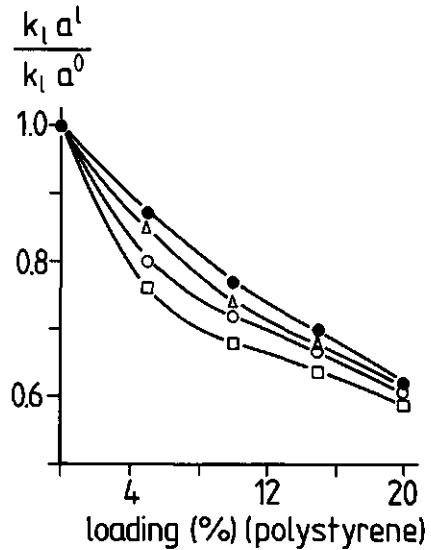


Fig. 10 The relative volumetric oxygen transfer coefficient as a function of the bead loading (Key: $10^2 v_{gs}$ [m/s]: ● 3.86; ▲ 7.71; ○ 11.6; □ 15.4)

paragraph. The effect on the mass transport coefficient k_1 will be of minor importance as for these large particles the increase in apparent viscosity for high loadings only has its effect on macro (reactor) scale but not on micro-scale where mass transfer takes place. Therefore the apparent viscosity has no effect on oxygen transfer. On the contrary it is reasonable to suppose that the k_1 value is slightly increased by surface renewal due to coalescence of the bubbles. On the other hand as mentioned in the previous section, turbulence is damped by the particle, having a negative influence on k_1 thus counterbalancing the effect of surface renewal on k_1 .

Our results agree with the results of Frijlink [2] who measured $k_1 a$ in a STR with a three-phase flow, the third phase being calcium-alginate beads and comparable to the beads in our research. The author found a slow linear decrease of $k_1 a$ in relation to the bead loading and compared his results with the present results in the ALR. Frijlink suggested that the decrease in $k_1 a$ as a function of the bead loading in the ALR could be a result of reduc-

tion of turbulence intensity resulting in larger stable bubbles, the effect being much stronger in a system with low energy input such as the ALR than in a system with high energy input such as the STR. However this explanation is in contrast to our discussion in the hydrodynamics and mixing section. In the latter section it was suggested that small eddies were damped by the particles while the larger eddies determine particle motion due to the negligible difference in density with water, as suggested in the first section. As the bubbles are larger in diameter than the particles are, the larger eddies which are not damped by the particles are responsible for bubble break up. As these eddies are hardly influenced by the particles no effect on bubble break up will occur. In fact the mechanism responsible for the reduction in the interfacial area, a , in an ALR is, apart from the mechanism in a STR as mentioned by Frijlink, also responsible for the decrease in the interfacial area in a STR. As the slenderness of the ALR is much larger than that of a STR the flowed area for the air-water mixture will be less in a STR than in an ALR, resulting in less coalescence and therefore less decrease of the interfacial area.

The reduction for alginate beads, shown in figure 9, being perfectly wetted is slightly more significant than for polystyrene beads, being poorly wetted. These findings are in accordance with the results of Kelkar and Shah [14] who reported that solids wettability was found to enhance the coalescence tendencies in the liquid phase thereby, in our case, reducing oxygen transfer.

CONCLUSION

The liquid velocity and the gas hold-up of a gas-liquid flow in an ALR can be easily modelled with a sufficient accuracy. Neutral buoyant particles with a diameter of 2-3 mm reduce the liquid velocity and the gas hold-up in an ALR significantly. The decrease in liquid velocity is caused by the decrease in gas hold-up and an increased friction. The gas hold-up is reduced mainly because the presence of the particles increases the collision frequency thereby increasing coalescence due to the diminished flowed area for the air-water mixture. In comparison to a gas-liquid flow axial dispersion is reduced in the three phase flow as the presence of the particles

damps the small eddies which are, apart from other mechanisms, responsible for the axial dispersion. Moreover, the increased coalescence also contributes to a decrease in axial dispersion. The presence of the particles negatively influences aeration due to a reduction in the gas-liquid interfacial area as a result of the coalescence process. The effect of the increase in apparent viscosity in the ALR was not supposed to contribute to the decrease in the aeration process.

REFERENCES

- [1] A.C. Hulst, P. Verlaan, H. Breteler and D.H. Ketel. Thiophene production by *Tagetes patula* in a pilot plant airlift-loop reactor. Proc. 4th Europ. Congress on Biotechnology, 1987, vol 2, pp 401-404. (O.M. Neijssel, R.R. van der Meer, K.Ch.A.M. Luyben eds.) Elsevier Science Publishers B.V., Amsterdam.
- [2] J.J. Frijlink. Physical aspects of gassed suspension reactors. Thesis, University of Technology, Delft, 1987.
- [3] B. Metz. From pulp to pellet, Thesis, University of Technology, Delft, 1976.
- [4] P. Verlaan, J. Tramper, K. van 't Riet and K.Ch.A.M. Luyben. A hydrodynamic model for an airlift-loop bioreactor with external loop. Chem. Eng. J. 33 (1986) B43-B53 (Chapter two of this thesis).
- [5] P. Verlaan, J. Tramper, K. van 't Riet and K.Ch.A.M. Luyben. Estimation of axial dispersion in individual sections of an airlift-loop reactor. Submitted (Chapter three of this thesis).
- [6] P. Verlaan, J. Tramper, K. van 't Riet and K.Ch.A.M. Luyben. Hydrodynamics and axial dispersion in an airlift-loop bioreactor with two and three phase flow. Proc. Int. Conf. on Bioreactor Fluid Dynamics (BHRA) Cambridge, England, 15-17 april, 1986.
- [7] P. Verlaan and J. Tramper. Influence of nearly floating particles on the behaviour of a pilot plant airlift-loop bioreactor. Proc. 4th Europ. Congress on Biotechnology, 1987, vol. 1, pp 101-104 (O.N. Neijssel, R.R. van der Meer, K.Ch.A.M. Luyben eds.) Elsevier Science Publishers B.V., Amsterdam.
- [8] A.C. Hulst, J. Tramper, K. van 't Riet and J.M.M. Westerbeek. A new technique for the production of immobilized biocatalysts in large quantities. Biotechnol. Bioeng. 27, pp 870-876 (1985).
- [9] N. Epstein. Three phase fluidisation: some knowledge gaps. Canadian J. of Chem. Eng. 59, 1981, pp 649-657.
- [10] W.-D. Deckwer and A. Schumpe. Transporterscheinungen in Dreiphasen-Reaktoren mit fluidisiertem Feststoff. Chem.-Ing.-Techn. 55, 1983, pp 591-600.
- [11] F.J. Brück and H. Hammer. Intensivierung des Stoffaustausches in Blasensäulen-Reaktoren durch suspendierten Feststoffen. Chem.-Ing.-Techn. 58, 1986, pp 60-61.
- [12] K.-W. Linnenweber and E. Bläß. Messung örtlicher Gas- und Feststoffgehalte in Blasensäulen mit in der Flüssigkeit suspendiertem Feststoff. Chem.-Ing.-Techn 54, (1982) pp 682-683.
- [13] Y. Kato, A. Nishiwaki, T. Fukuda and S. Tanaka. Chem. Eng. Japan, 5, 1972, p 112.
- [14] B.G. Kelkar, Y.T. Shah and N.L. Carr. Hydrodynamics and axial mixing in a three-phase bubble column. Effects on slurry properties. Ind. Eng. Chem. Process. Des. Dev. 29, 1984. pp. 308-313.
- [15] A.K.M. Krolikowski, M.H. Zwietering, D.P. van den Akker and P. Verlaan. Control of the dissolved oxygen concentration (DOC) in an airlift-loop bioreactor. Proc. 4th Europ. Congress on Biotechnology, 1987, vol. 3 pp. 149-152 (O.M. Neijssel, R.R. van der Meer, K.Ch.A.M. Luyben eds.) Elsevier Science Publishers, Amsterdam.
- [16] M. Miyachi, A. Iguchi, S. Uchida and K. Koide. Effect of solid particles in liquid-phase on liquid-side mass transfer coefficient.

- Canadian J. Chem. Eng. 59, 1981, pp 640-641.
- [17] R.S. Albal, Y.T. Shah, A. Schumpe and N.L. Carr. Mass transfer in multiphase agitated contactors. Chem. Eng. J. 27, 1983, pp 61-80.
- [18] G.E.H. Joosten, J.G.M. Schilder and J.J. Jansen. The influence of suspended material on the gas-liquid mass transfer in stirred gas-liquid contactors. Chem. Eng. Sci. 32, 1977, pp 563-566.

NOMENCLATURE

a	interfacial area	[m ²]
α	gas hold-up	[-]
D	dispersion coefficient	[m ² /s]
d	diameter	[m]
ρ	density	[kg/m ³]
g	gravitational constant	[m/s ²]
k	mass transfer coefficient	[m/s]
k_{1a}	volumetric mass transfer coefficient	[s ⁻¹]
K_f	friction coefficient	[-]
L	length	[-]
v	velocity	[m/s]

Subscripts

l	liquid
s	superficial
d	downcomer
g	gas

Superscripts

α	concerning the two-phase system
l	concerning the three-phase system with a bead loading l

CHAPTER EIGHT

SUMMARY

An airlift-loop reactor is a bioreactor for aerobic biotechnological processes. The special feature of the ALR is the recirculation of the liquid through a downcomer connecting the top and the bottom of the main bubbling section. Due to the high circulation-flow rate, efficient mixing and oxygen transfer is combined with a controlled liquid flow in the absence of mechanical agitators.

Liquid velocities and gas hold-ups in an external-loop airlift reactor (ALR) on different scales were modelled on the basis of a simple pressure balance. The model is adapted for non-isobaric conditions and takes into account non-uniform flow profiles and gas hold-up distributions across the duct. The friction coefficient together with the reactor dimensions are input parameters. It has been shown that the friction coefficient can be obtained from simple one-phase flow calculations based on known data of the separate reactor parts. The model predicts liquid velocities and local gas hold-ups in an ALR to within 10% and can be applied easily to an internal loop reactor.

Mixing in the individual sections of the ALR is determined by a newly developed parameter estimation procedure which has proven to be reliable for the estimation of axial dispersion coefficients in the individual sections of the ALR. From the results it can be concluded, that in an ALR the liquid flow behaves like plug-flow with superimposed dispersion except for the top-section for which it is not reasonable to assume plug-flow. The mixing results simplified the modelling of oxygen transfer in the ALR as it appeared not to be necessary to incorporate the dispersion contribution into the oxygen model.

The non-isobaric plug-flow model, presented in this thesis, predicts dynamic and stationary dissolved oxygen concentration (DOC) profiles in large-scale ALRs and has been applied also to estimate the volumetric oxygen transfer coefficient, k_{1a} , in the pertinent ALR. Comparison with the results on the basis of a simple isobaric stirred-tank-reactor model demonstrates, that such a model yields conservative values though for the present situation the underestimation did not exceed a value of 10% relative to the plug-flow

model. Therefore, due to its simplicity, it is recommended to use the stirred tank model for a rapid characterization of the overall aeration capacity of laboratory scale and pilot-scale ALRs. Oxygen depletion of the gas phase, even during a fermentation, appeared to be very limited and was fairly well predicted by the plug-flow model. For this reason an ALR is a very suitable reactor for aerobic processes having a high oxygen demand. If necessary, the aeration capacity of the ALR can be enhanced by injection of a small amount of gas at the entrance of the downflow region. This phenomenon is also accurately predicted by the plug-flow model. In the present ALR the aeration capacity of the air-sparger region did not significantly differ from the main aeration process in the upflow region due to its special geometry.

The intermediate flow region between the ALR and the bubble-column (BC) flow regime was investigated by gradually closing a butterfly valve at the bottom of the downcomer. When the valve is further shut and thus the friction is enhanced, the liquid velocity will be reduced thereby enlarging the gas hold-up. The maximum value for the gas hold-up is obtained when the ALR is operated as a BC. In the transition flow regime between ALR and BC flow, the liquid velocity was found to be a simple power law function of the gas flow rate. The coefficients of the power law depend on the flow characteristics in the reactor. In the transition flow regime the hydrodynamic calculations based on the plug-flow behaviour of an ALR are only valid up to a certain defined value of the total gas-liquid flow rate. For greater values, the ALR type of flow will change into a BC type of flow. A simple criterium qualifies the distinction between both flow patterns, determined by the superficial liquid velocity and the liquid circulation velocity.

The transition of ALR to BC flow coincides with the decrease of the Bodenstein number which also indicates a less established plug flow. As the dispersion coefficient at a constant gas-flow rate, remained constant for as well the ALR, the BC and the transition flow, the decreased Bodenstein number in the BC-type of flow is mainly attributed to the decreased convective transport as the liquid circulation is impeded. The number of circulations required to achieve complete mixing diminishes when the liquid circulation is impeded and appeared to be proportional to the Bodenstein number.

In the transition flow regime, the volumetric oxygen transfer coefficient was estimated by both the stirred-tank model and the plug-flow model. The

stirred-tank model yielded reliable results for the entire range of operation while the plug-flow model only appeared to be appropriate for the ALR operation mode. The volumetric oxygen transfer coefficient was found to increase for the BC operation mode and appeared to be a power law function of the ratio of the superficial liquid and gas velocity and the Bodenstein number.

Addition of immobilized biocatalysts to the ALR, in our case simulated by neutral buoyant particles with diameters ranging from 2.4-2.7 mm, significantly reduces the liquid velocity and the gas hold-up in an ALR. The decrease in liquid velocity is attributed to the decrease in gas hold-up and an increased friction in the ALR. The gas hold-up is reduced mainly because the presence of the particles increases the collision frequency of the air bubbles thereby increasing coalescence due to the diminished flowed area available for the air-water mixture. In comparison to a gas-liquid flow, axial dispersion in the three-phase flow is reduced as the presence of the particles damps the small eddies which are, apart from other mechanisms, responsible for the axial dispersion. Moreover, the increased coalescence also contributes to a decrease in axial dispersion. The presence of the particles negatively influences aeration due to a reduction in the gas-liquid interfacial area as a result of the increased coalescence. The effect of the increase in apparent viscosity in the ALR was not supposed to contribute to the decrease in the aeration process.

SAMENVATTING

Een airlift-loop reactor (ALR) is een bioreactor die zeer geschikt is voor aerobe biotechnologische productieprocessen. Het speciale kenmerk van de ALR is de recirculatie van de vloeistoffase door een daalbuis (downcomer) die onder en boven met het belangrijkste reactordeel, de stijgbuis (riser), verbonden is. Op deze manier ontstaat een sterke circulatiestroming in de reactor die een efficiënte menging en zuurstofoverdracht combineert met een gecontroleerde stroming zonder dat daarbij mechanische roerders aan te pas komen.

Vloeistofsnelheden en gas hold-ups in een airlift-loop reactor met een externe loop op zowel laboratorium als pilot-plant schaal, zijn gemodelleerd op basis van een eenvoudige drukbalans. Het model houdt rekening met de niet isobare condities en de niet-uniforme, radiale vloeistof en gas hold-up profielen. De afmetingen van de reactor en de frictie coefficient zijn invoer grootheden van het model. Er is aangetoond dat de frictie coefficient verkregen kan worden uit eenvoudige één-fase frictie berekeningen, toegepast op de verschillende reactor onderdelen en daarna gesommeerd over de reactor. Het hydrodynamische model voorspelt de gas hold-up en de vloeistofsnelheid met een afwijking van hoogstens 10% en is ook toepasbaar op een ALR met een interne loop.

De menging in de verschillende reactor onderdelen is gekarakteriseerd met behulp van een nieuw ontwikkelde parameterschattingsprocedure die betrouwbare resultaten oplevert voor het schatten van de axiale dispersie coefficient in de verschillende reactor delen. Uit de resultaten kan geconcludeerd worden dat in een ALR de vloeistofstroming zich inderdaad gedraagt als een propstroming met axiale dispersie behalve in de topsectie waar het niet aannemelijk is om het stromingsgedrag als een propstroming voor te stellen. Uit de verkregen meng-resultaten blijkt dat voor het modelleren van de zuurstofoverdracht in de ALR het niet nodig is om de dispersiebijdragen in het model op te nemen.

Het in dit proefschrift beschreven niet-isobare propstroom model voorspelt stationaire en niet-stationaire opgeloste-zuurstof concentratie profielen in grootschalige airlift-loop reactoren en is gebruikt om de volumetrische zuurstofoverdrachtscoefficient, $k_1 a$ in de ALR te schatten. Vergelijking met resultaten, verkregen op basis van een simpel, isobaar, geroerde-tank reac-

tormodel toont aan dat zo'n model te lage waarden oplevert ofschoon voor de bedoelde situatie deze afwijking niet meer dan 10% bedraagt. Door zijn eenvoud wordt dit model dan ook aanbevolen voor een snelle karakterisering van de overall beluchtingscapaciteit van zowel een laboratorium-schaal als van een pilot-plant ALR.

De zuurstofuitputting van de gasfase in de ALR bleek zeer gering te zijn, zelfs gedurende een fermentatie en werd goed beschreven door het propstroommodel. Hierdoor is een ALR een zeer geschikte reactor voor aerobe processen met een hoge zuurstofbelasting. Indien noodzakelijk, kan de zuurstofoverdrachtscapaciteit van de ALR vergroot worden door continu een kleine hoeveelheid gas bovenin de downcomer te injecteren. Dit verschijnsel wordt eveneens goed beschreven door het propstroom model. Voor de onderhavige ALR bleek de zuurstofoverdrachtscapaciteit in de buurt van de gasverdeler niet significant af te wijken van die in de rest van de riser, hetgeen toegeschreven kan worden aan de speciale geometrie van de gasverdeler.

De overgang tussen de typische ALR vloeistofstroming en de bellenkolom (BC) vloeistofstroming is onderzocht door middel van een vlinderklep onderin de downcomer van de ALR, die geleidelijk gesloten of geopend kon worden. Bij een grotere afsluitstand neemt de frictie toe als gevolg waarvan de vloeistofsnelheid af- en de gas hold-up toeneemt. De maximum waarde voor de gas hold-up wordt verkregen als de ALR wordt bedreven als een bellenkolom. In het overgangsregime blijkt de vloeistofstroming een simpele exponentiële functie van het gasdebiet te zijn. De coëfficiënten in deze exponentiële functie zijn afhankelijk van het stromingspatroon in de reactor. In het overgangsgebied blijkt het eerder genoemde hydrodynamische model alleen geldig te zijn tot een bepaald maximum van het totale gas-vloeistof debiet. Voor grotere waarden verandert de typische ALR stroming in een bellenkolomachtige stroming. Een eenvoudig criterium geeft aan wanneer de overgang tussen beide stromingspatronen plaatsvindt hetgeen bepaald wordt door de superficiële vloeistofsnelheid en de vloeistof circulatie snelheid. Het criterium strookt met de afname van het Bodenstein getal in het overgangsregime. Dit laatste verschijnsel wijst tevens op de minder ontwikkelde propstroming van een BC-achtig stromingspatroon. Aangezien de dispersiecoëfficiënt voor zowel de ALR als de BC situatie constant blijft bij een constant gasdebiet, betekent dit dat de genoemde afname van het Bodenstein getal hoofdzakelijk toegeschreven moet worden aan de verminderde convectieve bijdrage wanneer de vloeistof circulatie in toenemende mate wordt belemmerd.

Het aantal omlopen benodigd voor een totale menging in de ALR neemt af naarmate de vloeistofcirculatie steeds meer wordt belemmerd een blijkt evenredig te zijn met het Bodenstein getal. In de overgangssituatie is de volumetrische zuurstofoverdrachtscoëfficiënt geschat door zowel het geroerde-tank-reactor model als door het propstroommodel. Het geroerde-tank model geeft betrouwbare resultaten voor het gehele operationele gebied terwijl het propstroom model alleen toepasbaar blijkt voor de ALR. De volumetrische zuurstofoverdrachtscoëfficiënt neemt toe van de ALR naar de BC situatie en blijkt een exponentiële functie te zijn van de verhouding van de superficiële gassnelheid en de vloeistofsnelheid en het Bodenstein kental.

Toevoeging van een geïmmobiliseerde biofase, in ons geval gesimuleerd door deeltjes met een diameter variërend van 2.4-2.7 mm en een dichtheid ongeveer gelijk aan die van water, aan de ALR reduceerde de vloeistofsnelheid en de gas hold-up aanzienlijk. De afname van de vloeistofsnelheid kan toegeschreven worden aan de afname van de gas hold-up en een toename van de frictie in de ALR. De afname van de gas hold-up is hoofdzakelijk een gevolg van de aanwezigheid van de deeltjes die een positief effect heeft op de botsingsfrequentie van de luchtbellen en daarbij een toenemende coalescentie veroorzaakt door de afname van het beschikbare doorstromings oppervlak voor het water-lucht mengsel. In vergelijking met de gas-vloeistofstroming neemt de axiale dispersie in de drie-fasen stroming af aangezien de aanwezigheid van de deeltjes de kleine turbulenties dempt, die, naast andere mechanismen, verantwoordelijk zijn voor de axiale dispersie. Bovendien draagt een toename van de coalescentie óók bij tot een afname van de axiale dispersie. De aanwezigheid van de deeltjes heeft een negatieve invloed op de beluchting als gevolg van de afname van het gas-vloeistof uitwisselingsoppervlak als gevolg van de toename van de coalescentie. Het effect van de toename van de schijnbare viscositeit in de reactor is verondersteld niet bij te dragen tot een afname van de beluchtingscapaciteit.

CURRICULUM VITAE

De auteur van dit proefschrift is op 30 december 1955 geboren te Willemstad, Curaçao. In Vlissingen doorliep hij van 1968 tot 1974 het atheneum-B. Aansluitend hierop werd gestart met de studie Technische Natuurkunde aan de (toen nog) Technische Hogeschool Delft. Na de 3-jarige kandidaatsfase werd het doctoraalonderzoek verricht bij de vakgroep Fysische Technologie van de genoemde studierichting. De twee hoofdonderwerpen betroffen onderzoek aan waterstraalbeluchters en aan een deep-shaft reactor. Gedurende de doctoraalfase is de auteur enkele jaren in deeltijd werkzaam geweest als leraar in de natuurkunde aan een middelbare school en aan een HBO-opleiding, bovendien werd een eerste-graads lesbevoegdheid in de natuurkunde en mechanica behaald.

In 1983 rondde de auteur zijn studie af en werd hij aangesteld als wetenschappelijk assistent aan de sectie Proceskunde van de vakgroep Levensmiddelen-technologie van de (toen nog) Landbouwhogeschool Wageningen. Het onderwerp van onderzoek is beschreven in dit proefschrift en werd afgerond in 1986.

Vanaf 1 april 1986 is de auteur werkzaam als universitair docent aan de sectie Proceskunde van de Landbouwuniversiteit Wageningen.